AFAL-TR-77-158

PROJECT STRESS SATELLITE COMMUNICATION TEST RESULTS

System Development Branch
System Avionics Division

July 1977

TECHNICAL REPORT AFAL-TR-77-158

Final Report for Period June 1976 - March 1977

Approved for public release; distribution unlimited.

ORIGINAL CONTAINS COLOR PLATES: ALL DDC REPRODUCTIONS WILL BE IN BLACK AND WHITE

AIR FORCE AVIONICS LABORATORY
AIR FORCE WRIGHT AERONAUTICAL LABORATORIES
AIR FORCE SYSTEMS COMMAND
WRIGHT-PATTERSON AIR FORCE BASE, OHIO 45433

NOTICE

When Government drawings, specifications, or other data are used for any purpose other than in connection with a definitely related Government procurement operation, the United States Government thereby incurs no responsibility nor any obligation whatsoever; and the fact that the government may have formulated, furnished, or in any way supplied the said drawings, specifications, or other data, is not to be regarded by implication or otherwise as in any manner licensing the holder or any other person or corporation, or conveying any rights or permission to manufacture, use, or sell any patented invention that may in any way be related thereto.

This report has been reviewed by the Information Office (OI) and is releasable to the National Technical Information Service (NTIS). At NTIS, it will be available to the general public, including foreign nations.

This technical report has been reviewed and is approved for publication.

ALLEN L. JOHNSON
Project Engineer

FOR THE COMMANDER

FRANCIS J. LIBERATORI, Lt Col, USAF
Deputy Division Chief
System Avionics Division

"If your address has changed, if you wish to be removed from our mailing list, or if the addressee is no longer employed by your organization please notify _____,W-PAFB, OH 45433 to help us maintain a current mailing list".

Copies of this report should not be returned unless return is required by security considerations, contractual obligations, or notice on a specific document.

UNCLASSIFIED

SECURITY CLASSIFICATION OF THIS PAGE *(When Data Entered)*

REPORT DOCUMENTATION PAGE		READ INSTRUCTIONS BEFORE COMPLETING FORM
1. REPORT NUMBER AFAL-TR-77-158	2. GOVT ACCESSION NO.	3. RECIPIENT'S CATALOG NUMBER
4. TITLE *(and Subtitle)* PROJECT STRESS SATELLITE COMMUNICATION TEST RESULTS		5. TYPE OF REPORT & PERIOD COVERED Final Technical Report. June 76 - March 77
		6. PERFORMING ORG. REPORT NUMBER
7. AUTHOR(S) C. Prettie, T. Grizinski A. Johnson, R. Swanson J. Marshall		8. CONTRACT OR GRANT NUMBER(S) RDT & E RMSS Code B3220 76462 L 25AAXHX 63511 H2590D (DNA)
9. PERFORMING ORGANIZATION NAME AND ADDRESS Systems Avionics Division (AA) Air Force Avionics Laboratory Wright-Patterson Air Force Base, Ohio 45433		10. PROGRAM ELEMENT, PROJECT, TASK AREA & WORK UNIT NUMBERS Project 1227 Task 122722 Work Unit 12272205
11. CONTROLLING OFFICE NAME AND ADDRESS		12. REPORT DATE July 1977 13. NUMBER OF PAGES 124
14. MONITORING AGENCY NAME & ADDRESS *(if different from Controlling Office)*		15. SECURITY CLASS. *(of this report)* UNCLASSIFIED 15a. DECLASSIFICATION/DOWNGRADING SCHEDULE

16. DISTRIBUTION STATEMENT *(of this Report)*

Approved for public release; distribution unlimited

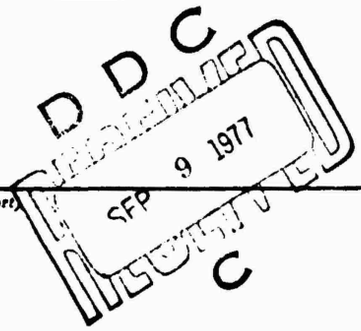

17. DISTRIBUTION STATEMENT *(of the abstract entered in Block 20, if different from Report)*

18. SUPPLEMENTARY NOTES

19. KEY WORDS *(Continue on reverse side if necessary and identify by block number)*

Barium Cloud
Ionospheric Scintillation
Satellite Communications
UHF Fading

20. ABSTRACT *(Continue on reverse side if necessary and identify by block number)*

In order to evaluate the effects of a nuclear disturbance of the ionosphere on UHF satellite communication, barium ions were released in the ionosphere. The test, nicknamed STRESS, was sponsored by the Defense Nuclear Agency. The drift of the barium ions across the magnetic field lines cause the ions to consolidate in rods, or sheets, causing diffraction of radio waves passing through the ionosphere. AFAL's Satellite Communication System aboard a C-135 type aircraft was flown in the shadow of the cloud and communicated through the ionospheric disturbance to the LES 8/9 UHF satellites. Measurements were made of the fading

DD FORM 1 JAN 73 1473 EDITION OF 1 NOV 65 IS OBSOLETE

711670

UNCLASSIFIED

SECURITY CLASSIFICATION OF THIS PAGE *When Data Entered)*

Key Words Cont'd Block No. 19

Airborne Communication
Propagation Anomalies
STRESS

Abstract Cont'd Block No. 20

characteristics and bit error rate performance when communicating through the ionospheric disturbance.

FOREWORD

The effort reported in this Technical Report was accomplished between 1 June 1976 and 15 March 1977 under Project #12272205, LES 8/9 Flight Test Effort. The effort was in support of the Defense Nuclear Agency's Project STRESS.

This Report is a cooperative effort between the Air Force Avionics Laboratory (AFAL) and ESL, Incorporated, the latter party with sponsorship of the Defense Nuclear Agency under RDT & E RMSS Code B3220 76462 L25AAXHX63511 H2590D.

The tests described herein were supported by the 4950th Test Wing, MIT Lincoln Laboratory, ESD's Test Management Facility, and an extensive test team located at Eglin AFB, Florida responsible for the rocket launch, aircraft positioning, photo/radar coverage, and physical analysis of the barium cloud.

The support of an extensive team of engineers/contractors at Wright-Patterson AFB, Ohio was also instrumental in the successful completion of this test.

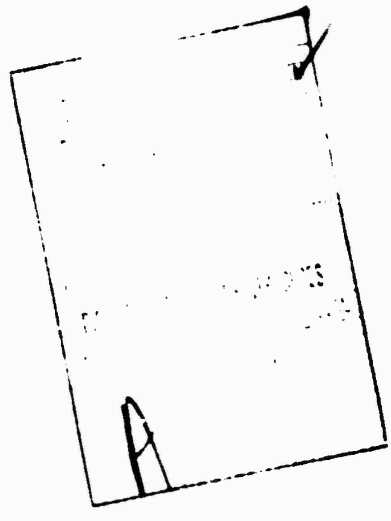

TABLE OF CONTENTS

I. TEST OBJECTIVES

The overall objective of the STRESS (Satellite Transmission Effects Simulation Study) Experiment was to evaluate the performance of a UHF satellite communication system in an artificially disturbed ionosphere in an effort to better predict the expected performance of such communication systems in a nuclear environment. The specific objectives of the experiment were:

a. To exercise the techniques used for and to verify assumptions made in predicting the performance of communications systems operating through striated plasmas. These techniques involve gradient drift plasma instability phenomenology for the determination of the striated environment, multiple thin phase screen propagation theory, and computer simulations of system performance that utilize propagation inputs.

b. To obtain data on late-time striation dissipation mechanisms. To date no theories exist that describe how long striations from barium or nuclear detonations are expected to persist.

c. To measure the performance of the LES 8/9 UHF command post force element forward and report-back communication links operating through a fading environment created by high altitude barium release and to assess the implications for operations in a nuclear environment. Since the LES 8/9 systems were chosen to meet objective (a) and since the system represents a design phase of future AFSATCOM concepts, an assessment of the performance of these systems through striated environments is called for.

II. TEST ORGANIZATION

The STRESS Project is under the direction of the Defense Nuclear Agency (DNA). The field operations necessary to accomplish the satellite measurements were planned and carried out by Stanford Research Institute (SRI). The Electro-magnetic Systems Laboratories (ESL) designed and built special test hardware for the satellite communication measurements. The Air Force Avionics Laboratory (AFAL) provided and operated the LES 8/9 airborne and ground satellite communication equipment. The collection of the satellite communication data was a joint effort of AFAL and ESL.

A list of the field experiment participants and their areas of responsibility is as follows:

DNA	Program Director
SRI	Test Planning and Direction, operation of the TV tracking system, FPS-85 radar, and ionosonde.
ESL	Construction of special measuring equipment and participation in satellite communication system measurements
AFAL	Provide and operate airborne and ground satellite communication system
4950th	Test aircraft support
TIC	Ground photography
SDC	Rocket operations
USU	Probe payloads
Thiokol	Barium payloads
LMSC	Optical interferometer
ESD	Satellite support
RDA	Probe rocket coordination
ADTC	Range operation

III. TEST CONCEPT

The basic concept of the STRESS Experiment involves at least two communication terminals, a striated plasma in the ionosphere, and a UHF satellite. In the experiment the two terminals attempt to communicate via the satellite with UHF signals between one terminal and the satellite traversing the striated plasma. The properties of the striated plasma perturb the UHF signals and, thereby, stress the communications link. The two communications terminals were the AFAL rooftop facility and aircraft C135/662 linked via the LES 8 (for two releases) or LES 9 (for three releases) satellites.

The first high altitude barium releases provided the plasmas which were diagnosed using rocket probe, optical, and RF techniques. The five STRESS releases were preceded by a pre-STRESS release with all bearing girl's names in alphabetical order as follows: pre-STRESS - ANNE, STRESS - BETTY, CAROLYN, DIANNE, ESTHER, and FERN. The pre-STRESS release was a field test to determine the capability of positioning the aircraft in the cloud shadow.

The use of chemicals to modify or artificially disturb the ionsophere is a technique which has received extensive development over the past years. An artificial barium ion cloud was used to produce propagation path disturbances during the ARPA SECEDE Program, which involved radar propagation through the disturbed ionosphere.

The barium clouds used in the STRESS Test were generated with the launch of 48 kilograms of barium chips to an altitude of approximately 185 kilometers. The barium was vaporized by a small thermite explosion. Action of the sun's ultra violet rays on the barium generated barium ions and free electrons. The barium which did not ionize formed spherical clouds (neutral clouds) which drifted according to the high altitude winds (30 to 100 meters per second generally away from the sun). The ionized barium also formed in spherical

clouds initially but soon changed into elliptical clouds tilted along the magnetic field lines. The ionized plasma was confined, and its diffusion spread occurred only in the direction of the magnetic field lines. Figure 1 from Reference 1 illustrates the subsequent ion cloud evolution from two different views. The bottom row of sketches represents the more typical view of an ion cloud in the process of striating as it would appear from sites with arbitrary magnetic field line aspect angles. The top row of sketches show the corresponding appearances of the ion cloud when viewed up the field lines. The typical cloud evolution from the elliptical form with the circular cross-section (labelled "AMBIPOLAR DIFFUSION") to a striated cloud is driven by the neutral wind attempting to drag the denser regions of the barium cloud with it (and thus with the neutral cloud) in conflict with the magnetic field confinement forces (or E x B forces) on the entire ion cloud. (If the neutral cloud were shown in this figure, it would be seen moving to the left.) Initially the denser portion of the cloud is dragged to one side of the cloud forming the "hard edge," or "BACKSIDE STEEPENING." Further wind drag pulls "fingers," or "sheets," of dense plasma from the "hard edge" which eventually pinch off to form isolated "striations." When viewed with a typical magnetic aspect as in the bottom row, the appearance of isolated striations embedded in a background plasma cannot be distinguished from the appearance of the overlap of several sheets of varying thicknesses. Both the sheets and striations cause UHF signal amplitude scintillations while the effect of the unstriated, or "smooth," ion cloud (farthest from the neutral cloud and to the right in the figure) is a slight phase shift due to the elevated integrated electron content through the medium. While the initial barium release occurs at approximately 185 kilometers altitude, the free electrons tend to drift up and down the magnetic field lines between altitudes of approximately 140

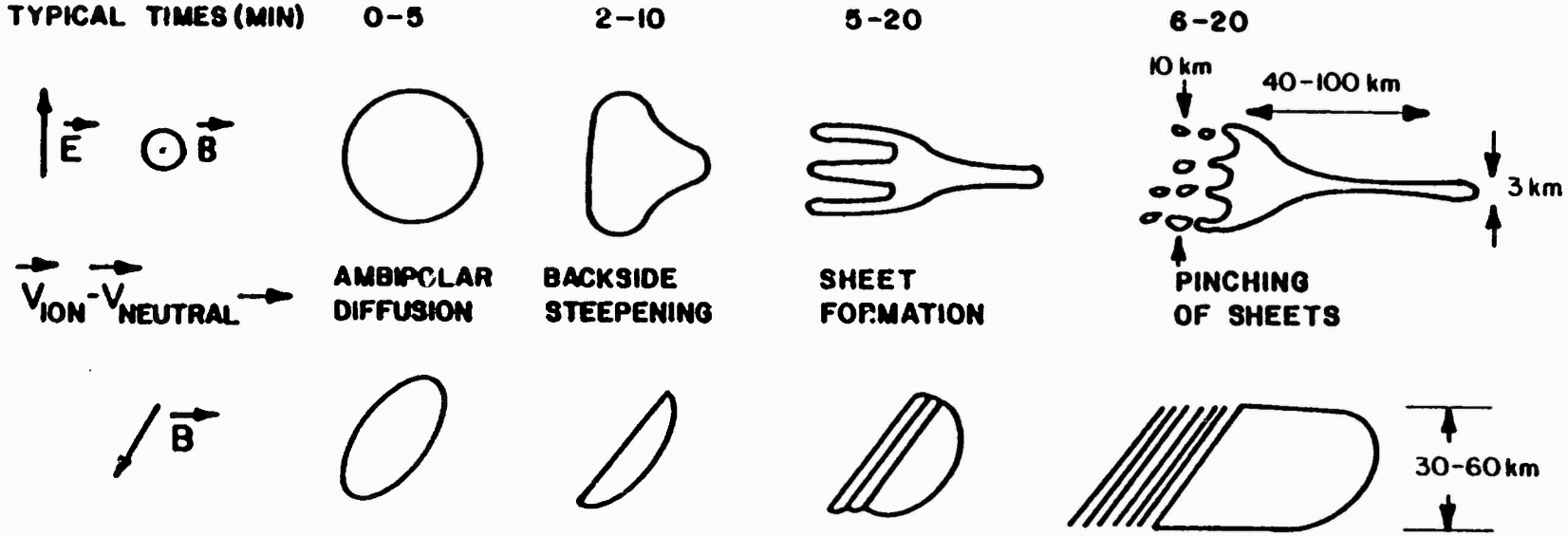

FIGURE 1 Schematic Diagram of Barium Ion Cloud Morphological Development

kilometers and 210 kilometers, Figure 2. The development of the striated line might appear as in Figure 3 when viewed across the field lines.

Barium clouds resemble weather clouds in that all of the significant observation light which comes from them is reflected sunlight; their glow due to molecular recombination is insignificant. Barium clouds launched at sunset are best observed after the time when the sun is 6° below the horizon and before sunset at the 185 kilometer altitude. The spherical neutral cloud reflects sunlight of a bluish and greenish tint. The ionized portion of the cloud reflects sunlight of a pinkish or reddish tint, Figure 4.

For Project STRESS the barium releases occurred at various times relative to the 6° sun depression angle, Table 1. The barium clouds which were released early and passed through their early stage of development obscured by the sky glow became visible well into their development and remained visible further into their development than those launched later. The variety of launch times allowed optical observation of the late-time cloud development and will provide data on structure dissipation mechanisms.

The Honest John-Hydac rocket launches carrying the barium payloads took place from Eglin's launch site, A-15 on Santa Rosa Island. A series of radars and optical TV trackers were located along the Florida coast at locations indicated in Figure 5 to position the aircraft beneath the ion cloud RF shadow to satellite emissions. A photographic coverage net, one mobile site omitted, is also indicated in the map.

The concept of using aircraft C135/662 to fly under the barium cloud projections from LES 8 or LES 9 was intrinsic to the test concept. Using satellite ephemeris data and nominal cloud drift assumptions two test windows for operation of the aircraft with the LES 8/9 satellites were generated

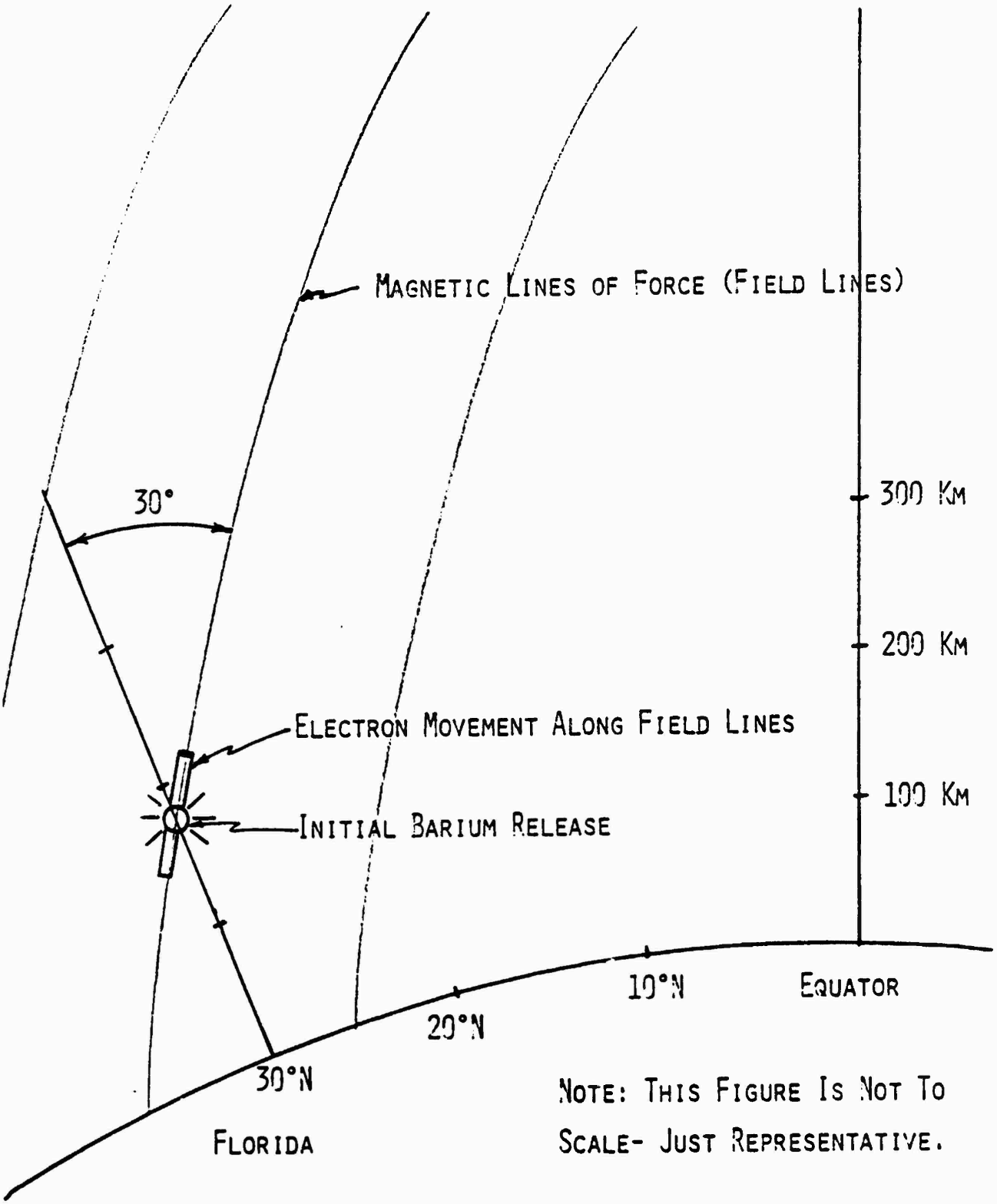

FIGURE 2 Propagation of Free Electrons Along Field Lines

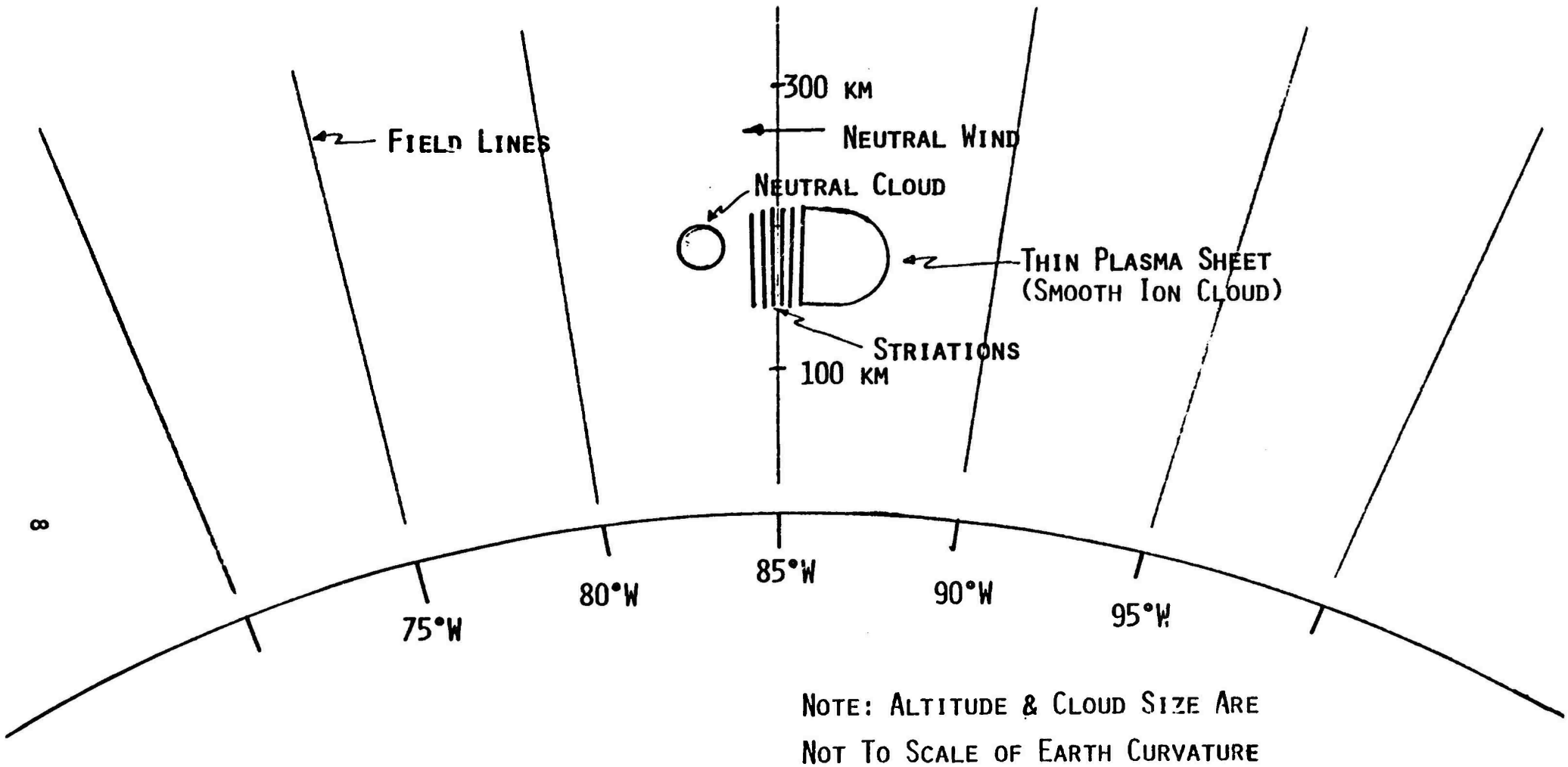

FIGURE 3 Movement of Barium Ion Cloud

FIGURE 4 Photograph of Barium Ion Cloud

TABLE 1: STRESS Events -- Summary
(Primary Source -- T.I.C., Bedford, Mass.)

Event Date	BETTY 26 Feb 77	CAROLYN 2 Mar 77	DIANNE 7 Mar 77	ESTHER 13 Mar 77	FERN 14 Mar 77
Release Time (Z)	2352:29	2354:10	0001:10	2301 :8	2246:09
Altitude of Release (Radar)	179	191	186	189	186
Optical Coverage (Z)	0012-0042	0005-0043	0010-0045	0015-0050	0015-0050
Optical Coverage (Release + min)	R+20 - R+50	R+11 - R+49	R+9 - R+44	R+74 - R+109	R+89 - R+124
Radar Track Duration	0047-0258	2358-0202	0004-0149	2304-0237	2246-0109
Duration of Fading	0012-0158	0010-0144	0009-0126	2301-0244	2247-0108
Speed of Drift (m/s) (all clouds moved east to southeast)	~45	~60	46	36	~20

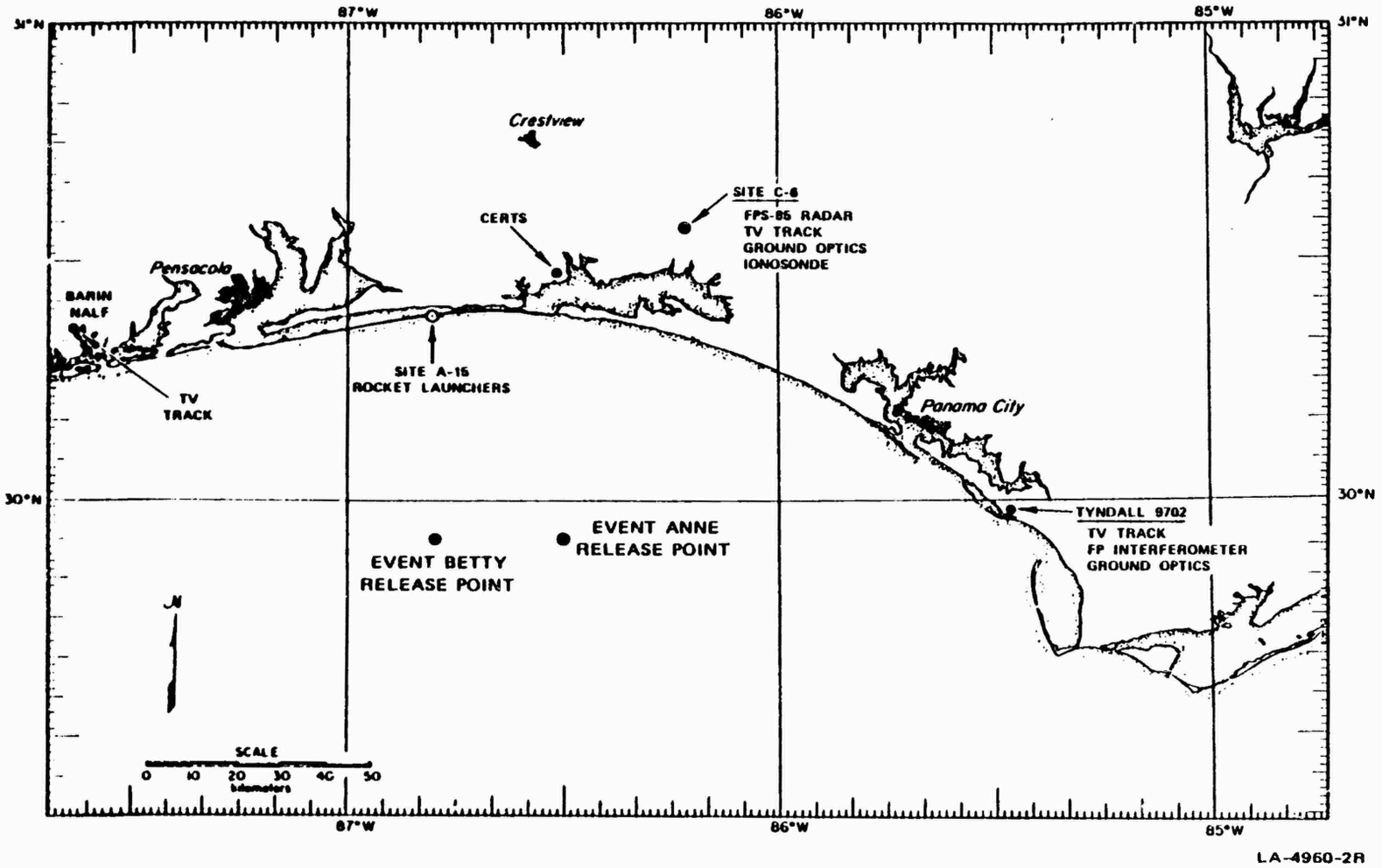

FIGURE 5 STRESS Instrum[illegible] Location

before the test and are shown in Figure 6. These windows give a qualitative feel for the geometry involved. Actual test operations windows differed somewhat in BETTY and CAROLYN from those shown due to cloud drift. The flight path of the aircraft in the shadow of the cloud was designed primarily to cut across the striations and to measure the signal fading caused by the diffraction pattern of the striations. Some passes, "parallel runs or end runs," were made along the striations to measure their extent and to investigate propagation phenomena. Figure 7 shows the cross striation aircraft flight pattern through an idealized cloud shadow. Figure 8 from Reference 2 shows an aircraft trajectory through an actual projection of the pre-STRESS event ANNE from LES 9. Figure 9 shows a similar projection, true to shape but not true to position, of the STRESS event DIANNE from LES 9 at about release +30 minutes for comparison.

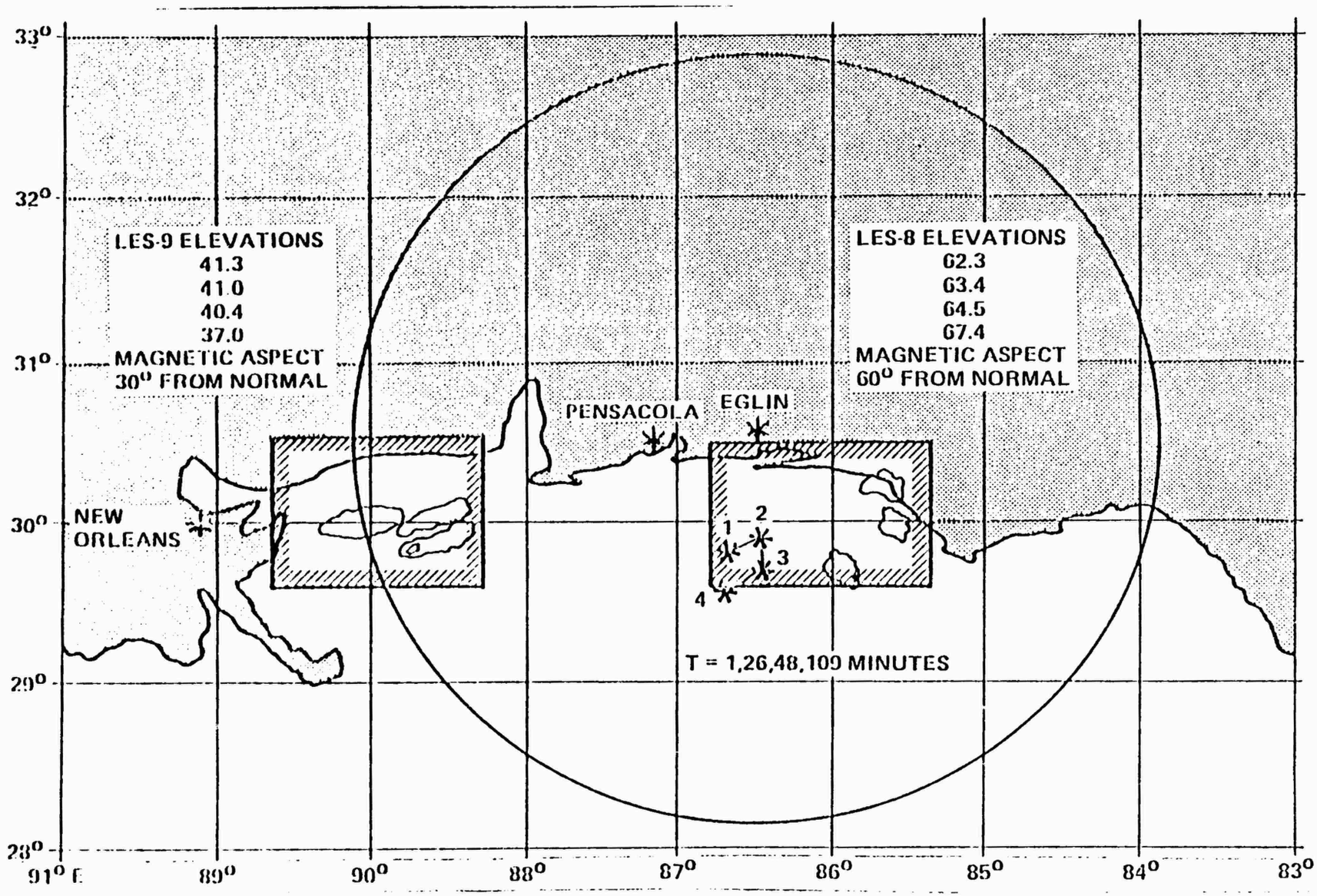

FIGURE 6 STRESS Late February Geometry

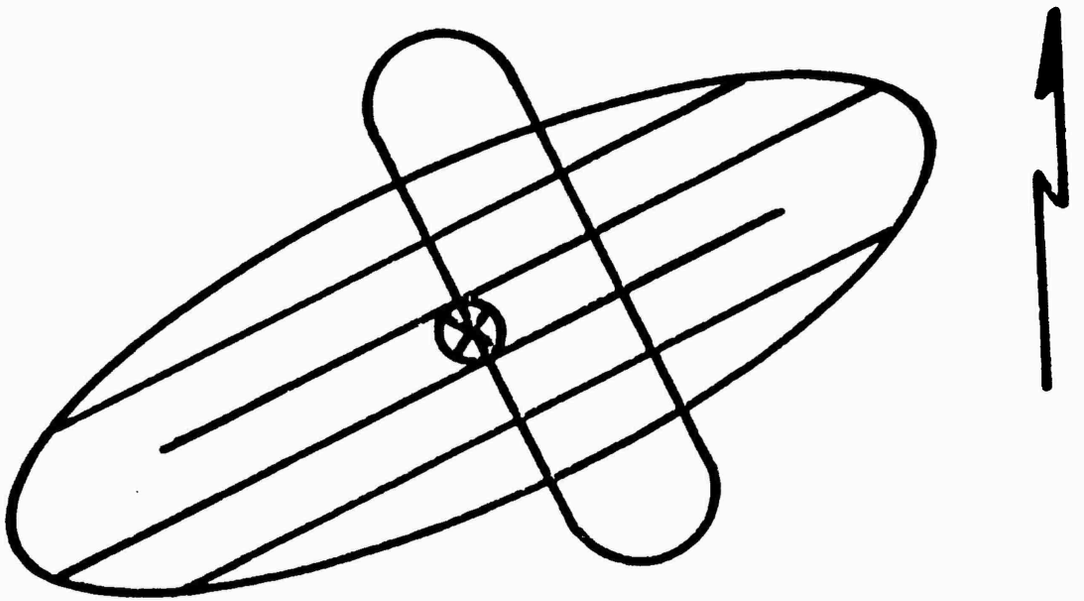

FIGURE 7 Desired Aircraft Flight Pattern in Cloud Shadow, LES 9 Geometry

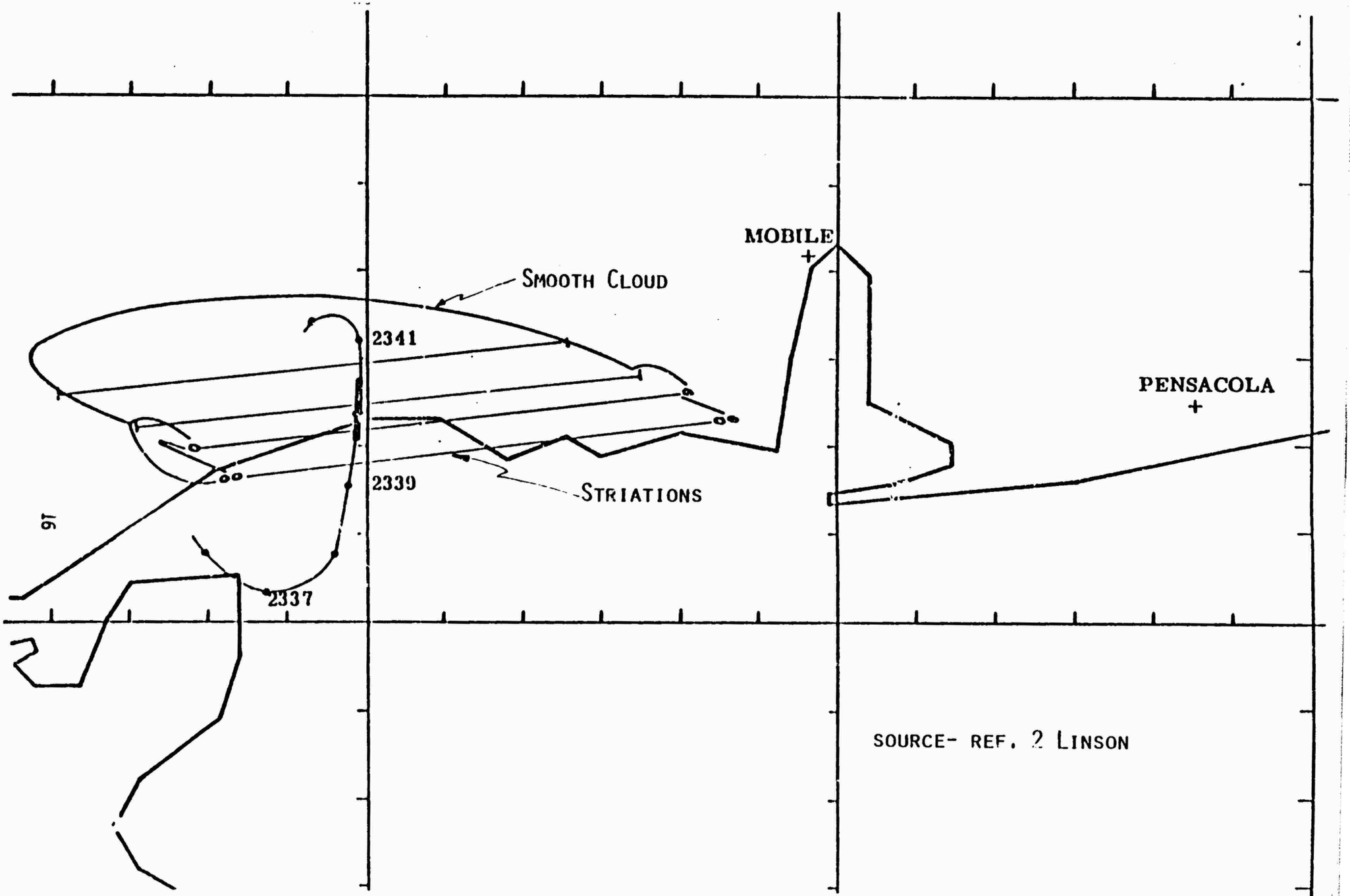

FIGURE 8 Barium Ion Cloud Projection on the Ground ,ANNE

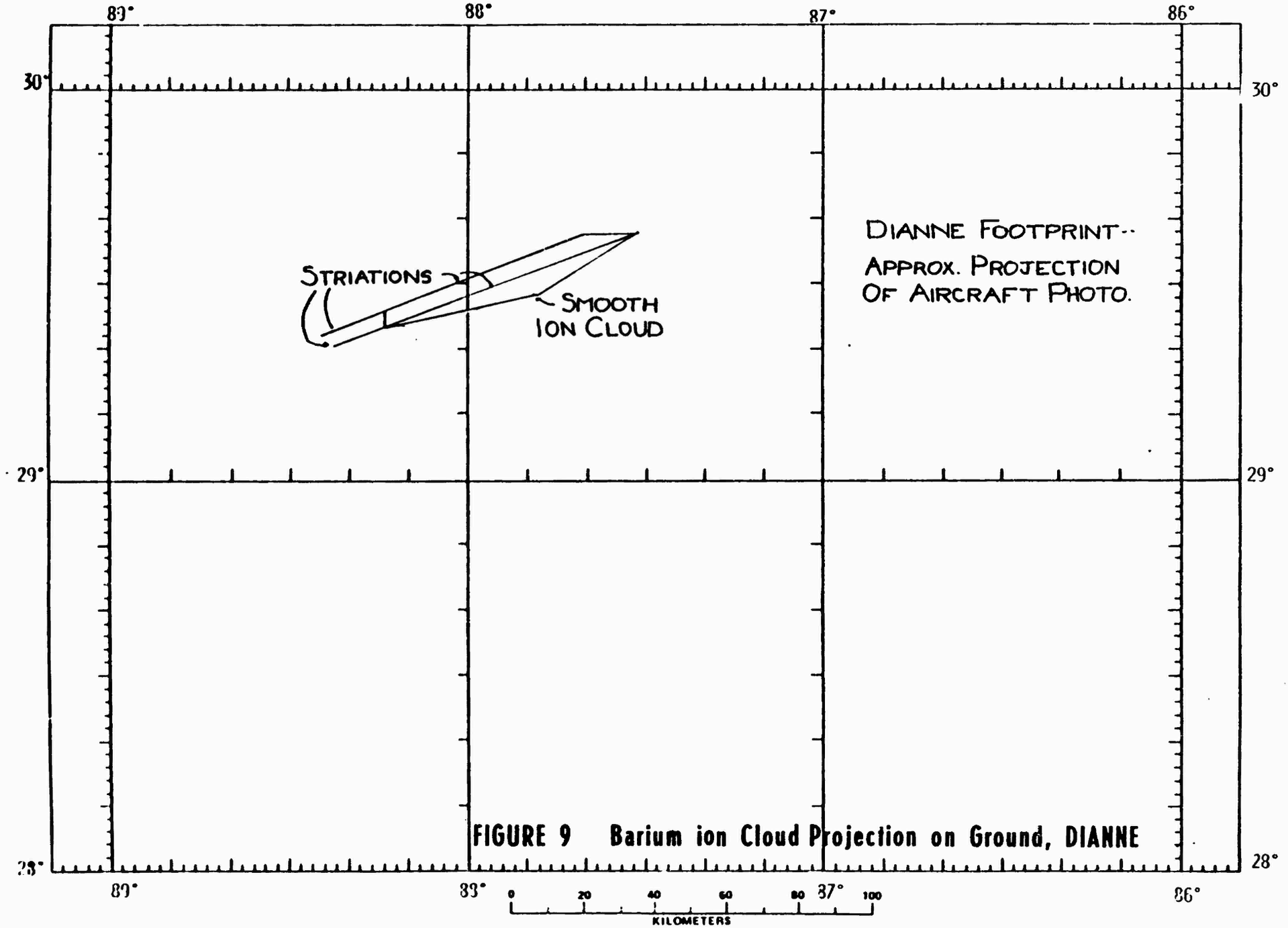

FIGURE 9 Barium ion Cloud Projection on Ground, DIANNE

IV. TEST CONFIGURATION

For the STRESS tests three basic satellite test configurations were utilized. Test Configuration #1, Figure 10, provided UHF forward downlink data to the aircraft and a CW UHF uplink probe from the aircraft through the barium cloud. The uplink probe was sampled at the satellite and sent down on the K band downlink to the rooftop where it was recorded. The K band forward uplink was provided either by the rooftop or by the aircraft.

Test Configuration #2 had been planned to test the report-back link. However, due to equipment problems this link was not tested during the STRESS test.

Test Configuration #3, Figure 11, involved an uplink and downlink UHF probe between the aircraft and the satellite. The downlink UHF tone was recorded on the aircraft. The uplink probe was sampled in the satellite and transmitted downlink via K band to the rooftop. Test Configuration #3 allowed a comparison of the uplink and downlink UHF fading at frequencies separated by approximately 90 MHz.

One other test configuration was used to evaluate multipath from the aircraft, Figure 12. The aircraft transmitted a UHF pseudo random (PRN) sequence through the transponder mode of the satellite. The UHF PRN sequence was downlinked from the satellite to the rooftop where a correlation process was used to indicate the relative strength of the direct and reflected UHF signals. Note that no barium cloud was needed for this configuration.

The block diagram of the aircraft equipment used in STRESS configuration #1 is shown in Figure 13. The K band received signal was used to measure doppler from the satellite. A scaled version of that doppler, derived in a divide by operation in the "frequency unit," was then used to precorrect the UHF uplink probe frequency to remove the effect of the doppler. The UHF forward downlink

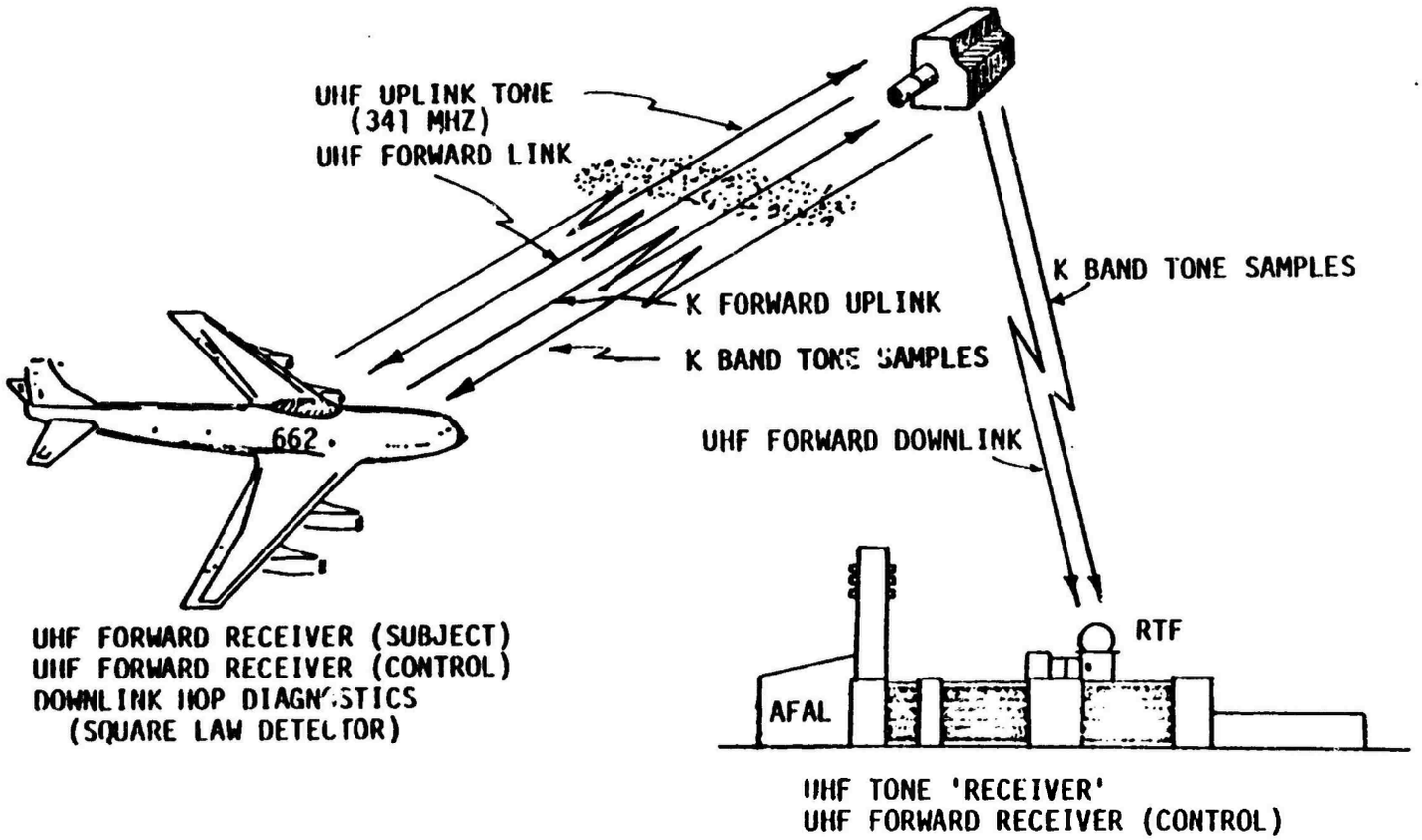

FIGURE 10 STRESS TEST CONFIGURATION NO. 1

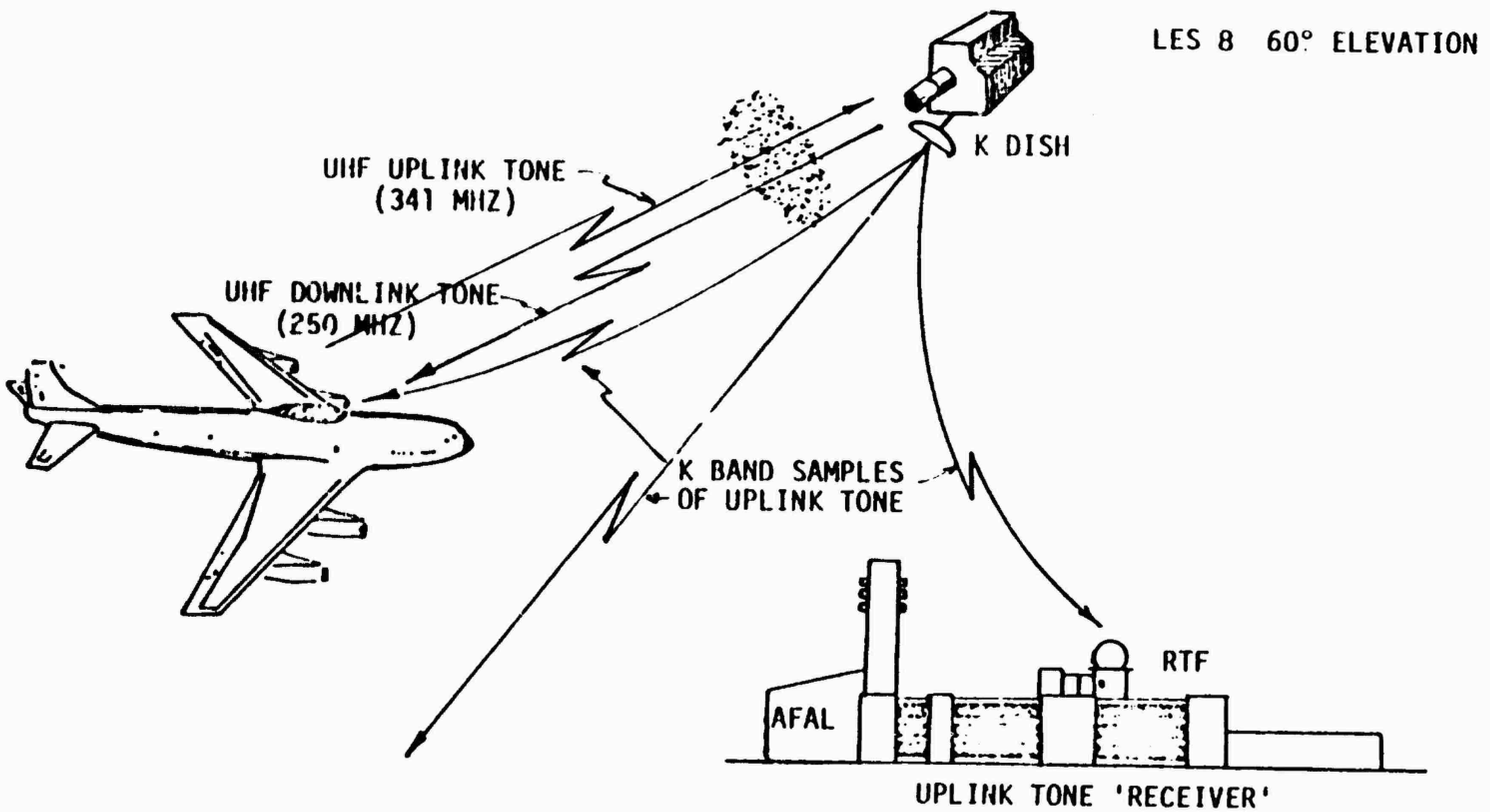

FIGURE 11 STRESS Test Configuration 3

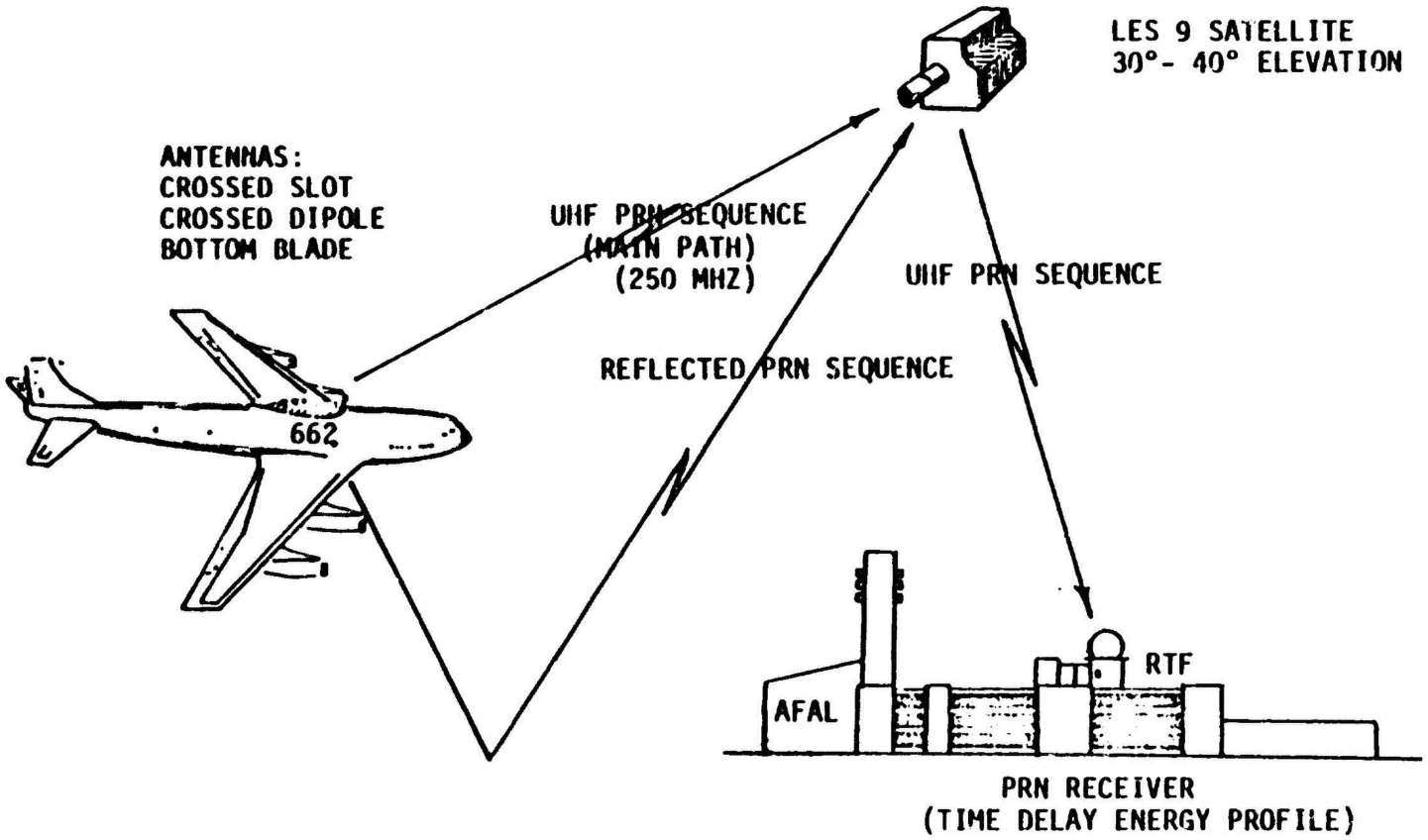

FIGURE 12 STRESS Multipath , PRN, Configuration

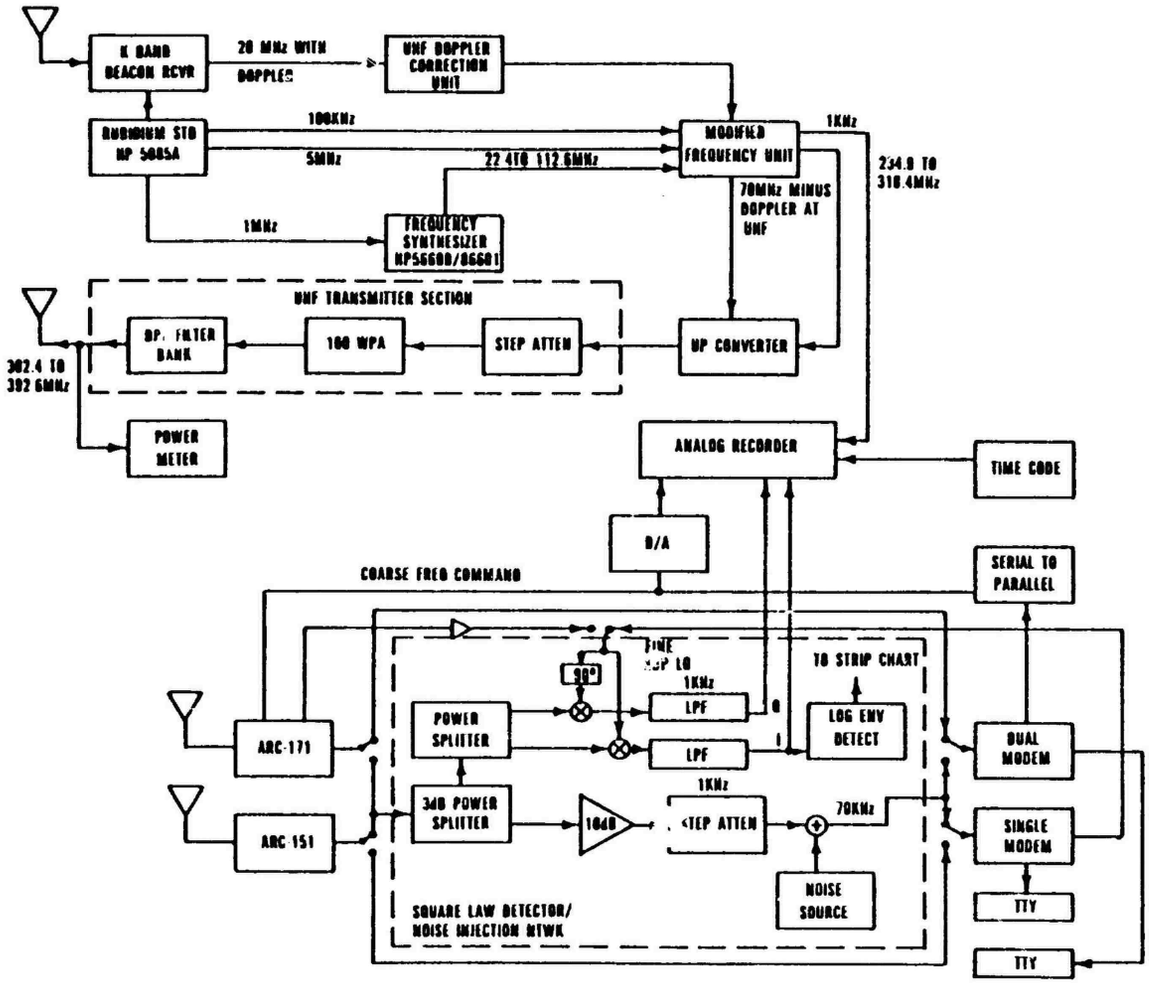

FIGURE 13 STRESS Test Configuration 1 Aircraft Equipment

was received and a dehopped version of the received signal used to indicate the UHF signal fading level. The coarse frequency command signal from the dual modem serial-to-parallel processor to the ARC-171 was tapped, processed, and recorded for later analyses to be performed in conjunction with recordings of the dehopped signal. The actual forward link data is received with two modems and typed out on teletypewriters for later error rate analysis. The signal strength into one of the modems (the subject modem) is attenuated while maintaining the same noise floor in order to sweep out performance versus received signal level. The other modem serves as a control. The block diagram of the rooftop equipment configuration for STRESS Test Configuration #1 is shown in Figure 14. The K band signal was received and demodulated. The I and Q samples were separated, processed, and recorded to obtain phase and amplitude information.

The block diagram of the aircraft equipment used in STRESS Test Configuration #3 is shown in Figure 15. The K band receiver determined the downlink doppler which was scaled to correct the UHF downlink and precorrect the UHF uplink signal to remove the effects of the doppler. The block diagram for the rooftop equipment used in STRESS is very similar to that used in Test Configuration #1, as shown in Figure 16. Again, the K band received signal was separated into I and Q channel samples, processed, and recorded for further analysis of the phase and amplitude variations.

The block diagram of the aircraft PRN sequence equipment used in the multipath test is shown in Figure 17. The 125 KHz (8 microseconds per symbol) pseudo random sequence (length 127) was transmitted from the aircraft ARC-146 UHF transmitter at a 1 kilowatt level. Various transmit antennas were used during the test to determine the isolation each provides between the direct

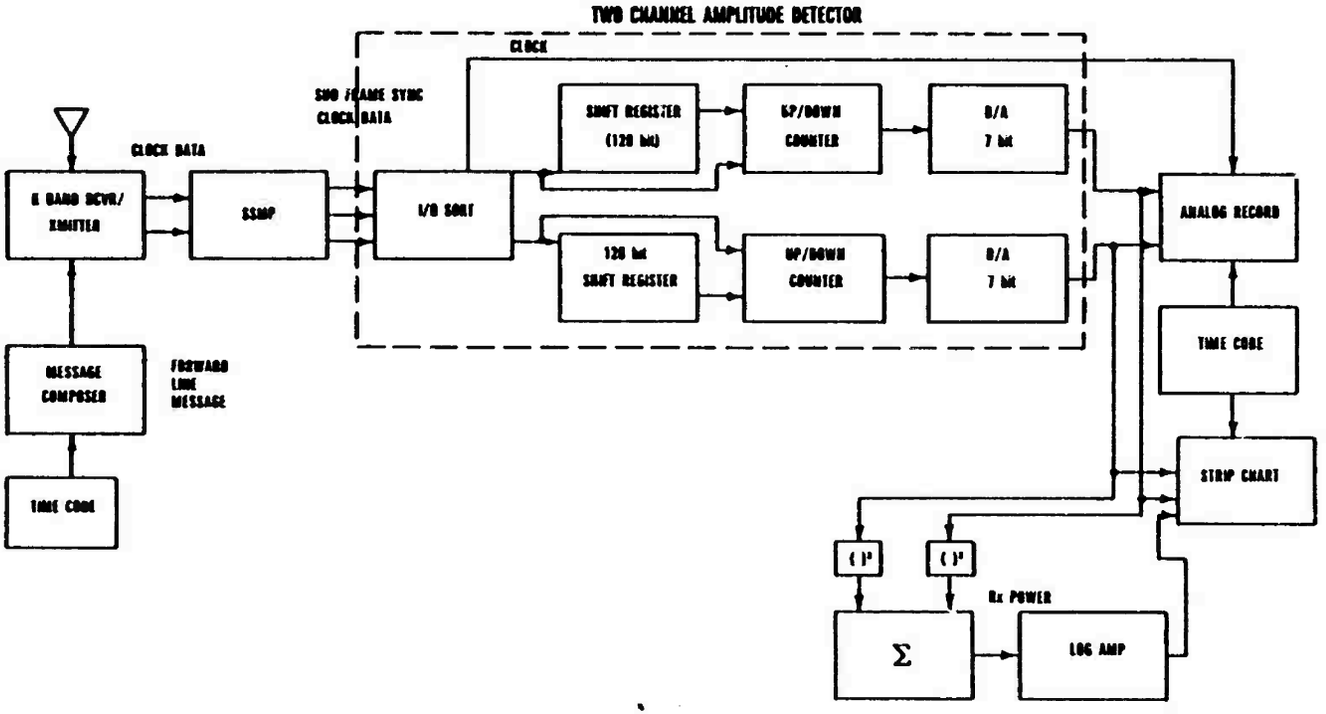

FIGURE 14 STRESS Test Configuration 1 Rooftop Equipment

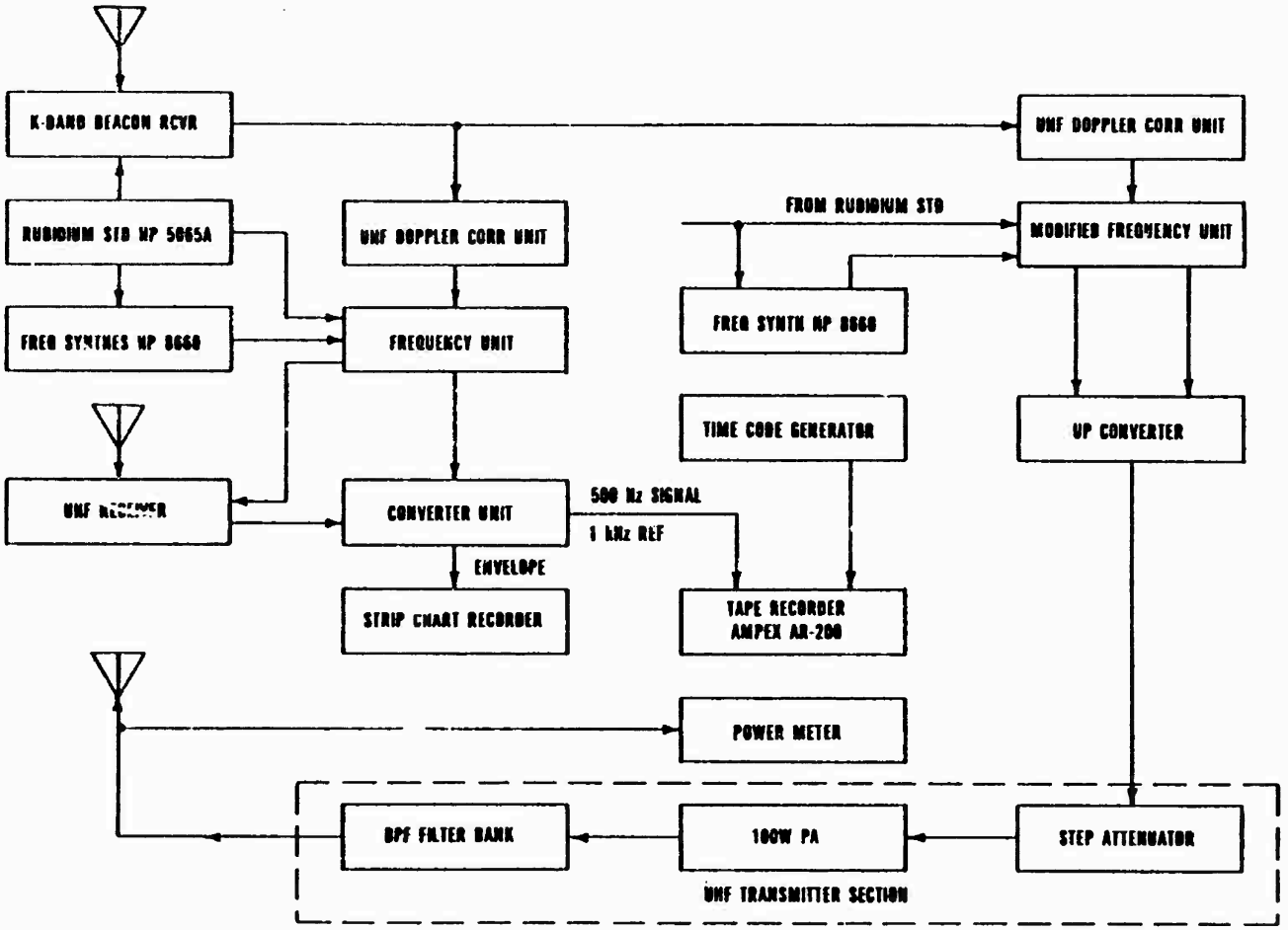

FIGURE 15 STRESS Test Configuration 3 Aircraft Equipment

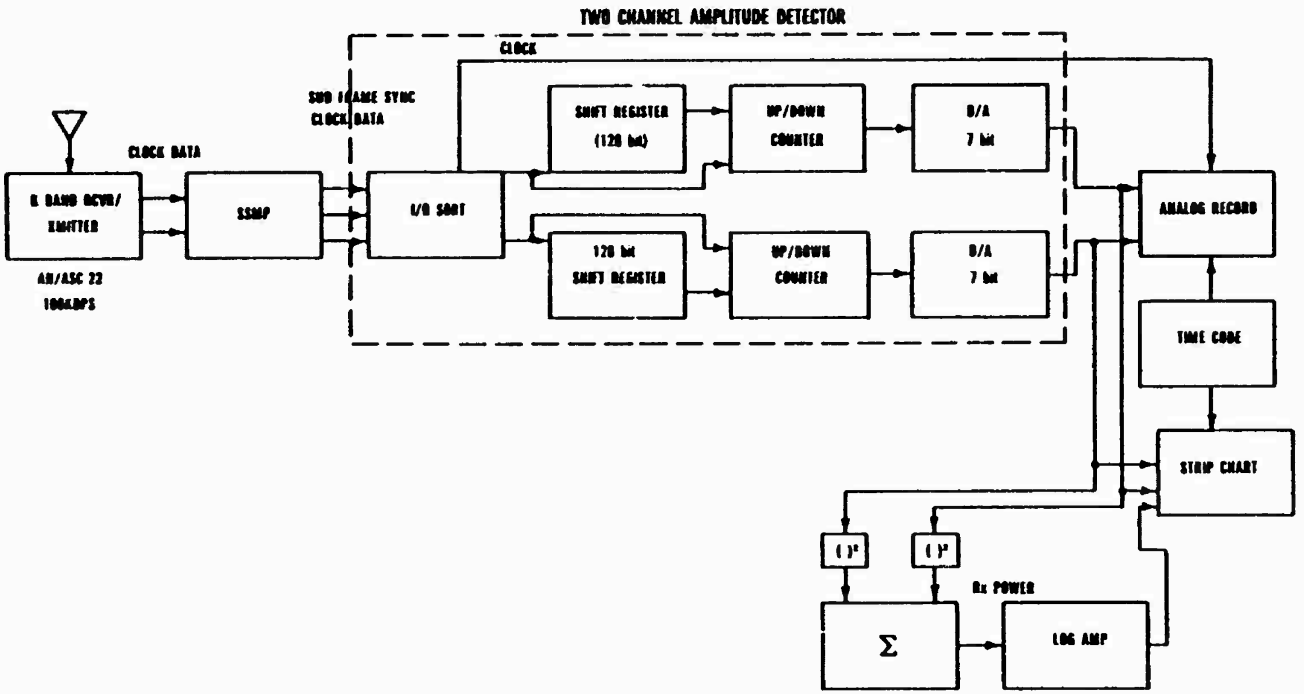

FIGURE 16 STRESS Test Configuration 3 Rooftop Equipment

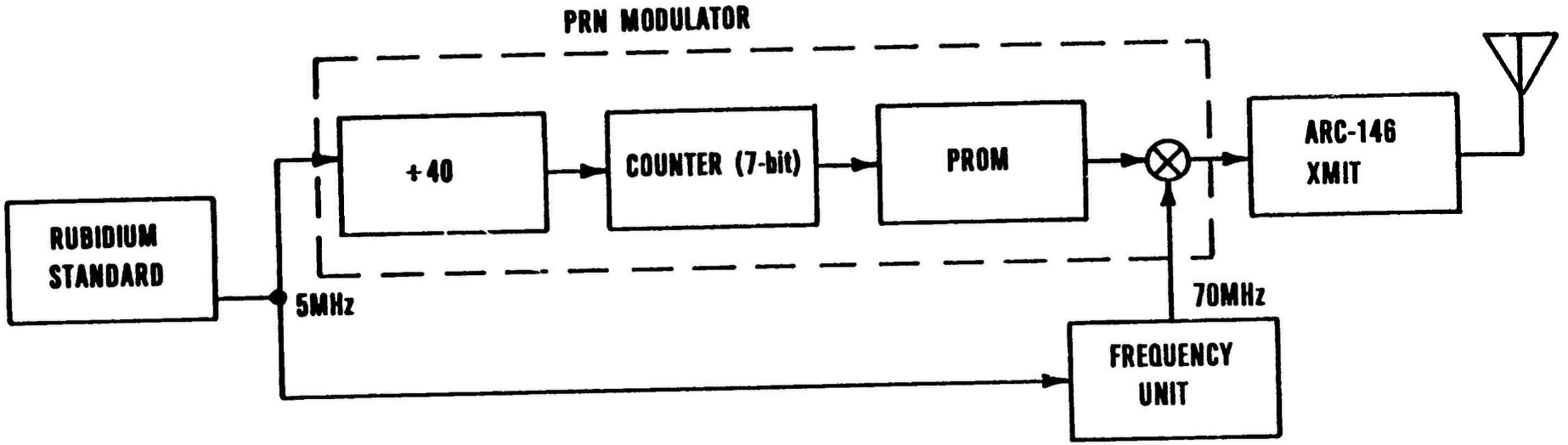

FIGURE 17 Block Diagram of Aircraft Multipath, PRN, Equipment

and each reflected signal. The block diagram of the rooftop PRN equipment is shown in Figure 18. By eliminating occasional bits in the repetitive sequence the rooftop correlated the locally generated PRN sequence with first the direct path PRN sequence and at a later time with the reflected PRN sequence coming from the aircraft through the satellite.

The frequency plan used during STRESS is shown in Table 2. Shown is the nominal frequency of the uplink tone used in each of the five releases and the nominal frequency of the downlink tone used simultaneously with the uplink tone during ESTHER. These tones were doppler corrected using AN/ASC-22 20 MHz plus doppler estimates derived from received K band signals from the LES 9 dish at 36.84 GHz or from the LES 8 dish at 38.04 GHz. The doppler correction ideally would divide the K band doppler by the ratio of the K band frequency to the UHF frequency to produce an estimate of UHF doppler. In the actual hardware realization the divide-by ratio was limited to integral values. The ratio chosen for each release is shown with the parenthetical entries indicating offsets from ideal. The suboptimal choices for the BETTY and CAROLYN uplink frequency allows a small component of the aircraft-to-satellite doppler to enter into the phase data. While changes in aircraft heading are obvious in the data with a 400 Hz change in uncorrected doppler producing a 0.7 Hz change in the doppler corrected signal, the phase data corruption produced by bumpiness of flight on straight and level data runs is insignificant.

Shown in Table 2 are the synthesizer settings used to adjust the uplink and downlink frequencies. The 1 Hz settability of the HP 8660 frequency synthesizers used is reflected in the table with parenthetical entries indicating the fractional offset required for a zero frequency demodulator offset. Ideally the resulting measurements should reflect these offsets, but the long term drift of the aircraft rubidium standards and of the satellite

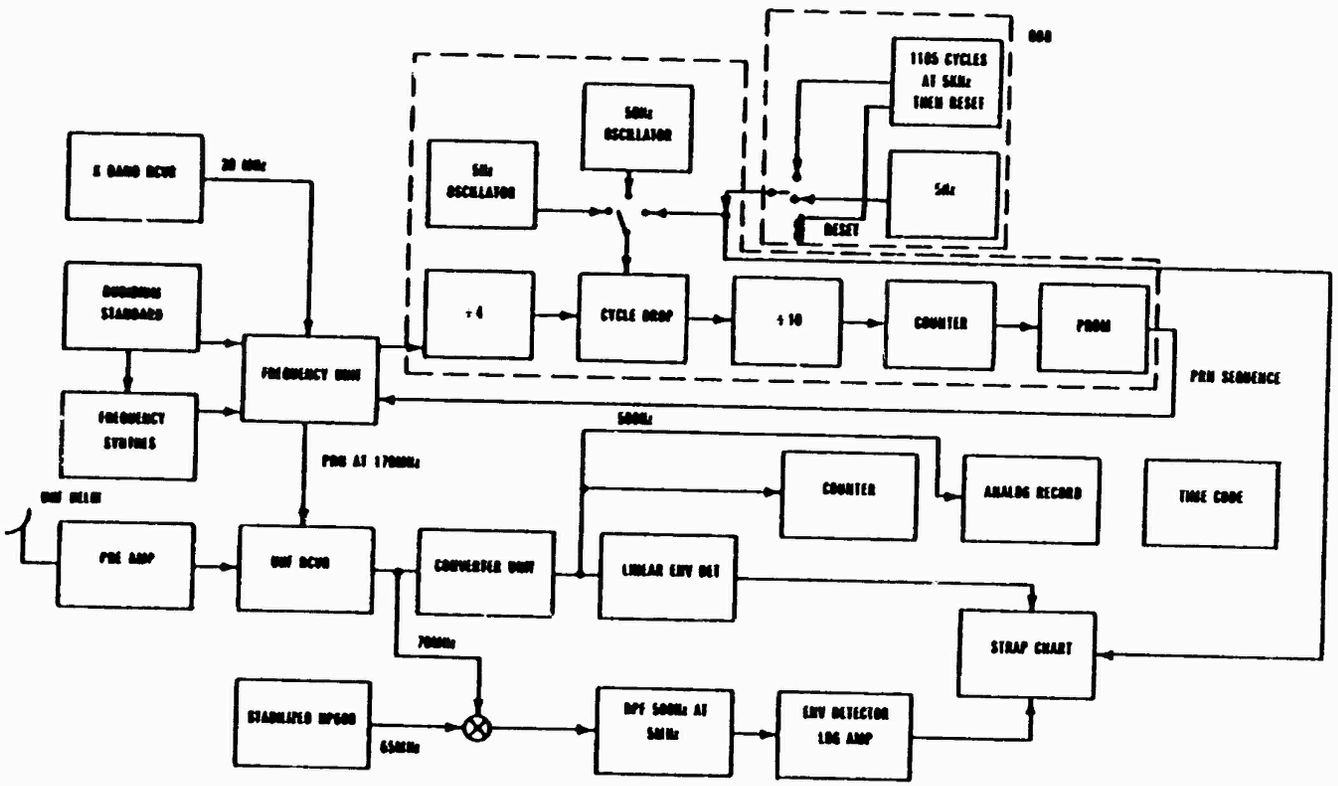

FIGURE 18 Block Diagram of Rooftop Multipath, PRN, Equipment

Table 2: Uplink Tone Frequency Plan

Event	Frequency Hz	K-Band Reference Source	÷ Setting	HP 8660 Setting (Hz)	Satellite Uplink Synth Octal
BETTY & CAROLYN	341 666 602	LES 9 Dish	108 (-.18)	61 851 787 (-.25)	0674525
DIANNE	341 111 132	LES 9 Dish	108 (-.000007)	61 296 318 (-.00)	0667071
ESTHER & FERN	339 644 727	LES 8 Dish	112 (-.0006)	59 823 297 (-.01)	0650345
DOWNLINK TONE FREQUENCY PLAN USED IN ESTHER					
ESTHER	250 326 392	LES 8 Dish	152 (-.04)	40 184 313 (-.35)	4650344 (DOWNLINK SYNTH OCTAL)

clock apparently caused the observed demodulator offsets to deviate from ideal.

Also shown in the table are the satellite telemetry display values in octal for the downlink and uplink synthesizers. It should be noted that the choice of the UHF frequency synthesizer settings in the satellite for the uplink and for the downlink are not independent, and that the ESTHER downlink frequency shown corresponds to the uplink frequency used simultaneously in ESTHER.

V. DESCRIPTION OF STRESS EVENTS

The dates and launch times of the five STRESS events are listed in Table 1.

The first barium release on 26 February 1977, BETTY, occurred at 2352:29Z at an altitude of 179 kilometers. Radar returns from the ion cloud were received as late as 0258Z. However, fading was observed only as late as 0158Z, indicating either a problem with the radar positioning of the aircraft or a dissipation of the barium cloud. Radar track of the ion cloud did not commence until 0047Z, although fading was observed much earlier as the aircraft maneuvered in the vicinity of the expected projection location. BETTY moved in a general eastward or southeastward direction, as did all the STRESS ion clouds, at a moderate velocity (40 meters/second). The BETTY ion cloud was unusual in that it was exceedingly narrow as viewed up the field lines during times when it was optically visible. Whether this narrowness was due to improper venting of the barium vapor at release is not known. In most other aspects BETTY was a normal cloud. Strong fading was observed on at least 5 of the 29 total passes.

The second barium release, CAROLYN, occurred on 2 March 1977 with a release time of 2354:10Z at an altitude of 191 kilometers. Radar returns were received from the cloud until 0202Z. However, radar positioning as indicated by fading at the aircraft was valid only until 0144Z. CAROLYN moved at a relatively high velocity (60 m/s). In most other respects it was a nominal cloud. Good up-the-field line photographs were obtained from CAROLYN at times later than those taken up to that date in previous barium release programs. A total of 21 data passes were made by the aircraft with the strong Rayleigh-like fading observed on 6 of them. Some fading was obvious on a total of 16 passes.

The third barium release of STRESS, DIANNE, occurred on 8 March 1977 (7 March local time) at 0001:10Z at an altitude of 186 kilometers. Radar track was maintained until 0149Z with fading observed until 0126Z. Of the total 18 data passes made by the aircraft some fading was observed on 15 with strong fading, either early-time-like or Rayleigh-like, being observed on 11 passes. DIANNE was unusual in that the ion cloud developed a right angle bend as viewed up the field lines. The cause of this bend is currently believed by plasma phenomenologists to be high altitude wind shear because of a deformation of the neutral barium cloud that was also observed. Some of the strongest fading to be observed during the series was seen in DIANNE, which may be atrributed to its unusual geometry.

The fourth barium release, ESTHER, occurred on 13 March 1977 with a release time of 2301:08Z and an altitude of 189 kilometers. This release occurred earlier than the preceding three by more than 50 minutes. The cloud drifted at a slower rate than the previous releases, 36 m/s. Optical coverage extended from 74 to 109 minutes after release, late into the cloud development, and may reveal information about late-time striation dissipation mechanisms. Radar returns for cloud tracking were received as late as 0237Z, three hours and thirty minutes after release. The aircraft by maneuvering in the proper vicinity observed fading until 0244Z. Of the total 45 data passes made by the aircraft fading was observed on 42 with early-time, or Rayleigh-like, fading on 29 passes. An unexpected patch of fading was fortuitously observed at release because of the aircraft's proximity to the initial release point projection. While most of the ionization in the ion cloud is produced by solar ultraviolet nominally 30 seconds after release, some of the barium is ionized thermally by the heat of the thermite explosion that initiates

release. Structure in this thermally produced ionization was observed to cause fading and phase effects as early as 10 seconds after release, Figures 19 and 20.

The fifth and last release, FERN, occurred on 14 March 1977 with a release time of 2246:09Z at an altitude of 186 kilometers. Radar returns from the cloud were received as late as 0109Z. Fading was observed at the aircraft until about the same time. Of a total of 33 passes made by the aircraft fading was observed on 29 with Rayleigh-like, or early-time, fading observed on 22 passes. The optical appearance of FERN (release plus 89 to release plus 124 minutes) is enigmatic. The ion cloud resembles none of the barium ion clouds observed in the past. The drift of FERN was the slowest of the releases (approximately 20 meters per second). Several of the late-time passes produced fading usually typical of early-time fading. The interpretation of FERN phenomenological data may be complicated by sporadic E at the end of the test.

The aircraft trajectories with fading occurrences indicated and the radar cloud track projection positions are shown in Figures 21 to 36 for each of the five barium releases.

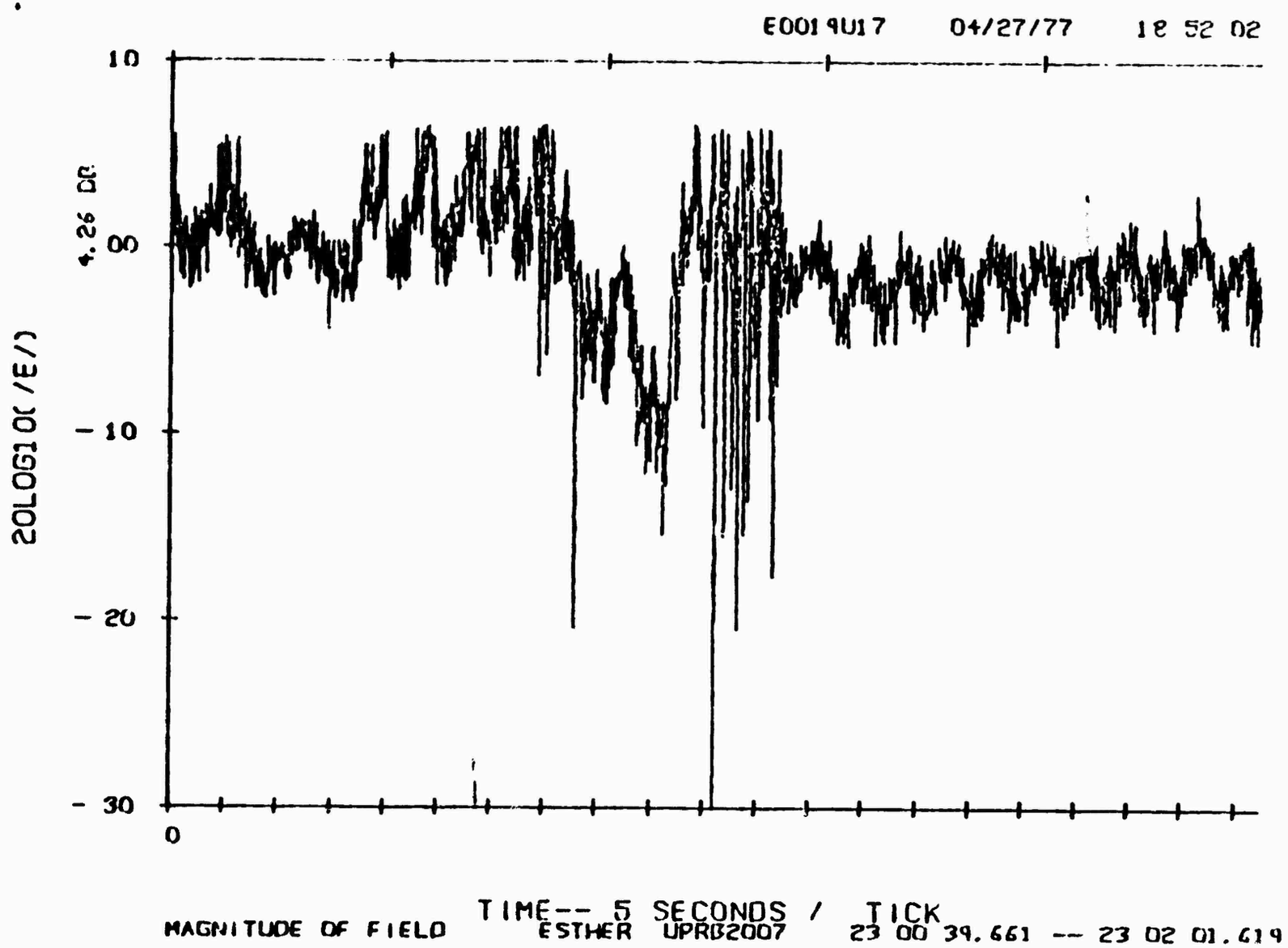

FIGURE 19 Fading of Uplink Tone Due to Release Thermal Ionization

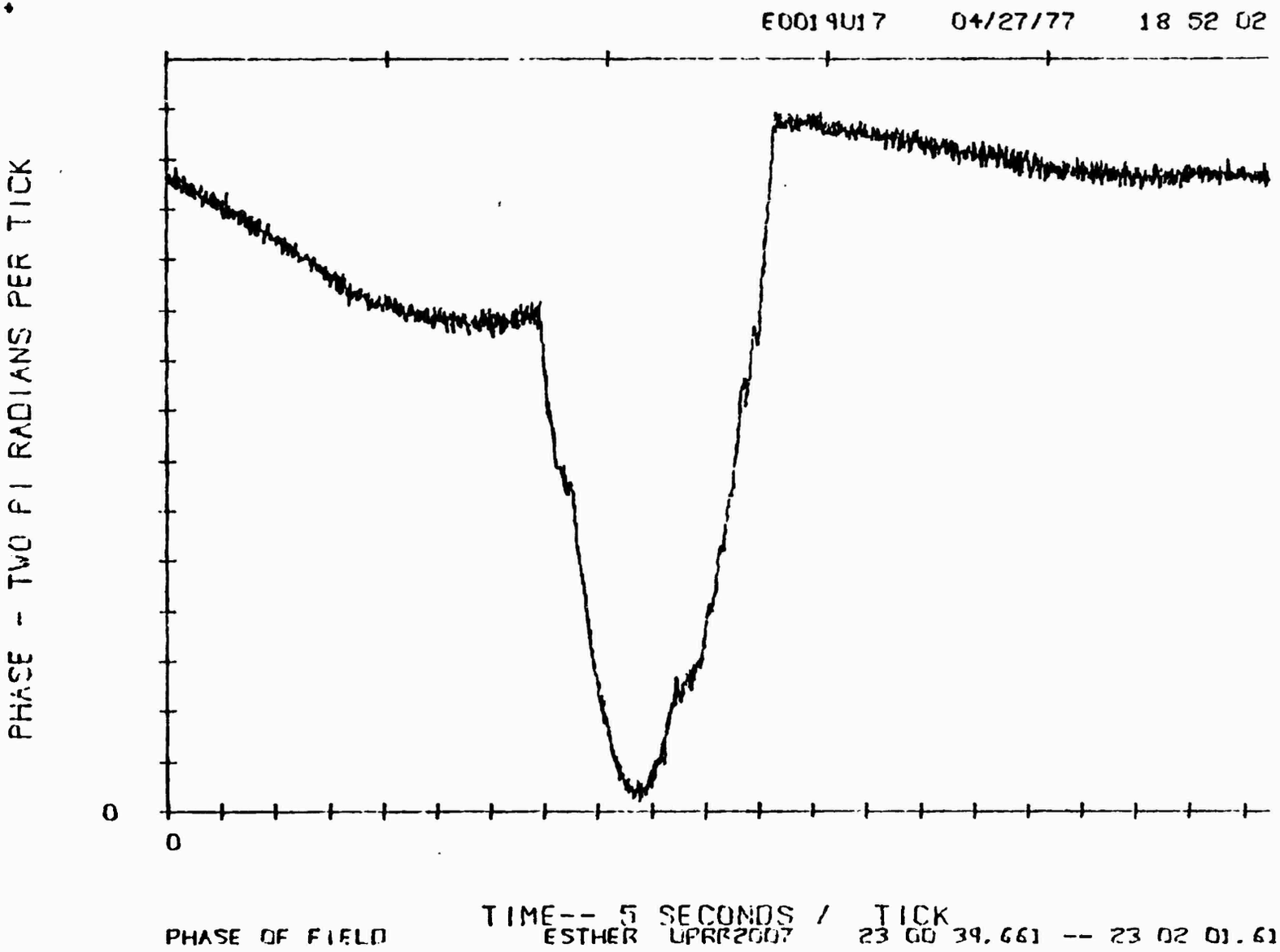

FIGURE 20 Phase Shift of Uplink Tone Due to Release Thermal Ionization

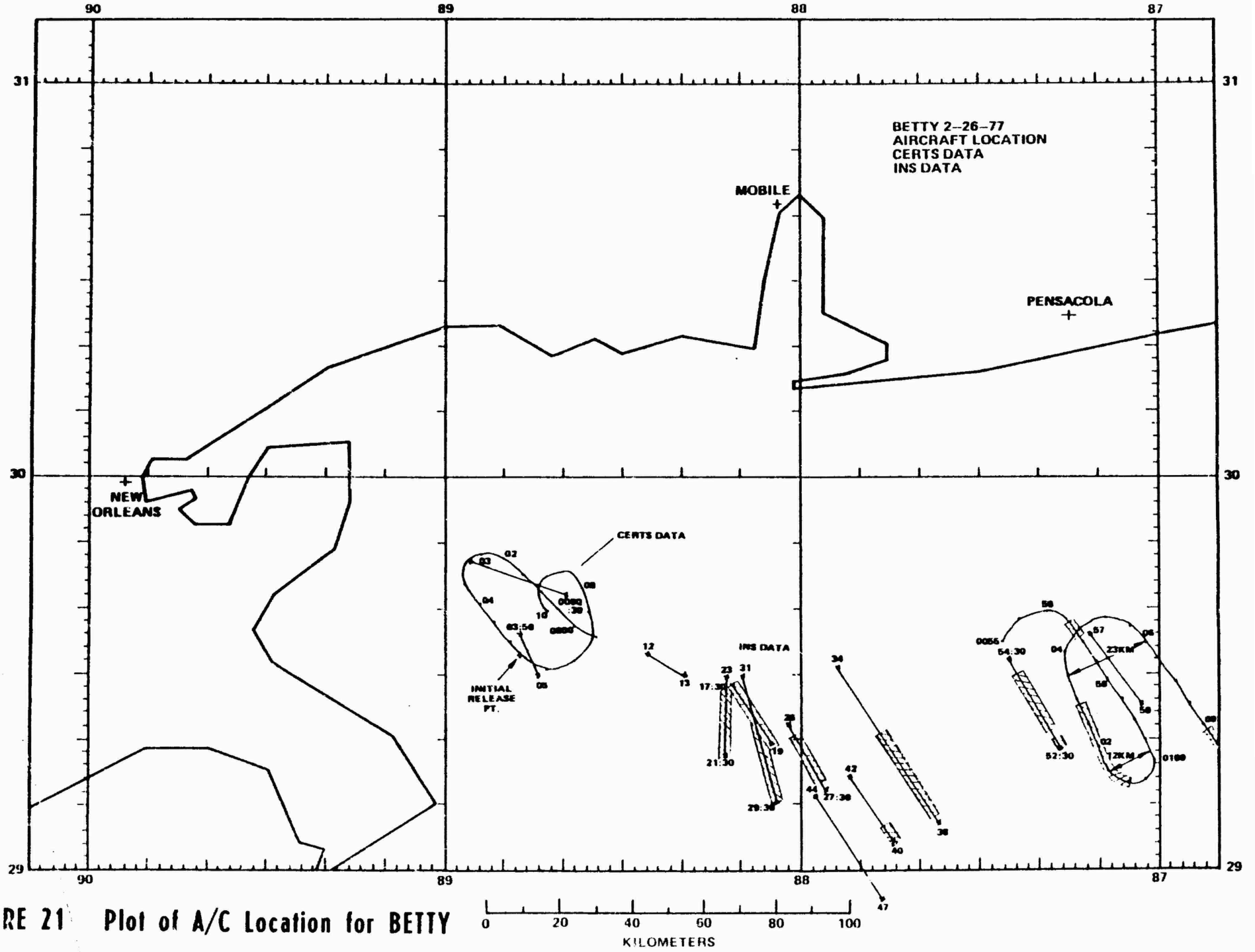

FIGURE 21 Plot of A/C Location for BETTY

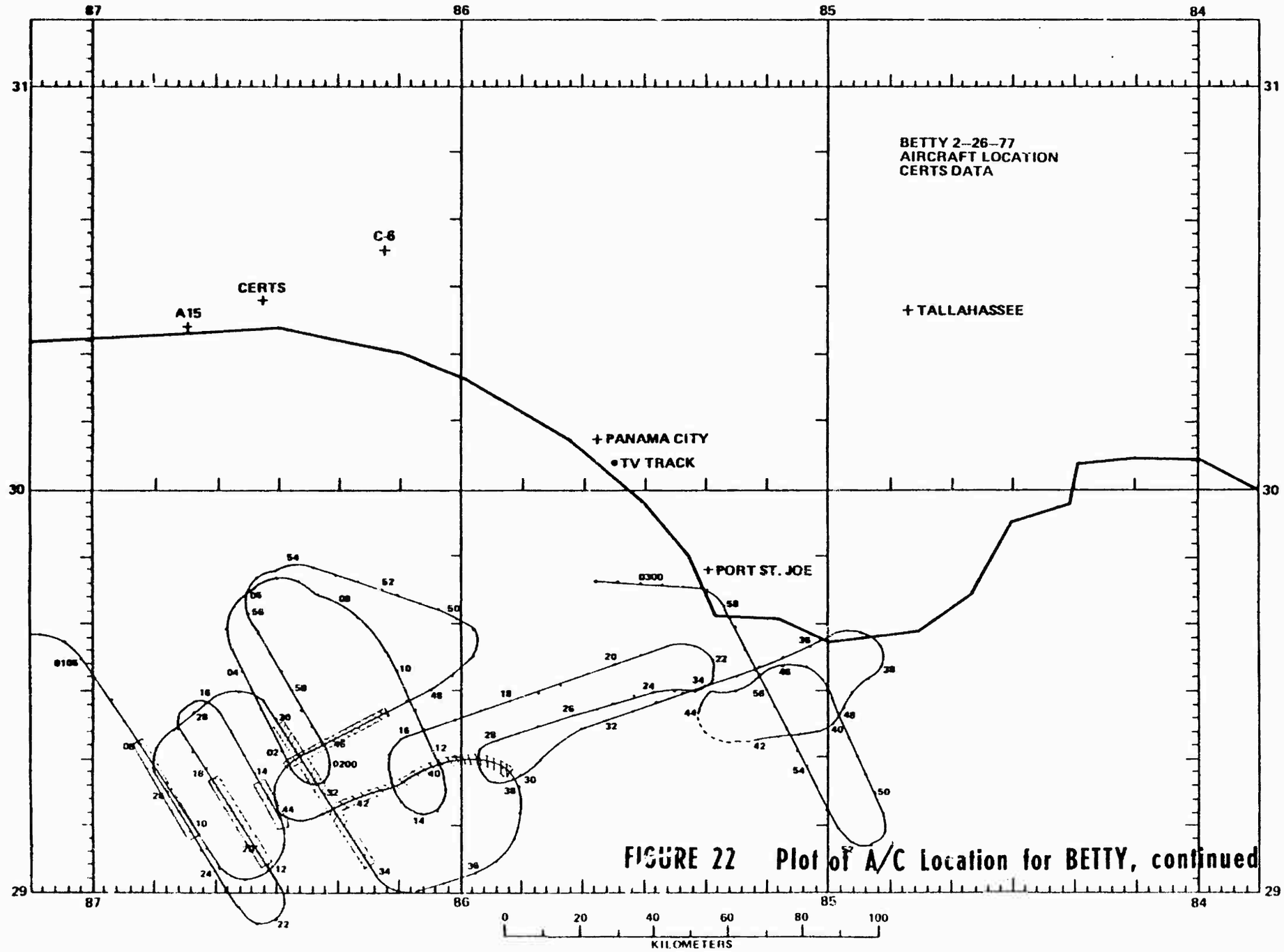

FIGURE 22 Plot of A/C Location for BETTY, continued

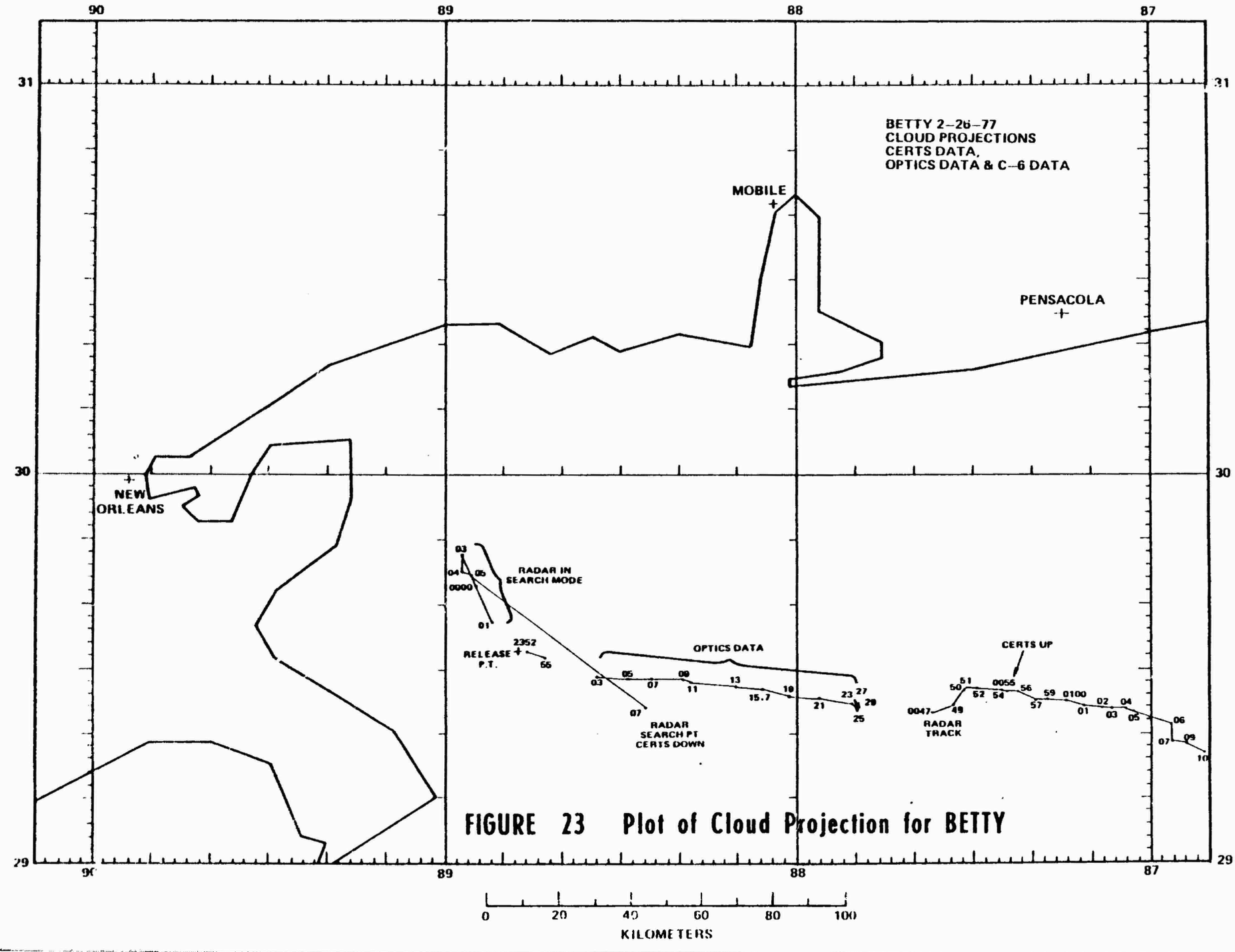

FIGURE 23 Plot of Cloud Projection for BETTY

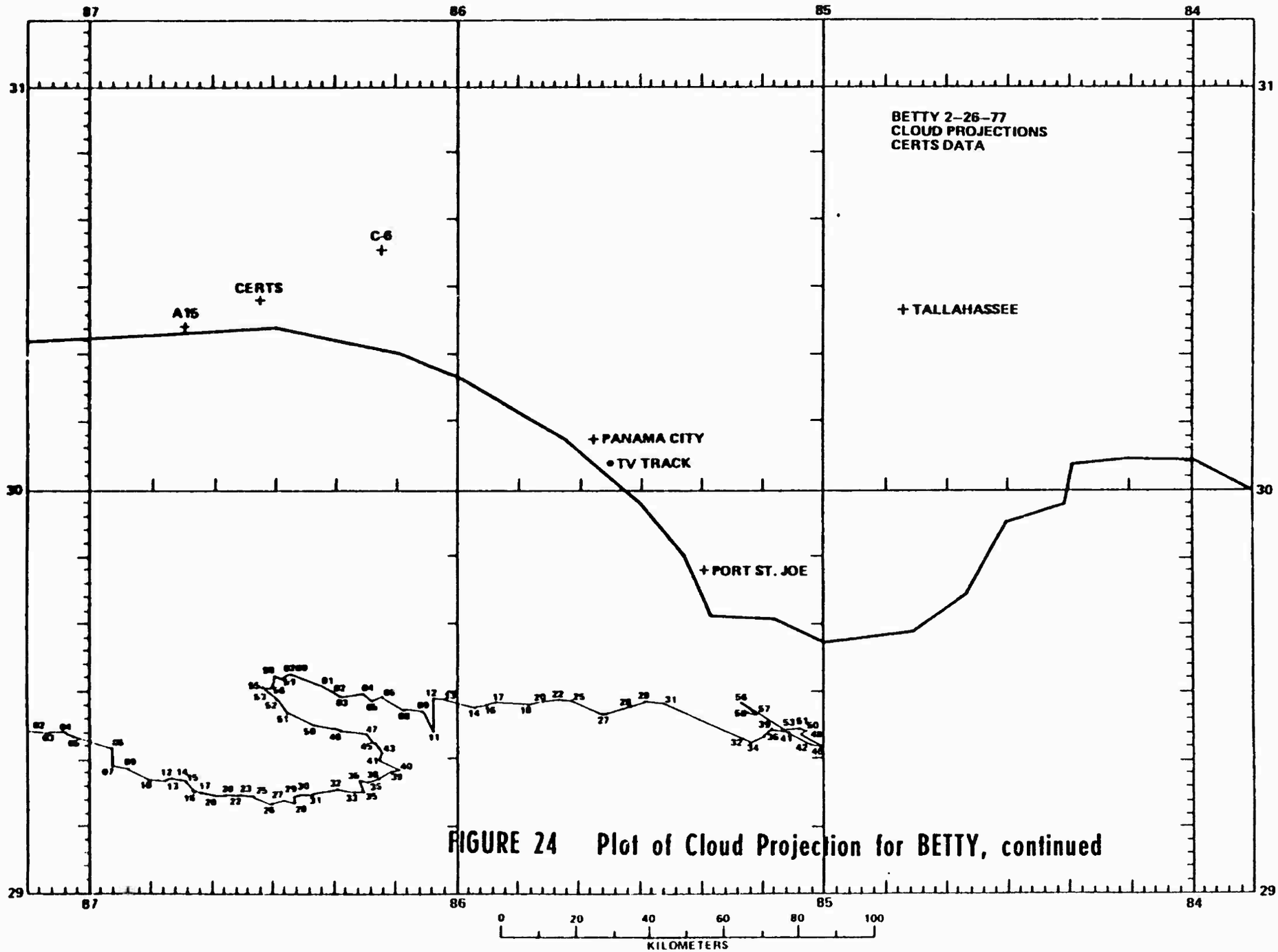

FIGURE 24 Plot of Cloud Projection for BETTY, continued

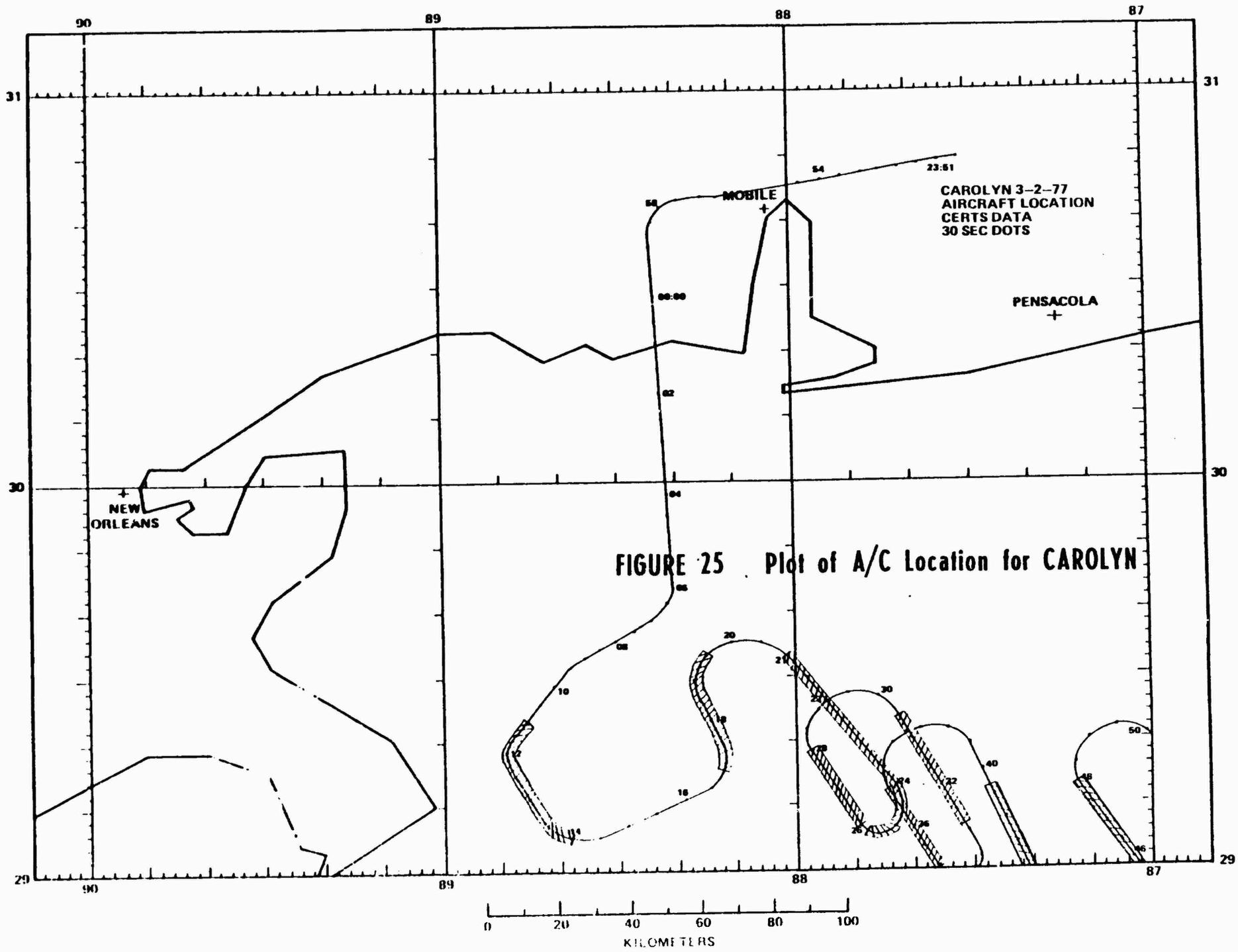

FIGURE 25 Plot of A/C Location for CAROLYN

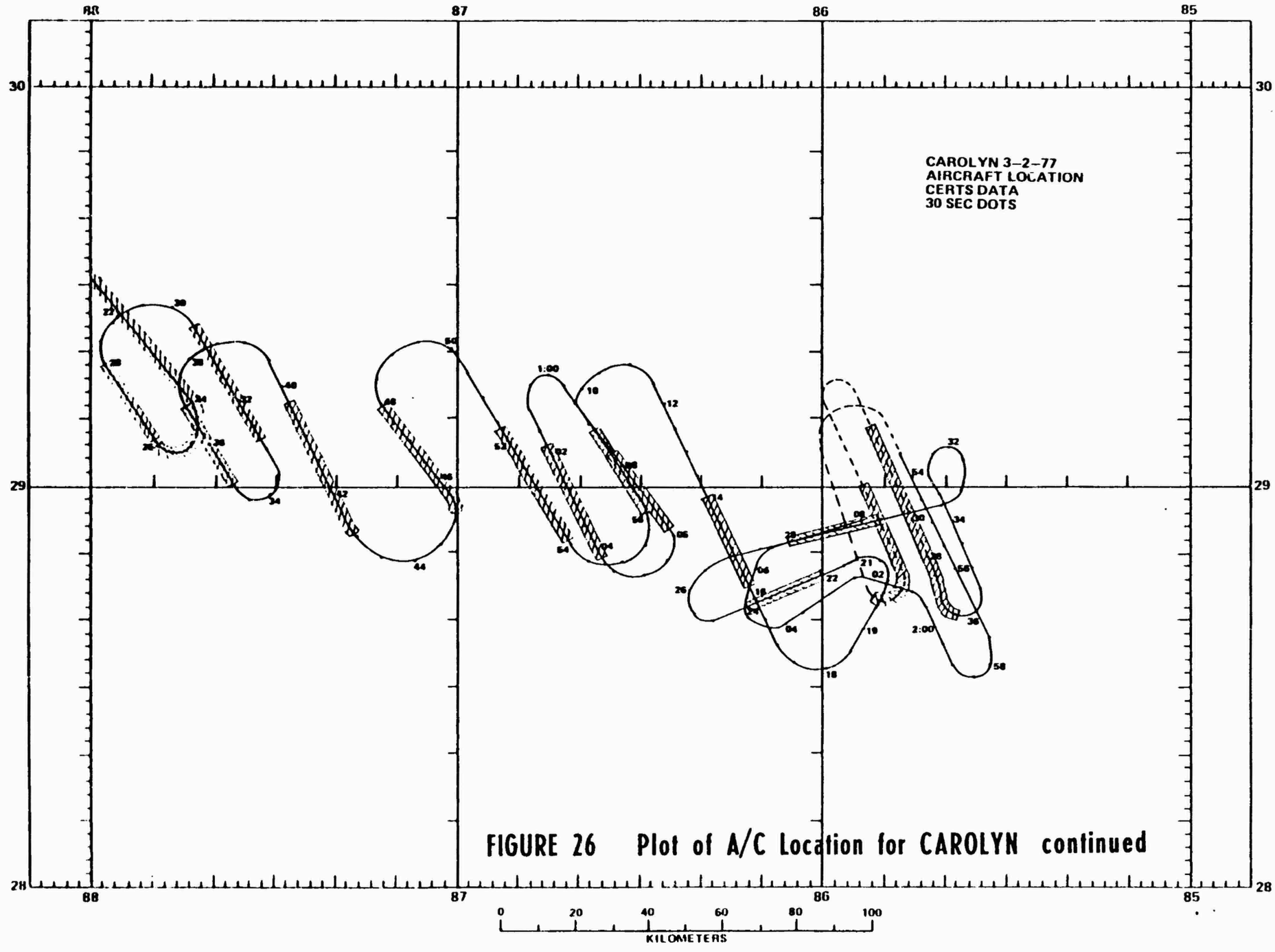

FIGURE 26 Plot of A/C Location for CAROLYN continued

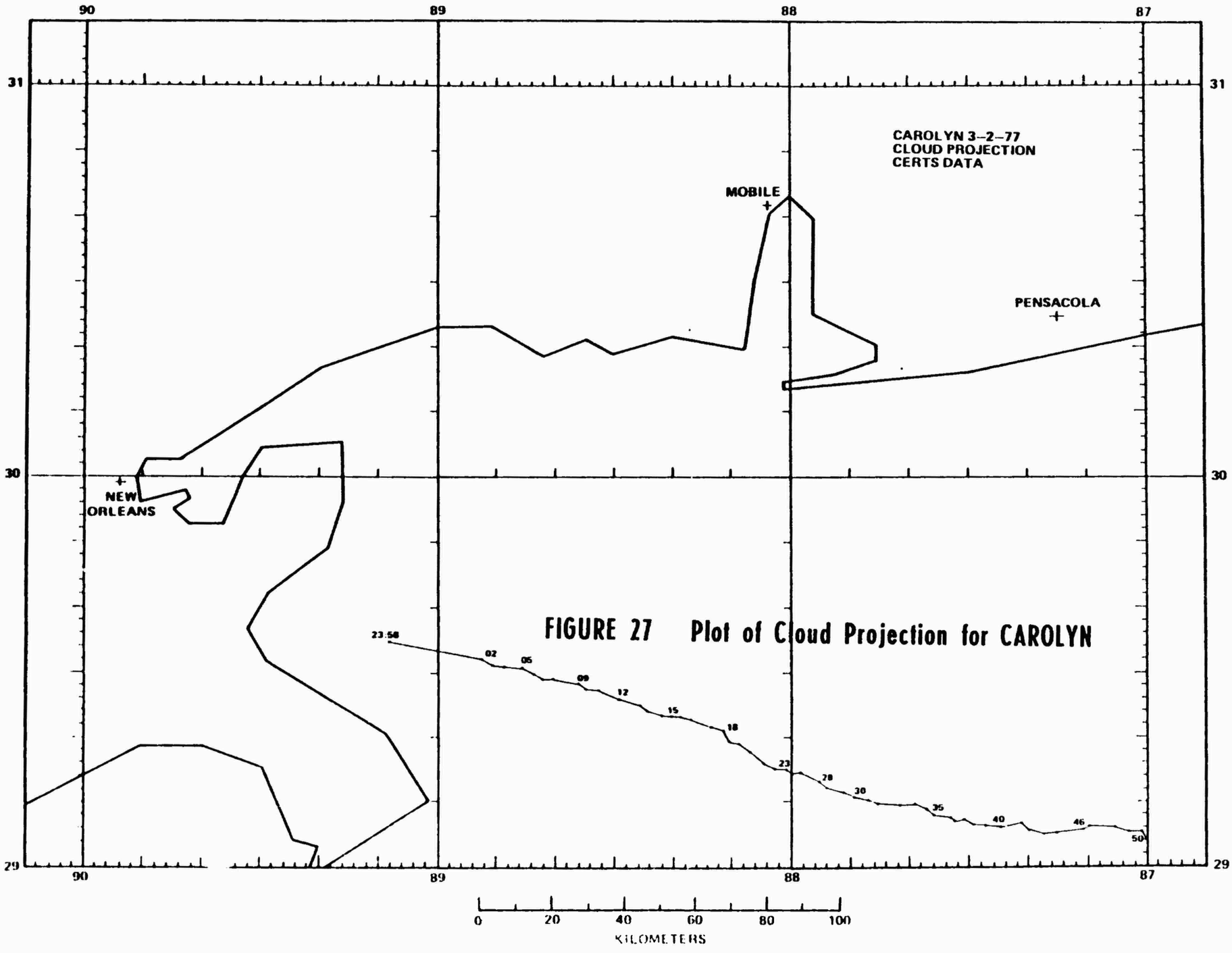

FIGURE 27 Plot of Cloud Projection for CAROLYN

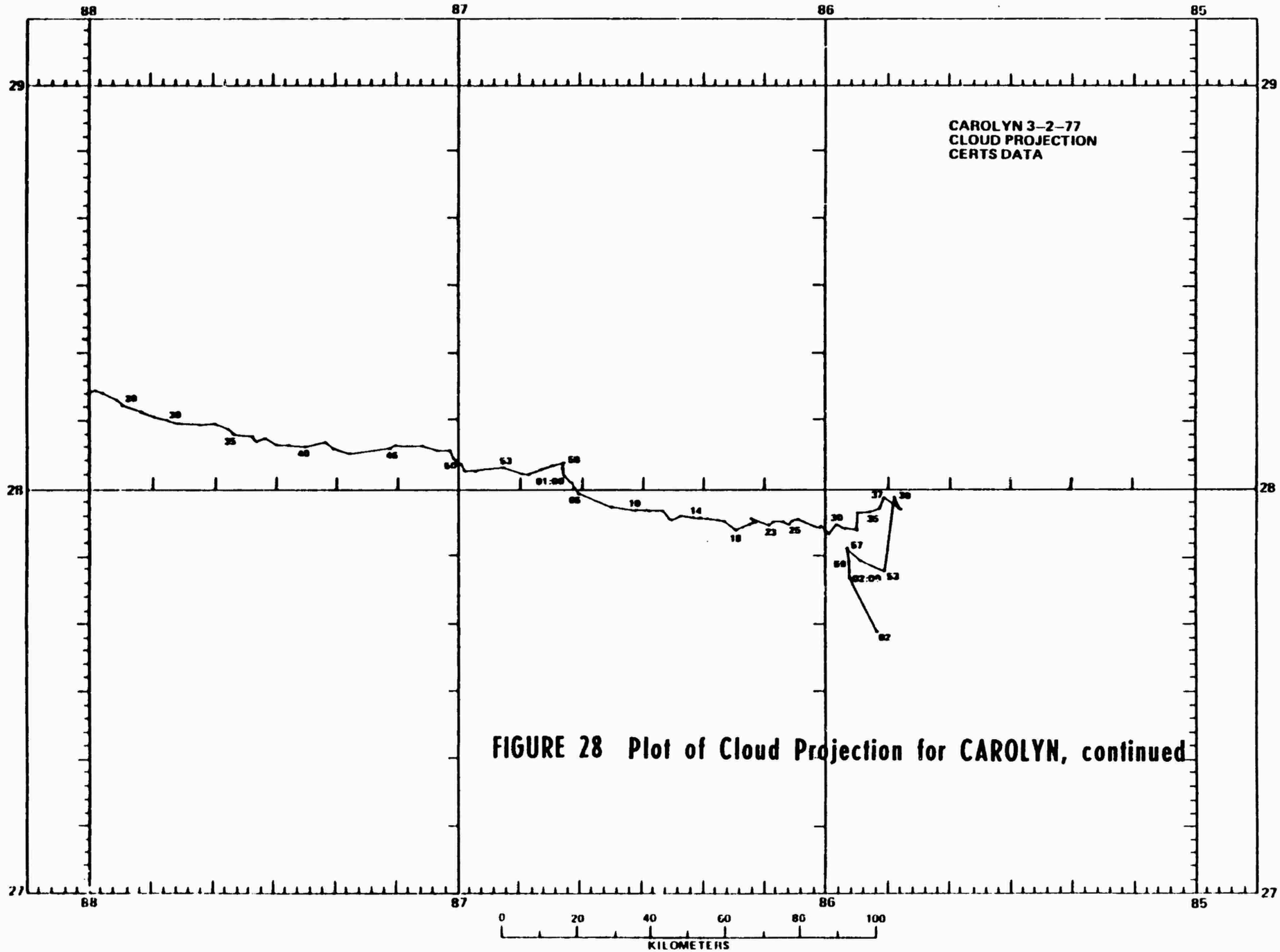

FIGURE 28 Plot of Cloud Projection for CAROLYN, continued

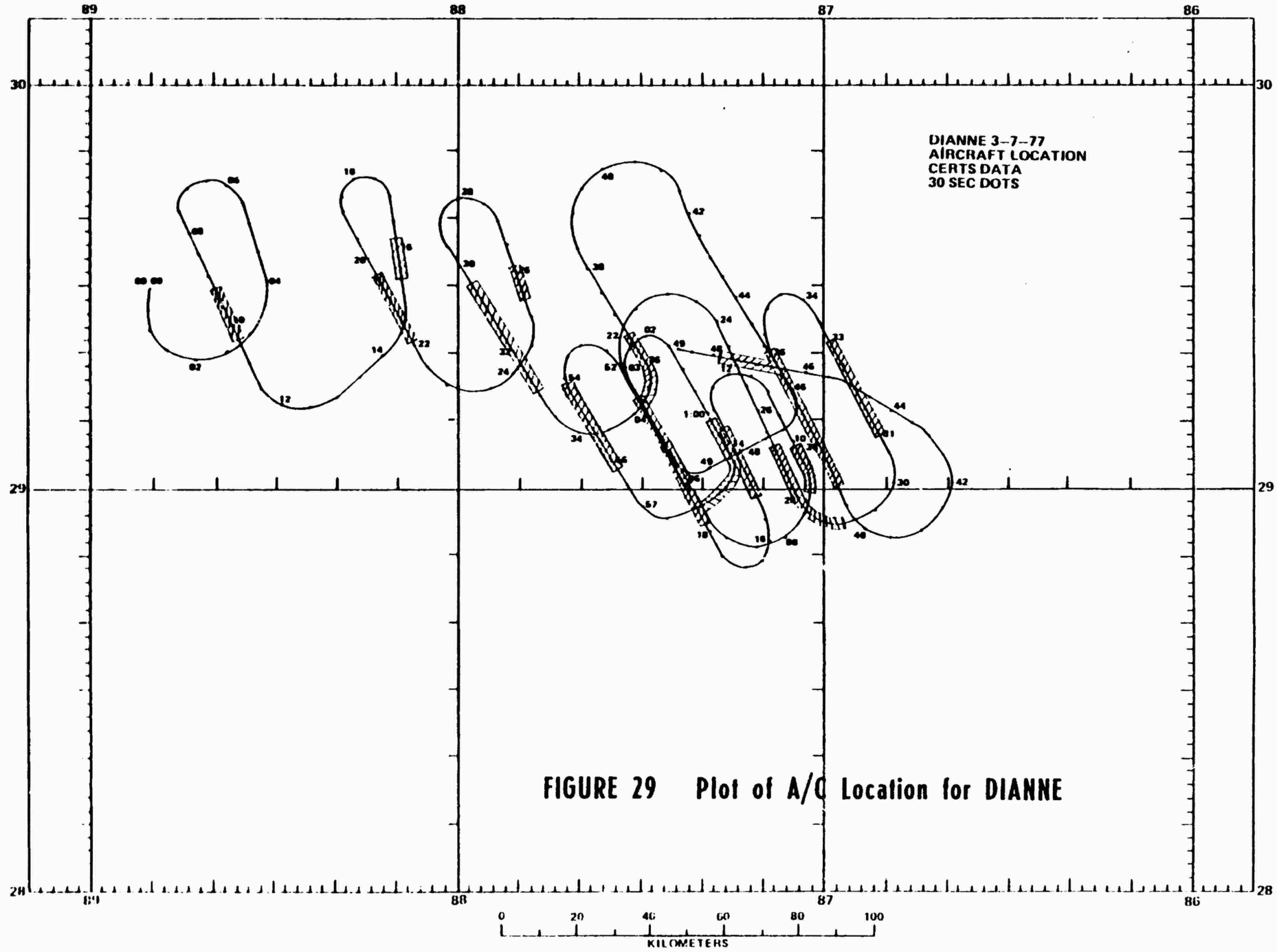

FIGURE 29 Plot of A/C Location for DIANNE

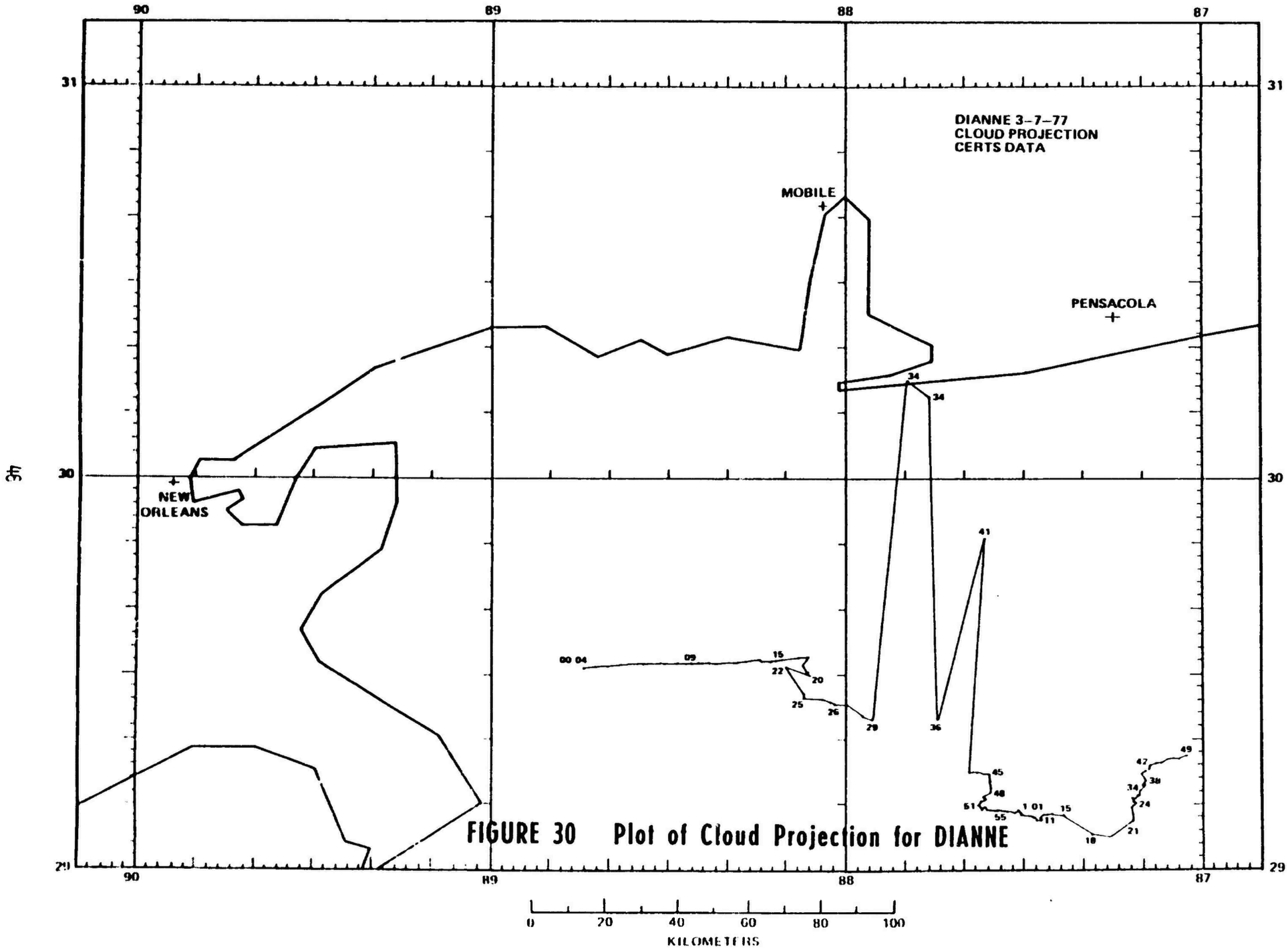

FIGURE 30 Plot of Cloud Projection for DIANNE

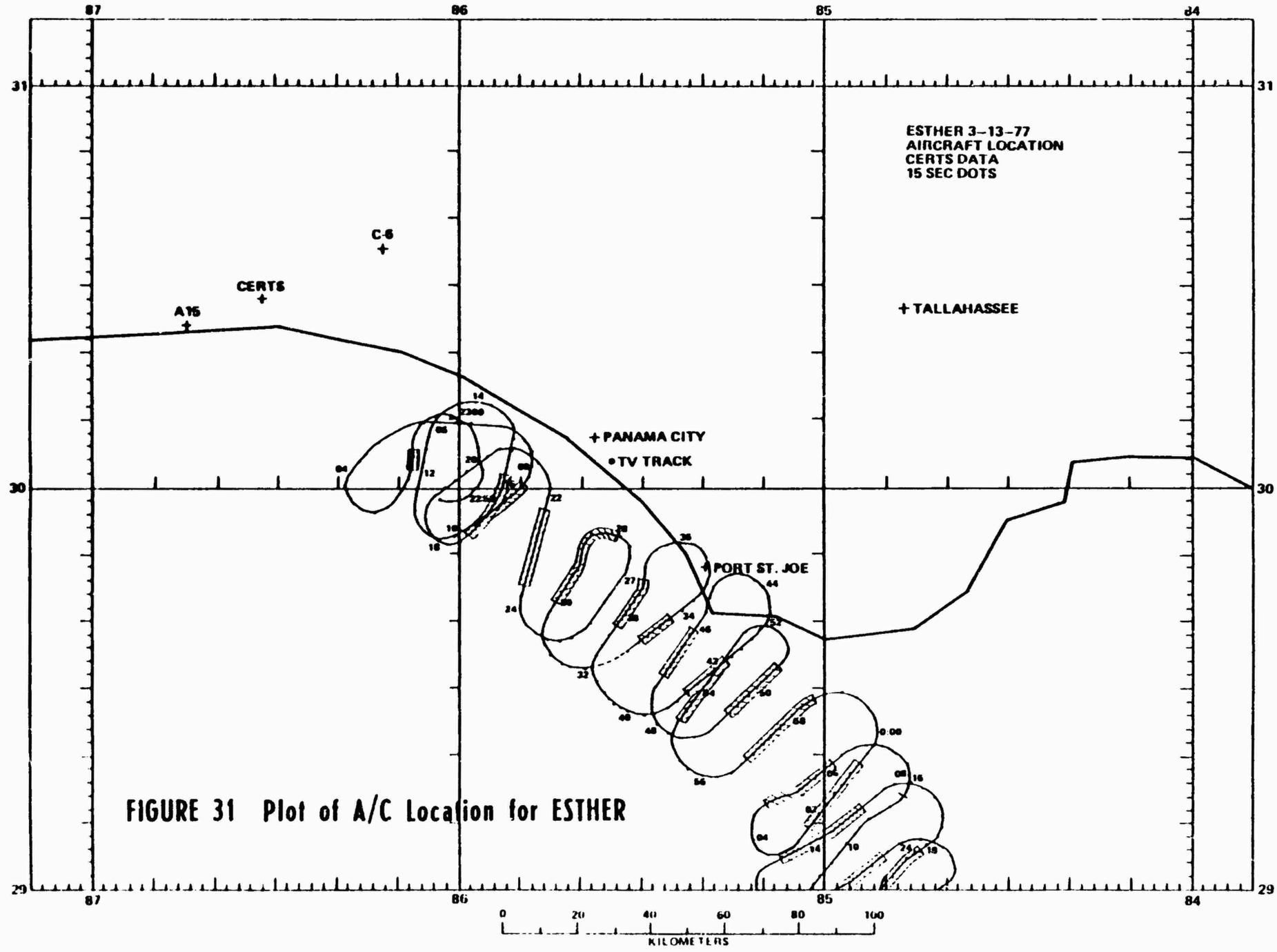

FIGURE 31 Plot of A/C Location for ESTHER

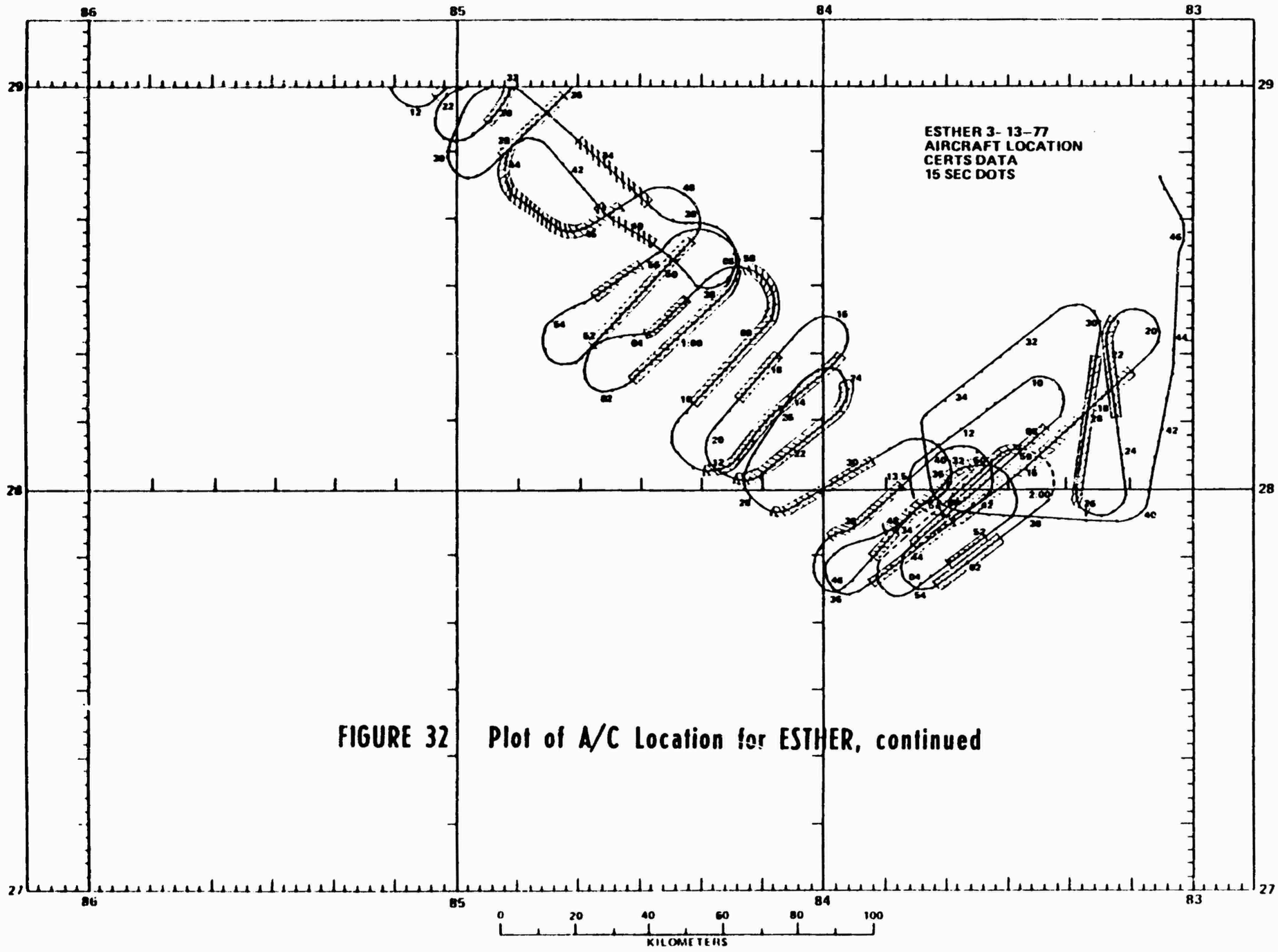

FIGURE 32 Plot of A/C Location for ESTHER, continued

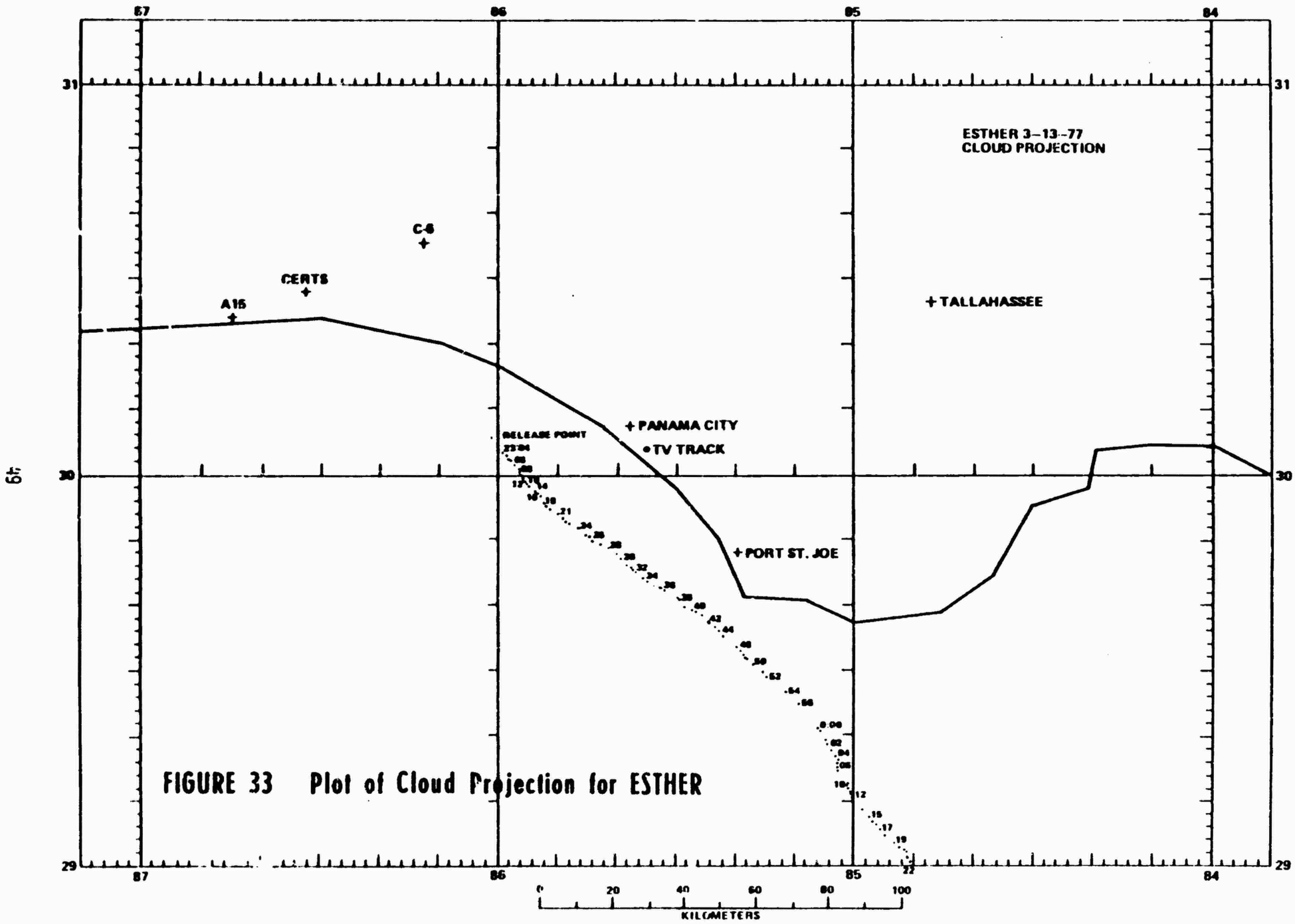

FIGURE 33 Plot of Cloud Projection for ESTHER

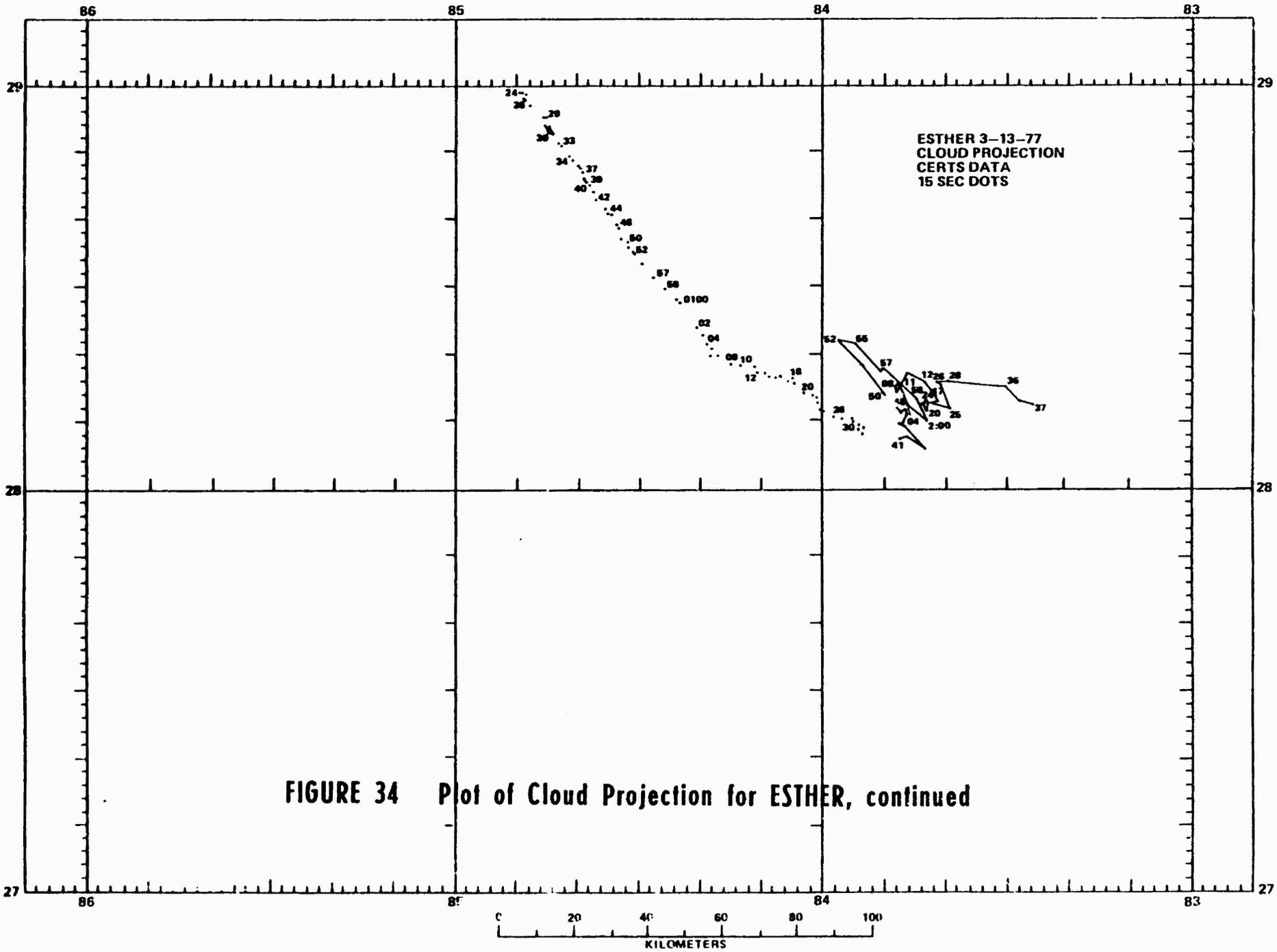

FIGURE 34 Plot of Cloud Projection for ESTHER, continued

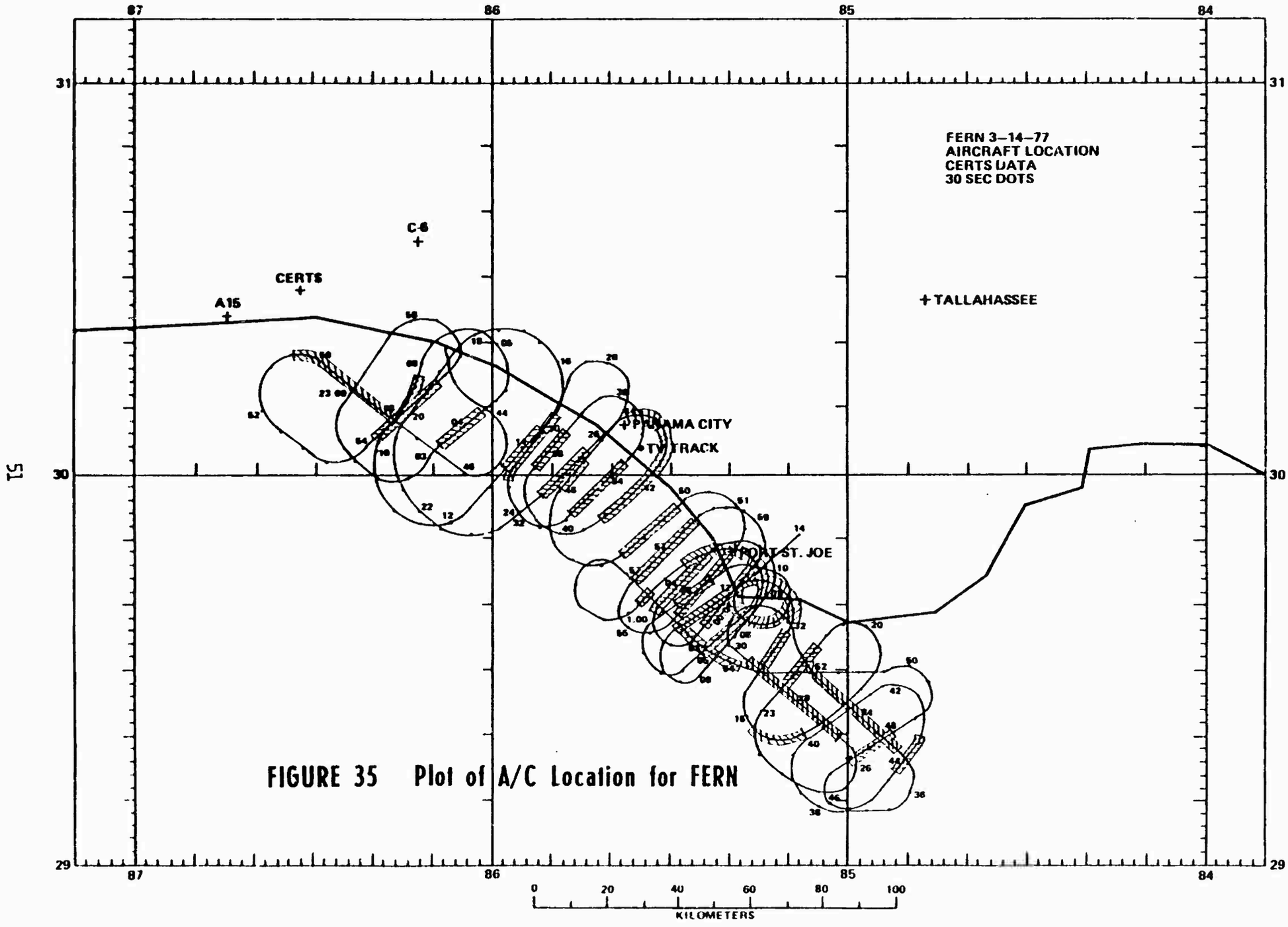

FIGURE 35 Plot of A/C Location for FERN

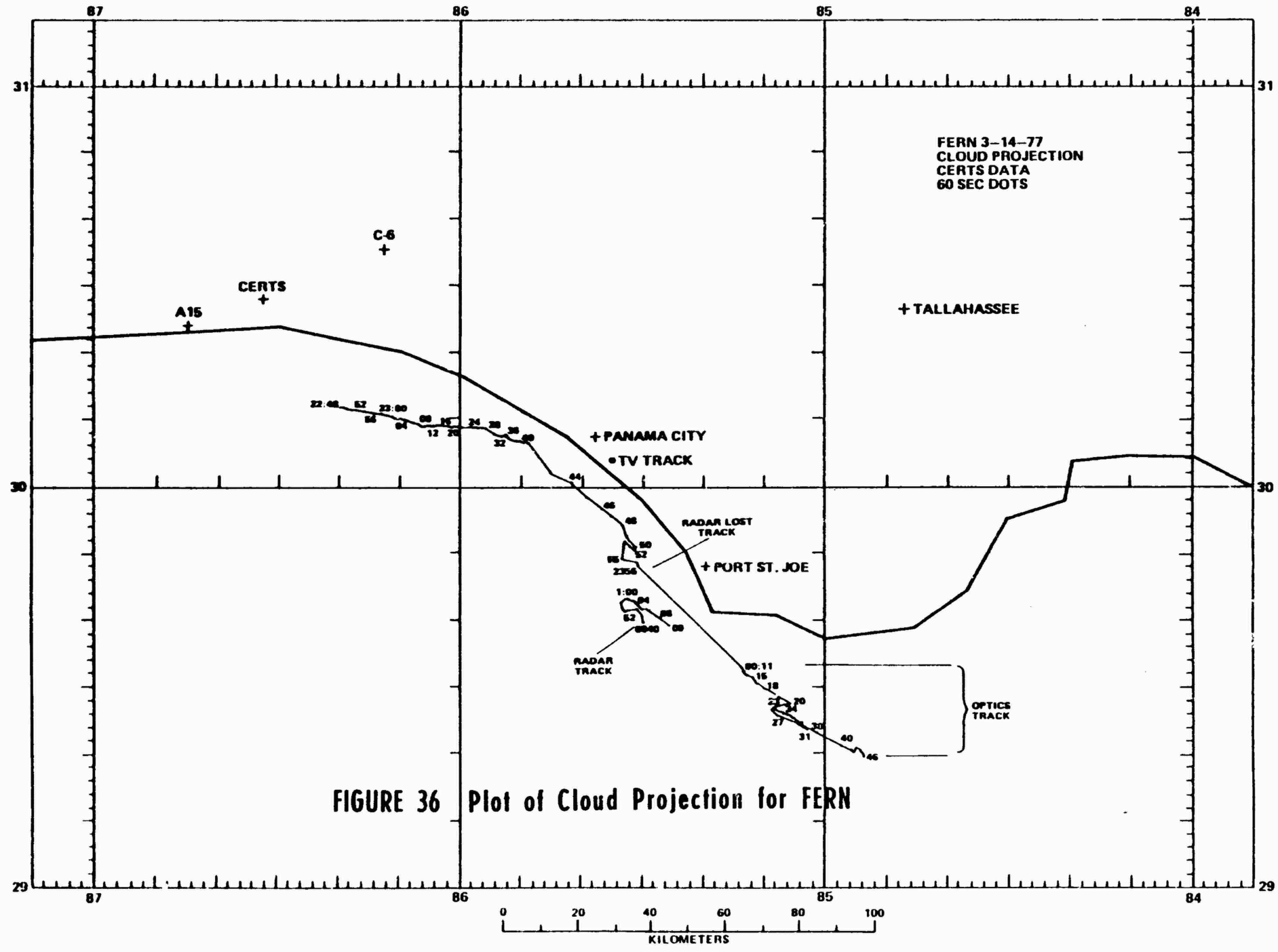

FIGURE 36 Plot of Cloud Projection for FERN

VI. TEST RESULTS

A summary of the results for each pass of each test is contained in Tables 3 through 7. The fading is characterized according to early-time like, Rayleigh-like, or Rician-like, and parallel pass fading. Some characteristic examples are taken from aircraft strip chart data on downlink fading from FERN and from semi-processed rooftop uplink phase and amplitude fading from FERN and ESTHER. System effects are also discussed.

A. Early-Time Fading: The downlink received signal strength for Pass 1 FERN, Figure 37, shows a classical diffraction pattern for a single, spherical or cylindrical cloud. The UHF signal level had a sharp rise of approximately 10 db as the aircraft reached the edge of the cloud shadow and then fell rapidly with a very broad fade lasting 80 seconds. As the aircraft flew out from under the shadow, the characteristic signal enhancement occurred and the signal returned to the unfaded signal level. A similar result was observed during the next pass, Pass 2 FERN, with a ringing, or multipath, occurring at the end of the pass, Figure 38. Pass 4 also shows the characteristic decrease of signal with a broad multipath-like ringing occurring at the end of the pass, Figure 39. The ringing is caused by interference between the rays passing outside of or near the edge of the ion cloud with rays diffracted outward from the portions of the cloud with steepest gradients of ray path integrated electron contents. The ion cloud evolution of its "hard edge" is reflected in the results of FERN, Passes 2 and 4, by the fact that this multipath-like effect occurs predominantly on one side of the cloud, presumably, the edge where the gradient steepening is occurring. Similar results are seen in Figures 40 through 43, showing uplink amplitude and phase for Pass 1 of FERN and Pass 2 of ESTHER. These plots represent unfiltered data and the hashy appearance is due to a combination of thermal and digitization noise. The

TABLE 3: TEST RESULTS FOR 26 FEBRUARY (BETTY)

PASS	COMMENTS	PASS start	PASS stop	POP-TOP FADING start	POP-TOP FADING stop	DEPTH % Avg	DEPTH % Max	DURATION sec Avg	DURATION sec Max	Comments	AIRCRAFT FADING start	AIRCRAFT FADING stop	DEPTH % Avg	DEPTH % Max	DURATION sec Avg	DURATION sec Max	COMMENT	TTY MESS SENT	SINGLE ATTEN	SINGLE MODEM ERROR FREE	SINGLE MODEM WITH ERROR	SINGLE MODEM CHAR ERROR	DUAL DIF MODEM ERROR FREE	DUAL DIF MODEM WITH ERROR	DUAL DIF MODEM CHAR ERROR	AIRCRAFT DIRECTION	PASS
1		000030	0307	000000	-	-	-	-	-	No fade	000100	-					No fading observed	36	0	36	0	0					1
2		0320	0510	0330	-	-	-	-	-	No fade	0400	-					No fading observed	22	0	22	0	0					2
3		1152	1241	1100	-	-	-	-	-	No fade	1100	-					No fading observed	11	0	11	0	0					3
4		173	1903	1718	1850	15	30	2	4	Rayleigh slow fade	1800	-					No fading observed	20	0	20	0	0					4
5		2130	2240	2100	2210	10	30	2	3	Rician	2200	-					No fading observed	13	0	13	0	0					5
6		255	2726	2510	2715	10	30	1	2	Rayleigh slow fade	2600						No fading observed	21	0	21	0	0					6
7		293	3055	2918	3020	10	12	2	4	Rician	3000	-					No fading observed	18	0	18	0	0					7
8		3400	3758	3548	3750	10	80	1	2	Rayleigh slow fade	3600						No fading observed	53	0	53	0	0					8
9		4010	4142	4000	4030	3	6	1	2	Rician	4100						No fading observed	24	0	24	0	0					9
10		4400	4645	4400	-	-	3	-	-	No fading	4500	-					No fading observed	35	0	0	0	0					10
11		5230	5431	5145	5250	6	20	2	20	Deep defocus/Rician	5300	5400					Rician potentially	27	0	17	0	0					11
12		5702	5856	5630	5650	3	6	1	2	Brief Rician Patch	5800	-					No fading	26	18	12	0	0					12
13		010200	0328	010110	0250	-	3	-	-	Rician	010300	-					No fading	20	14	3	2						13
14		0600	1035	0800	1015	6	20	1	2	Rician	0700	-					No fading	61	10	23	23						14
15		1310	1514	1250	1350	-	3	-	-	Rician	1400	-					No fading	27	10	27	0	0					15
16		1711	2054	1815	2020	10	20	2	3	Rayleigh slow fade	1800	-					No fading	51	5	45	4						16
17		2330	2616	2500	-	-	3	-	-	No fade	2400	-					No fading	37	16	2	1						17
18		3010	3359	3020	3335	20	35	1	3	Rayleigh fast fade	3002	12					Rayleigh fast fade	48	12	4	0	0					18
19		3950	4319	3820	4250	10	20	1	5	Parallel Run	3830	4115					Rician slow	47	12	15	10						19
20		4532	4820	4510	4640	6	25	1	5	Parallel Run	4500	4700					Rician slow	36	8	26	6					61°	20
21		5610	5937	5700	-	-	3	-	-	No fade	5700	-					No fade	45	2	45	0	0				161°	21
22		020140	020430	020200	-	-	-	-	-	No fade	020200	-					No fade	38	0	36	0	0				324°	22
23		0939	1224	1100	-	-	-	-	-	No fade	1200	-					Lost lock	38	18	2	0	0				164°	23
24		1605	2056	1600	-	-	-	-	-	No K signal	1800	-					Lost lock	65	14	3	0	0				79°	24
25		2420	2725	-	3000	-	-	-	-	No K signal	2600	-					No fade	42	10	10	0	0				250°	25
26		3142	3625	3300	-	-	-	-	-	No fade	3400	-					No fade	64	10	37	0	0				73°	26
27		4010	4240	4100	-	-	-	-	-	No fade	4100	-					No fade	0	5	-	-	-					27
28		4705	5010	4700	-		-	-	-	No fade	4800	-					No fade/lost lock	0	16	-	-	-				164°	28
29		5300	5730	5500	-	-	-	-		No fade	5200	-					No fading	0	0		-	-				325°	29

TABLE 4: TEST RESULTS FOR 2 MARCH (CAROLYN)

PASS	COMMENT	PASS start	PASS stop	ROOFTOP FADING start	ROOFTOP FADING stop	DEPTH db Avg	DEPTH db Max	DURATION sec Avg	DURATION sec Max	COMMENT	AIRCRAFT FADING START	AIRCRAFT FADING stop	DEPTH db Avg	DEPTH db Max	DURATION sec Avg	DURATION sec Max	COMMENT	TTY MESS SENT	Single Modem Atten	SINGLE MODEM error free	SINGLE MODEM with error	SINGLE MODEM char error	DUAL MODEM error free	DUAL MODEM with error	DUAL MODEM char error	AIRCRAFT HEADING	PASS
1	Hop mode message 18 - 24	0740	1115	001100	1400	2	20	1	2	some data	001220	1250	-	-	-	-	fading in turn	7	0	7	0	0	7	0	0	245	1
2	79 14	1745	1835	1650	1930	-	-	-	-	some phase data	1500	-	-	-	-	-	out of lock	36	0	7	0	0	27	6	15	322	2
3	no uplink messages	2120	2350	2100	2420	20	30	1	2		2225	2450	5	10	.5	1.0	Rayleigh fast fade	-	0	-	-	-	-	-	-	154	3
4	no uplink messages	2615	2750	2600	2800	-	-	-	-		2610	2640	10	20	1.0	1.0	Rayleigh/lost lock	-	0	-	-	-	-	-	-	316	4
5	went to HFP mode	3040	3255	3030	3245	-	-	-	-	no K signal	-	3300	10	15	.5	.5	fading late	-	0	-	-	-	-	-	-	165	5
6	went to HFP mode	3510	3655	3510	3610	-	-	-	-		3542	3700	15	30	.5	.5	Rayleigh slow fade	-	0	-	-	-	-	-	-	318	6
7	went to HFP mode	3945	4240	-	4250	-	-	-	-	no K lock	4020	4250	10	15	.5	.5	Rayleigh	-	0	-	-	-	-	-	-	168	7
8	went to HFP mode	4605	4750	4510	4750	25	35	0.5	1	Rayleigh fade	4525	4740	10	20	.5	1.0	Rayleigh	-	0	-	-	-	-	-	-	316	8
9	went to HFP mode	5040	5350	5140	5340	20	35	0.5	1	Rayleigh fade	5240	5350	10	15	.5	2.0	Rician	-	0	-	-	-	-	-	-	162	9
10	poor uplink messages	5650	5920	5610	5820	20	35	1	2	Rayleigh fade	5615	5815	10	20	.5	2.0	Rayleigh	-	0	-	-	-	-	-	-	317	10
11	poor uplink messages	010120	0355	010200	0410	20	30	1	4	Rayleigh fade	010150	0400	10	15	1.0	3.0	Rician	-	0	-	-	-	-	-	-	167	11
12	poor uplink messages	0650	0855	0610	0745	10	25	2	20	Rician - deep fade	0615	0825	10	20	1.0	4.0	Rician	-	0	-	-	-	-	-	-	312	12
13	poor uplink messages	1215	1650	1450	1525	6	30	2	4	Rayleigh fade	1400	1550	5	10	1.0	4.0	Rician	-	0	-	-	-	-	-	-	170	13
14	poor quality uplink	2150	2440	2145	2330	10	20	5	15	parallel/slow fade	2115	2400	10	15	7.0	5.0	slow fade	24	0	15	1	2	10	11	61	253	14
15		2735	3015	2800	2920	20	30	5	10	2 slow fades	2800	2935	-	-	-	-	2 or 3 small fades	14	0	2	5	14	14	0	0	75	15
16	no fades	3330	3510	3400	-	-	3	-	-	no fades	3400	-	10	15	.5	1.0	out of lock	-	0	-	-	-	-	-	-	167	16
17	scheduled HFP hop mode	3820	4125	3630	3950	3	6	1	2	Rician	3900	-	3	5	-	.5	out of lock	-	0	-	-	-	-	-	-	328	17
18	6 25	4345	4605	4320	4440	3	6	2	4	Rician	4300	4410	3	5	-	.5	light fading	18	0	4	0	0	18	0	0	167	18
19	no fading	4815	5035	4900	-				-	no fading	4800	-	3	5	-	1.0	no fading	-	0	-	-	-	-	-	-	328	19
20	no fading	5335	5655	5600	-					no fading	5500	-	3	3	-	1.0	no fading	-	0	-	-	-	-	-	-	167	20
21	no fading	5900	020025	5900	-	-	-	-	-	no fading	5900	-	5	15	.5	2.0	no fading	-	0	-	-	-	-	-	-	320/240	21

TABLE 5: TEST RESULTS FOR 7 MARCH (DIANNE)

PASS	COMMENT	PASS start	PASS stop	ROOFTOP FADING start	ROOFTOP FADING stop	DEPTH db AVG	DEPTH db Max	DURATION sec AVG	DURATION sec Max	COMMENT — 0 1055	AIRCRAFT FADING start	AIRCRAFT FADING stop	DEPTH db AVG	DEPTH db MAX	DURATION sec AVG	DURATION sec MAX	COMMENTS	TTY MESS SENT	SINGLE ATTEN	SINGLE MODEM error rate	SINGLE MODEM with error	SINGLE MODEM char error	DUAL MODEM error free	DUAL MODEM with error	DUAL MODEM char error	Aircraft Direction	Pass
1	Message 71 - 86	0008	1110	00091	1020	–	3	–	–	early time phase			–	–	–	–	No strip chart output	16	0	7	9	44	4	12	29	168°	1
2	46 - 54	1510	1630	1525	1607	3	10	1	5	early time strong sig			–	–	–	–	" " "	9	0	9	0	0	2	7	16	343°	2
3	3 - 22	1930	2210	2025	2153	10	20	2	30	hashy			–	–	–	–	" " "	20	0	9	0	0	8	9	41	163°	3
4	70 - 79	2515	2635	2520	2604	10	20	2	20	defocus			–	–	–	–	" " "	10	0	4	0	0	0	4	10	323°	4
5	Rec one garble	2945	3305	3030	3250	10	20	1	25	–			–	–	–	–	" " "	–	0	–	–	–	–	–	–	161°	5
6	out of lock	3625	3815	3516	3635	15	25	1	3	short but intense			–	–	–	–	" " "	–	0	–	–	–	–	–	–	319°	6
7	no effect # 4518	4155	4535	4510	–	–	–	–	–	some very weak effect	4510	4520	5	5	–	–	isolated fades	–	0	–	–	–	–	–	–	166°	7
8	message gen. problem	5025	5145	5000	5108	10	20	0.5	2	Rayleigh fade-fast	5010	5128	10	10	.5	1.0	Rayleigh fast	–	0	–	–	–	–	–	–	320°	8
9	44 - 66	5420	5625	5418	5602	20	30	1	3	Rayleigh fade-slow	5410	5605	12	15	1.0	2.0	Rayleigh slow	23	0	22	1	6	7	5	51	164°	9
10	out of lock	5920	10030	5852	5950	20	30	1	?	Rayleigh- intense	5855	5955	15	20	.5	2.0	Rayleigh in turn	15	0	0	0	–	2	5	16	320°	10
11	76 - 99	0315	0620	010408	0555	10	20	2	4	Rician slow	010415	0600	12	15	.5	1.0	Rayleigh	24	6	21	3	7	0	19	70	163°	11
12	45 - 52 8 - 19	0920	1050	0900	0950	15	30	1	2	Rayleigh in turn	0858	0952	15	15	.5	1.0	Rayleigh	8	8	8	0	0	1	7	12	321°	12
13	errors before & after	1320	1530	1355	1445	15	30	2	3	Rayleigh slow/Rician	1320	1500	12	15	.5	1.0	Rayleigh slow	12	10	0	3	24	2	10	26	168°	13
14	83 - 98 72 - 88	1805	2110	1932	2042	–	–	–	–	Rician	1915	2044	10	15	1.0	3.0	Rayleigh slow	16	9	14	2	5	8	7	11	321°	14
15	errors before & after	2815	2745	2640	2705	–	–	–	–	Rician	2812	2900	10	15	1.5	2.0	Rician intense f.	6	10	1	1	9	0	4	20	167°	15
16		3050	3320	3100	–	–	–	–	–	no fading	3100	3300	–	–	–	–	no fading	–	11	–	–	–	–	–	–	321°	16
17		3550	3700	3600	–	–	–	–	–	no fading	3600	3900	3	3	–	–	small fade near end	–	12	–	–	–	–	–	–	168°	17
18		4545	4852	4455	–	–	–	–	–	no fading	4630	4750	3	3	–	–	slow weak fading	–	–	–	–	–	–	–	–	289°	18

TABLE 6: TEST RESULTS FOR 13 MARCH (ESTHER) PAGE 1 OF 2

PASS	COMMENTS	PASS start	PASS stop	GROUNDTOP FADING start	GROUNDTOP FADING stop	DEPTH dB Avg	DEPTH dB Max	DURATION sec Avg	DURATION sec Max	COMMENTS	AIRCRAFT FADING start	AIRCRAFT FADING stop	DEPTH dB Avg	DEPTH dB Max	DURATION sec Avg	DURATION sec Max	COMMENT	TTY MESS SENT	Sinold Atten	SINGLE MODEM error free	SINGLE MODEM with errors	SINGLE MODEM char error	DUAL MODEM error free	DUAL MODEM with error	DUAL MODEM char error	AIRCRAFT direction	PASS
1	Message 2 - 18	2308 5	0930	2308 2	0942	-	3	-	-	weak defocus (phase	2308 4	0920	4	4	-	55	focus	17	10	16	1	3	17	0	0	234°	1
2	6 - 18	1625	1655	1606	1705	-	-	-	-	trong amp & defocus	1603	1710	5	5	-	58	small leading edge osc.	13	10	2	4	15	13	0	0	225°	2
3		1910	2000	1930	-	-	-	-	-	o fade	1920	-	0	0	0	0	no fading	-	10	-	-	-	-	-	-	45°	3
4	22 - 05	2220	2348	2228	2336	-	10	1	25	early time hard edg	2215	2335	4	5	-	45	more oscillations	14	10	11	3	25	11	3		200°	4
5	71 - 81	2900	3015	2820	2912	6	15	1	2	ard edge then phase	2800	3003					" "	11	10	10	0	0	11	0	0	205°	5
6	51 - 42	3307	3403	3302	3344	10	30	0.5	1	Rayleigh fading	3306	3346					" "	9	10	7	1	2	9	0	0	44°	6
7	93 - 03	3735	3823	3724	3815	20	30	0.5	10		3721	3813	8	10	1.0	20.0	early time defocus	11	12	6	0	0	9	1		223°	7
8	45 - 56	4133	4225	4118	4212	—	-	-	-		4116	4210	15	20	1.0	2.0	Rayleigh fading	12	14	6	2	4	12	0	0	42°	8
9	9 - 22	4554	4715	4605	4706	18	30	0.5	1	" "	4606	4713	10	15	1.0	2.0	" "	14	14	5	3	18	14	0	0	222°	9
10	53 - 67	4920	5035	4918	5028	20	30	0.5	1	" "	4917	5031	10	15	0.5	2.0	" "	15	13	7	3	11	15	0	0	40°	10
11	7 - 20	5240	5435	5321	5424	10	30	0.5	2	" "	5322	5430	15	20	0.5	2.0	" "	14	13	6	2	7	12	2		222°	11
12	54 - 81	5656	5812	5649	5829	20	30	0.5	1	" "	5647	5809	10	15	0.5	1.0	" "	28	14	16	6	18	26	2		39°	12
13	Start Test #3 - No TTY	0000 50	0240	0039	0219	20	30	0.5	2	Rayleigh fading slow	0040	0250	20	25	0.5	1.0	" Test 3	NO TTY		-	-	-	-	-	-	222°	13
14		0505	0615	0454	0607	15	30	0.5	1	Rayleigh fading fast	0450	0610	20	25	0.5	1.0	"	-	-	-	-	-	-	-	-	58°	14
15		0925	1120	0832	1028	20	30	0.5	15		0830	1130	25	30	0.5	1.0	"	-	-	-	-	-	-	-	-	225°	15
16		1435	1535	1353	1455	15	30	0.5	1	" "	1350	1510	25	30	0.5	0.5	"	-	-	-	-	-	-	-	-	42°	16
17		1825	2020	1835	2011	-	-	-	-	" "	1810	2020	25	30	0.5	0.5	" start good data	-	-	-	-	-	-	-	-	227°	17
18		2300	2355	2228	2313	10	25	1	3	" "	2225	2320	25	30	0.5	0.5	" "	-	-	-	-	-	-	-	-	45°	18
19		2650	2830	2753	2816	10	30	0.5	4	" "	2610	2820	25	35	0.5	1.0	" "	-	-	-	-	-	-	-	-	242°	19
20	Parallel Run	3235	3502	3332	3519		-	-	-	" "	3400	3525	20	35	0.5	1.5	" "	-	-	-	-	-	-	-	-	137°	20
21		4025	4225	3920	4040	10	30	1	3	" "	3930	4100	25	35	0.5	2.0	" K band Lost lock	-	-	-	-	-	-	-	-	312°	21
22		4610	4650	4515	4615		30	-	10	" "	4525	4625	25	35	0.5	2.0	" "	-	-	-	-	-	-	-	-	45°	22
23		4915	5200	4900	5153	20	30	1	2	" "	4900	5200	30	35	0.5	1.0	" K band Lost lock	-	-	-	-	-	-	-	-	232°	23
24		5500	5615	5500	5550		-	-	-	RICIAN	5450	5555	25	35	0.5	1.5	Rician	-	-	-	-	-	-	-	-	50°	24
25		5845	010114	5930	010055	15	30	1	3	Ray/Rician from 5820	5810	010120	30	35	0.5	2.0	Rayleigh fading	-	-	-	-	-	-	-	-	233°	25
26		0418	0525	0450	0505	3	10	-	-	eak fading	0420	0520	15	35	0.5	1.5	Rician	-	-	-	-	-	-	-	-	43°	26
27		0747	1010	0720	0940	10	25	2	3	Rician	0620	1000	30	40	0.5	2.0	Rayleigh fading fast	-	-	-	-	-	-	-	-	231°	27
28		1215	1415	1140	1550	15	30	1	2	Rician-some deep	1140	1510					" "									25°	28

TABLE 6: TEST RESULTS FOR 13 MARCH (ESTHER) PAGE 2 OF 2

PASS	COMMENTS	PASS start	PASS stop	RECEIVE LEVEL start	RECEIVE LEVEL ADING stop	DEPTH dB Avg	DEPTH dB Max	DURATION sec Avg	DURATION sec Max	COMMENTS		AIRCRAFT FADING	DEPTH dB Avg	DEPTH dB Max	DURATION sec Avg	DURATION sec Max	COMMENTS	TTY MESS SENT	Single Modem Atten	SINGLE MODEM error free	SINGLE MODEM with error	SINGLE MODEM char error	DUAL MODEM error free	DUAL MODEM with error	DUAL MODEM char error	Aircraft Heading	PASS
29	Test 3 no TTY	011650	1909	011700	-	-	-	-	-	phase only - weak	11740	1850					Rician weak	-	-	-	-	-	-	-	-	228°	29
30		2120	2305	2100	2215	5	10	-	-	Rician		2050	2355	15	30	0.5	1.0	Rayleigh	-	-	-	-	-	-	-	-	41°	30
31		2503	2700	2600	-	10	20	1	3	No fading		2600	-	-	3	-	-	one little fade	-	-	-	-	-	-	-	-	222°	31
32		2855	3040	2835	3000	-	-	-	-	Rayleigh then Rician		2840	3020	30	35	0.5	1.5	Rayleigh then Rician	-	-	-	-	-	-	-	-	50°	32
33		3315	3520	3404	3444	-	10	-	-	Rician		-		-	-	-	-	out of lock	-	-	-	-	-	-	-	-	238°	33
34	end Test 3	3730	3955	3733	3920	10	25	1	3	Rician		-		-	-	-	-	out of lock	-	-	-	-	-	-	-	-	52°	34
35	start Test 1 mess 80 92	4210	4505	4250	4350	15	30	1	2	Rayleigh - slow		4250	4455	20	30	1.0	2.0	2 Rician patches	13	13	1	2	23	10	3		244°	35
36	45-79	4809	4920	-	-	-	-	-	-	no K signal		4740	5020	10	15	1.0	2.0	Rayleigh fading	35	11	29	4	25	34	1		42°	36
37	3-16	5140	5355	-	-	-	-	-	-	no K signal		5200	5300	7	10	2.0	4.0	Rician	14	11	13	1	8	13	1		245°	37
38	77 80	5700	5812	5729	5748	3	15	-	-	few deep spikes		5600	5750	10	15	1.0	4.0	Rician	4	13	0	0	0	1	1		41°	38
39	39-40	020030	0302	02020	0214	10	25	3	5	5 spikey fades		020120	0300	7	15	1.0	5.0	Rician	2	13	1	0	0	1	1		240°	39
40	91-99 + 9 - 17	0551	0818	0555	0800	5	25	-	-	Rician then Rayleigh		0750	0810	5	15	1.0	4.0	Rician then Rayleigh	18	13	5	6	30	18	0	0	40°	40
41		1025	1244	1100	-	-	-	-	-	no fading		1100	-	0	1	-	-	No fading	-	13	-	-	-	-	-	-	240°	41
42	9-18 & 25 58	1548	1913	1443	1855	10	20	2	2	spikey then Rayleigh		1420	1900	15	20	0.5	2.0	Rician then Rayleigh	44	14	11	5	27	36	7		44°	42
43	84 93 & 98 01	2140	2415	2120	2240	-	5	-	-	Rician + 4 deep fades		2110	2310	10	15	1.0	5.0	Ripple then Rician	14	0	9	0	0	8	5		183°	43
44	42 55 & 60 85	2622	2930	2600	2705	10	15	-	-	Rician		2600	2920	15	20	1.0	4.0	Rayleigh then Rician	40	11	30	6	29	32	6		0°	44

TABLE 7: TEST RESULTS FOR 14 MARCH (FERN) PAGE 1 OF 2

PASS	COMMENT	PASS start	PASS stop	ROOFTOP FADING start	ROOFTOP FADING stop	DEPTH dB Avg	DEPTH dB Max	DURATION sec Avg	DURATION sec Max	COMMENT	AIRCRAFT FADING start	AIRCRAFT FADING stop	DEPTH dB Avg	DEPTH dB Max	DURATION sec Avg	DURATION sec Max	COMMENTS	TTY MESS SENT	SINGLE ATTEN	SINGLE MODEM ERROR FREE	SINGLE MODEM with char error	SINGLE MODEM char error	DUAL MODEM error free	DUAL MODEM with error	DUAL MODEM char error	AIRCRAFT HEADING	PASS
1	Message 21 - 29	24725	4940	24744	4926	-	-	-	-	Early Time Phase	24742	5019	7	7	-	60	Early time/defocus	22	12	13	1	7	18	3		311	1
2	no data	5415	5555	5413	5529	-	3	-	40	ET Phase-Hard edge	5423	5542	7	7		50	early time large defocus	-	0	-	-	-	-	-	-	36	2
3	no fade	5845	30010	5900	-	-	-	-	-	No fade	5850	-	0	1	-	-	no fading	-	10	-	-	-	-	-	-	220	3
4	no data	0320	0425	30324	041	-	20	-	-	E.T. phase	30324	0426	5	10	.5	40	small defocus	-	0	-	-	-	-	-	-	45	4
5	92 - 02	0805	0927	0813	090	-	-	-	-	Phase - no amplitude	0820	-	1	3	-	-	no fading	11	10	11	0	0	11	0	0	203	5
6	no data	1300	1434	1335	142	10	25	0.5	2	Phase then hard edge	1342	1427	10	12	1.0	2.0	Rayleigh fast fade	-	0	-	-	-	-	-	-	37	6
7		1835	1955	1900	-	-	-	-	-	No fade	1900	-	0	1	-	-	no fading	-	10		-	-	-	-	-	218	7
8	08 - 20	2405	2605	2440	2540	15	25	1	2	Rayleigh fast fade	2434	2540	10	20	.5	1.0	Rayleigh fast fade	13	13	7	3	17	12	1		43	8
9	69 - 81	2925	3044	2940	3040	20	30	0.5	2	Rayleigh fast fade	2941	3054	15	25	.5	1.0	Rayleigh slow fade	13	13	5	3	9	12	1		220	9
10	17 - 31	3305	3432	3315	425	15	30	0.5	2	Rayleigh fast fade	3314	3426	10	20	.5	1.0	Rayleigh fast fading	15	12	8	2	6	13	2		32	10
11	75 - 85	3705	3825	3733	3825	18	30	0.5	5	Early time with scint	3734	3821	15	25	.5	2.0	Rayleigh fast fading	11	13	5	1	2	10	1		222	11
12	21 - 32	4100	4205	4100	4156	20	30	0.5	3	Rayleigh slow fade	4254	4406	15	25	.5	2.0	Rayleigh fast fading	12	10	6	3	26	9	2		45	12
13	79 - 84	4430	4558	4518	454	20	25	1	3	Rayleigh slow fade	4513	4552	10	20	.5	3.0	Rayleigh fast fading	6	14	1	0	0	4	2		225	13
14	22 - 34	4840	4950	4842	494	20	30	1	2	Rayleigh fast fade	4835	4948	15	25	.5	2.0	Rayleigh fast fading	13	12	4	4	14	12	1		42	14
15	69 - 84	5210	5350	5152	532	10	30	2	4	strong Rician	5155	5350	15	20	.5	2.0	Rayleigh slow fade	20	8	16	2	12	19	1		227	15
16	22 - 39	5550	5740	5610	573	15	25	1	3	Rayleigh fast & slow	5610	5747	15	20	.5	2.0	Rayleigh fast fade	18	12	5	6	19	16	2		38	16
17	74 - 80	000010	0130	00000	003	10	25	2	4	Rayleigh slow fading	5955	000133	10	20	1.0	2.0	parallel run	7	10	4	3	17	4	3		222	17
18	19 - 32	0338	0442	0320	042	12	18	2	4	Rayleigh slow fading	0332	0454	15	20	.5	2.0	Rayleigh slow fade	14	12	6	6	32	14	0	0	40	18
19	67 - 81	0700	0838	0655	081	3	12	1	4	Rician	0646	0818	15	20	1.0	4.0	Rayleigh fast fade	18	10	15	2	5	18	0	0	225	19
20	20 - 50	1016	1158	1050	114	15	30	1	3	Rayleigh slow fale	1048	1210	15	20	1.0	3.0	Rayleigh slow fade	11	12	8	2	7	11	0	0	63	20
21	60 - 66	1400	1500	1348	142	12	30	2	3	Rayleigh slow fade	1338	1445	15	20	.5	2.0	Rayleigh fast fade	7	12	7	0	0				220	21
22	99 - 07	1711	1825	1635	172	3	10	2	3	Rician	1641	1734	5	15	1.0	4.0	Rayleigh slow fade	11	12	11	0	0	11	0	0	46	22
23	60 - 75	2055	2240	2115	225	13	30	2	5	Rayleigh slow fale	2149	2235	15	20	.5	4.0	Rayleigh fast fade	16	12	7	4	19	16	0	0	225	23
24	15 - 66	2610	2952	2735	291	-	-	-	-	parallel run	2645	2931	10	20	1.0	5.0	parallel run	22	12	9	1	8				309	24
25	11 - 36	3250	3445	3243	344	3	20	6	15	parallel run	3240	3456	10	20	3.0	0.	parallel run	23	10	20	2	17	21	2		138	25
26	1 - 2	4016	4116	4005	405	5	15	2	5	Rayleigh slow fade	3957	4118	10	25	2.0	4.0	Rayleigh slow fade	10	12	6	3	28	-	-	-	43	26
27	no fading	4325	4451	4410	-	-	-	-	-	no fading	4326	4414	-	5	-	-	weak Rician	-	12	-	-	-	-	-	-	221	27
28	0 - 1	4705	4815	4650	471	-	3		-	weak Rician	4700	4757	5	8	1.0	5.0	Rician	12	12	12	0	0	11	1		57	28

TABLE 7: TEST RESULTS FOR 14 MARCH (FERN) PAGE 2 OF 2

PASS	COMMENT	PASS start	PASS stop	MOON-TOP FADING start	MOON-TOP FADING stop	DEPTH dB Avg	DEPTH dB Max	DURATION sec Avg	DURATION sec Max	COMMENT	AIRCRAFT FADING start	AIRCRAFT FADING stop	DEPTH dB Avg	DEPTH dB Max	DURATION sec Avg	DURATION sec Max	COMMENT	TTY MESS SENT	SINGLE ATTEN	error free	with error	char error	error free	with error	char error	AIRCRAFT HEADING	PASS
29	94 - 22	0055	5656	0053	5603	-	10	-	30	parallel run	5340	5600	10	20	1.0	50	early time	29	14	28	1	12	24	2		315	29
30	00 - 01	0100	0129	0100	0055	-	10	-	5	defocus-hard edge	0100	0100	5	15	.5	10	early time-hard edge	2	14	2	0	0	2	0	0	43	30
31	36 - 38	0310	0511	0428	0443	-	20	-	10	defocus-hard edge	0423	0500	10	20	.5	15	early time	3	12	0	0	0	2	0	0	230	31
32	79 - 84	0715	0852	0739	0805	-	20	-	10	defocus-hard edge	0740	0822	10	20	.5	20	early time	6	10	2	2	17	5	1		46	32
33	29 - 45			1120	-	-	-	-	-	saw something	1042	1240	5	10	-	10	Rician	17	7	17	0	0	17	0	0	-	33

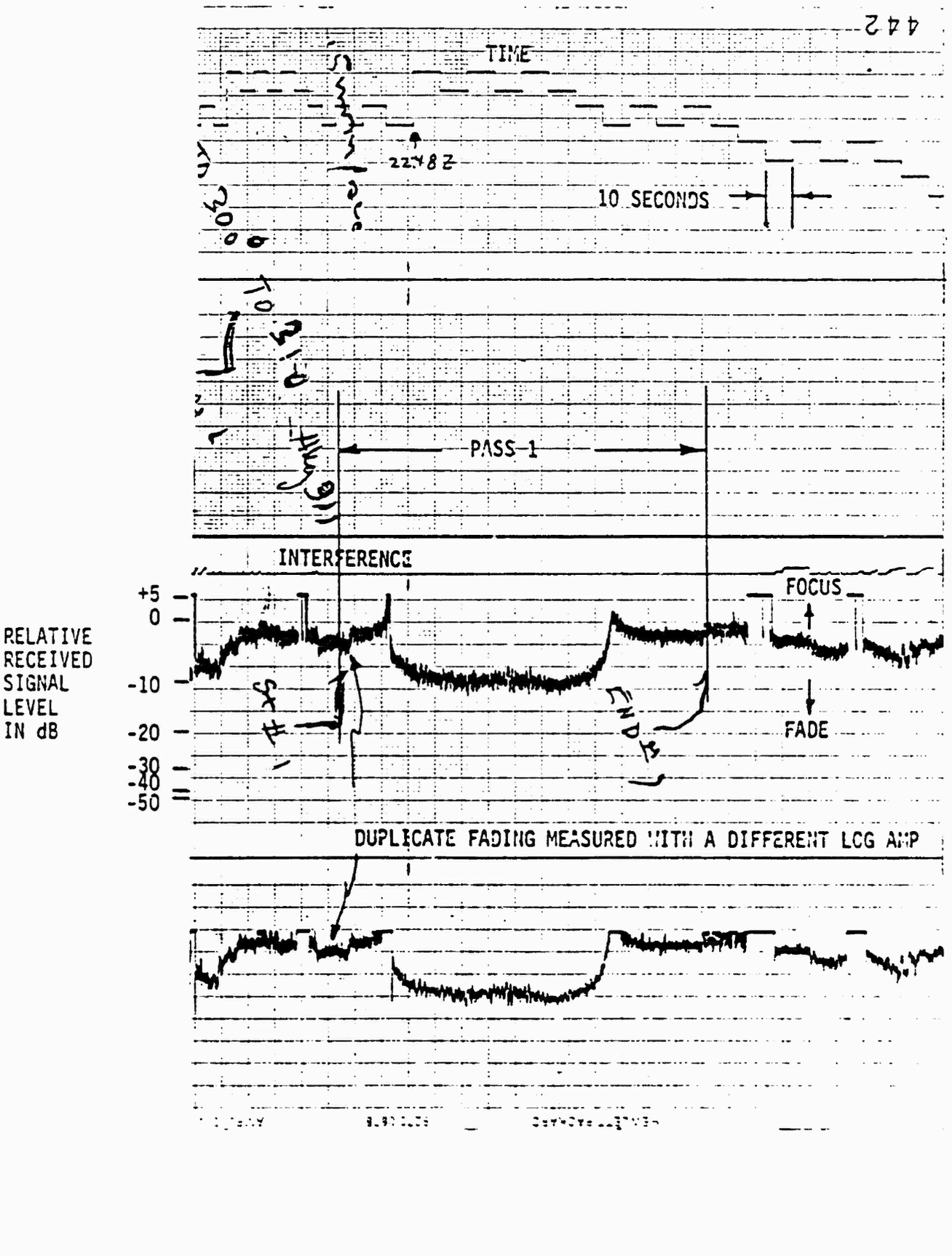

FIGURE 37 Downlink Fading, FERN, Pass 1

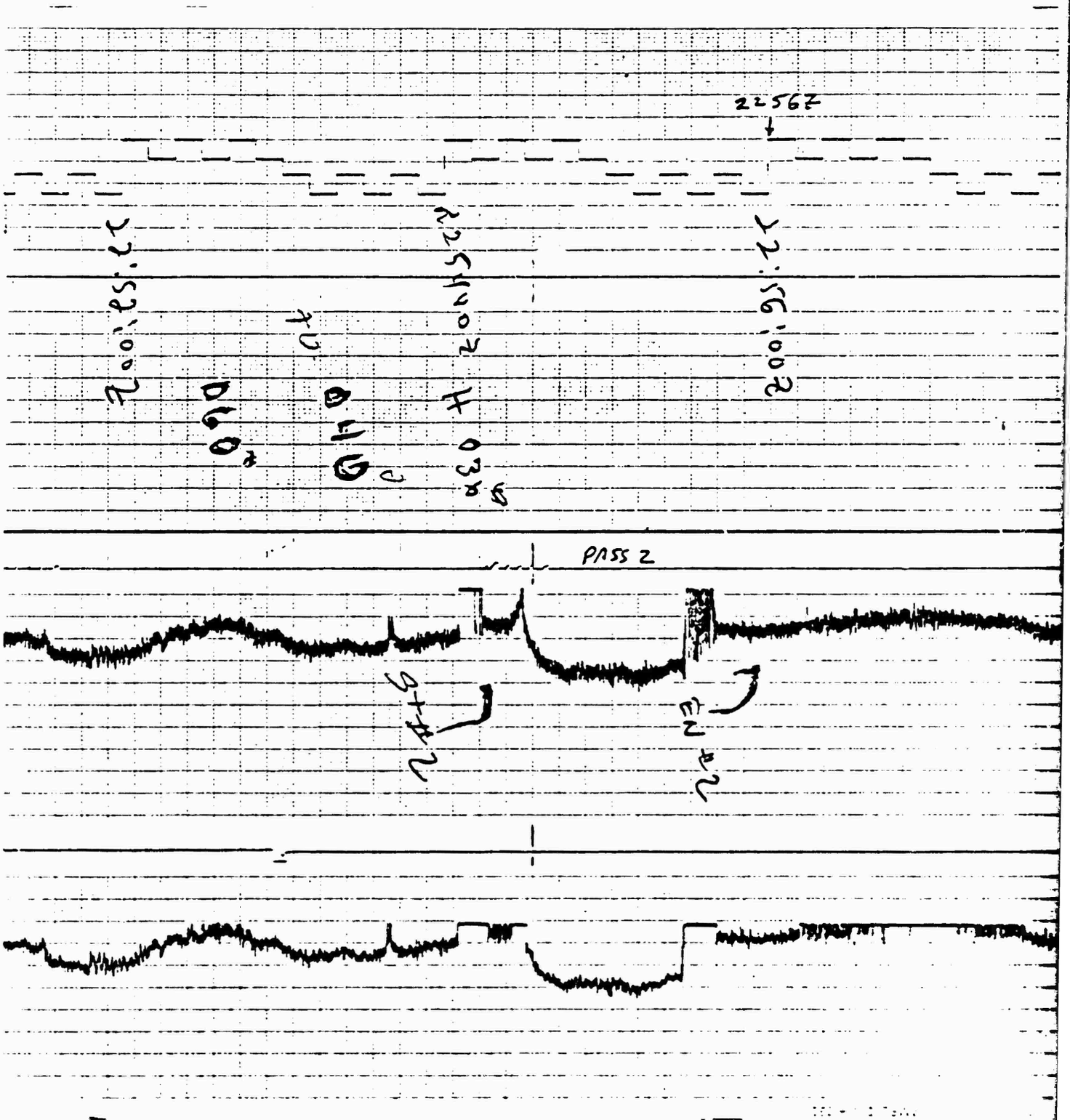

FIGURE 38 Downlink Fading, FERN, Pass 2

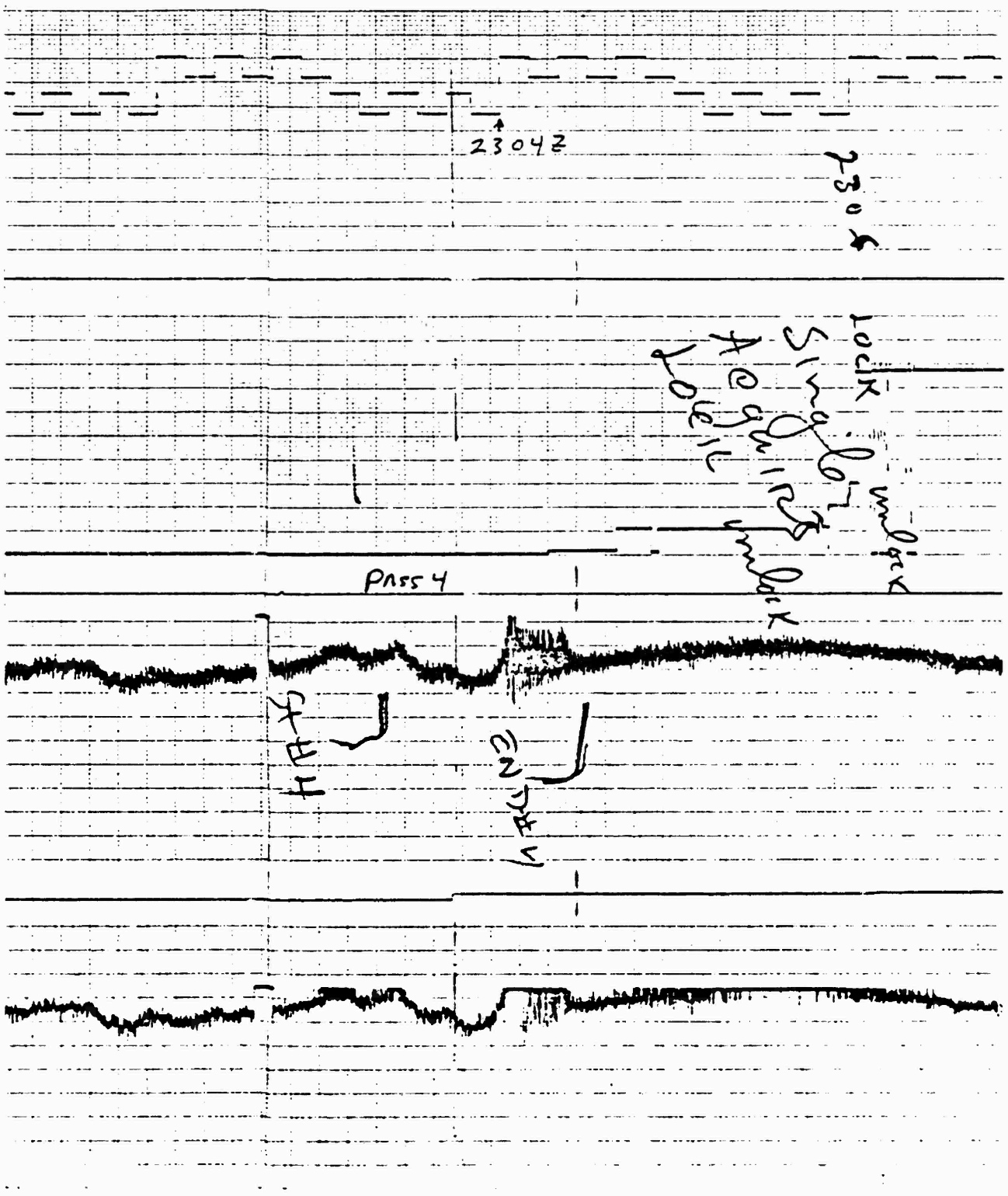

FIGURE 39 Downlink Fading, FERN, Pass 4

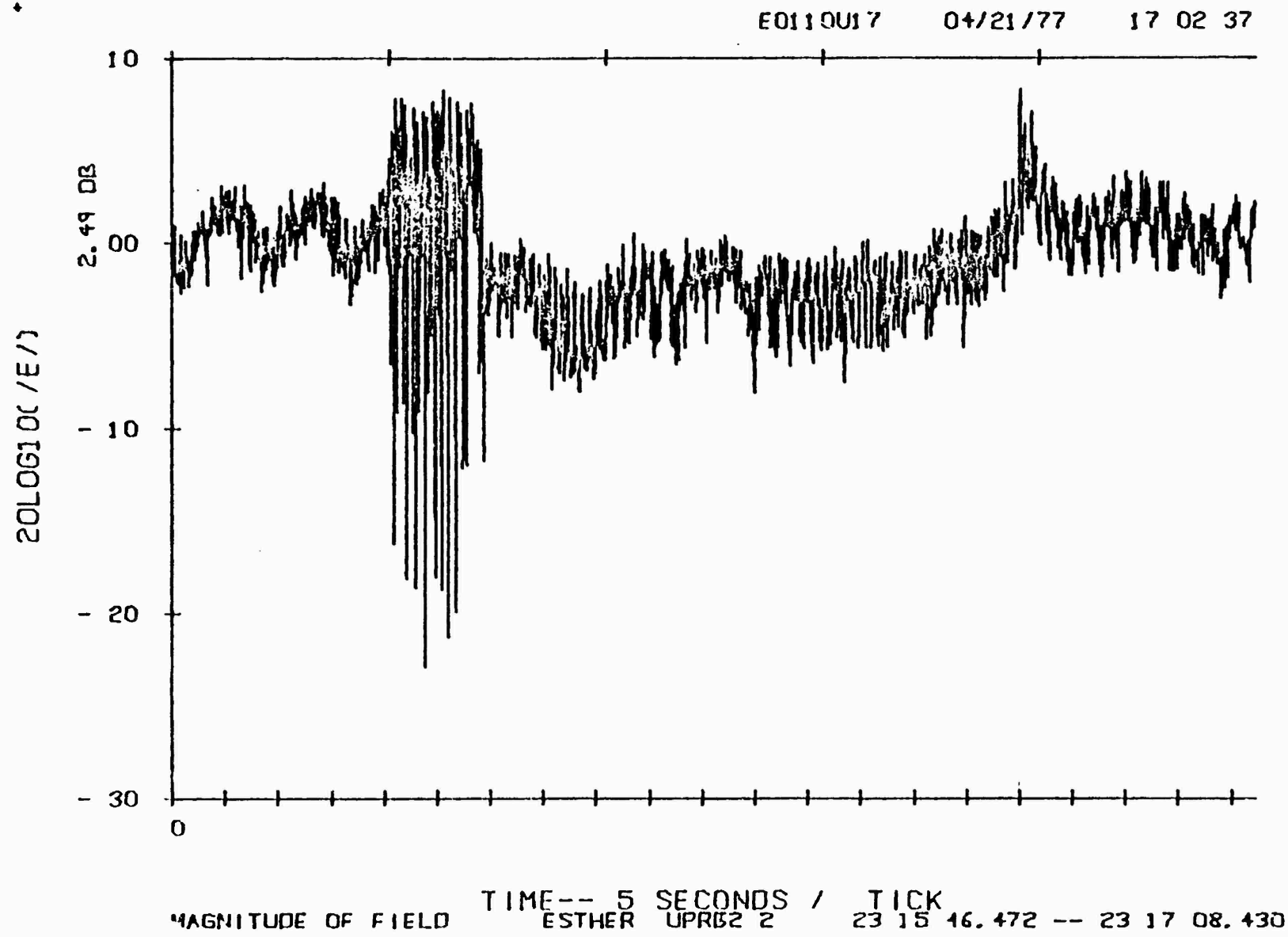

64

FIGURE 40 Uplink, 339 MHz, Amplitude Fading for ESTHER Pass 2

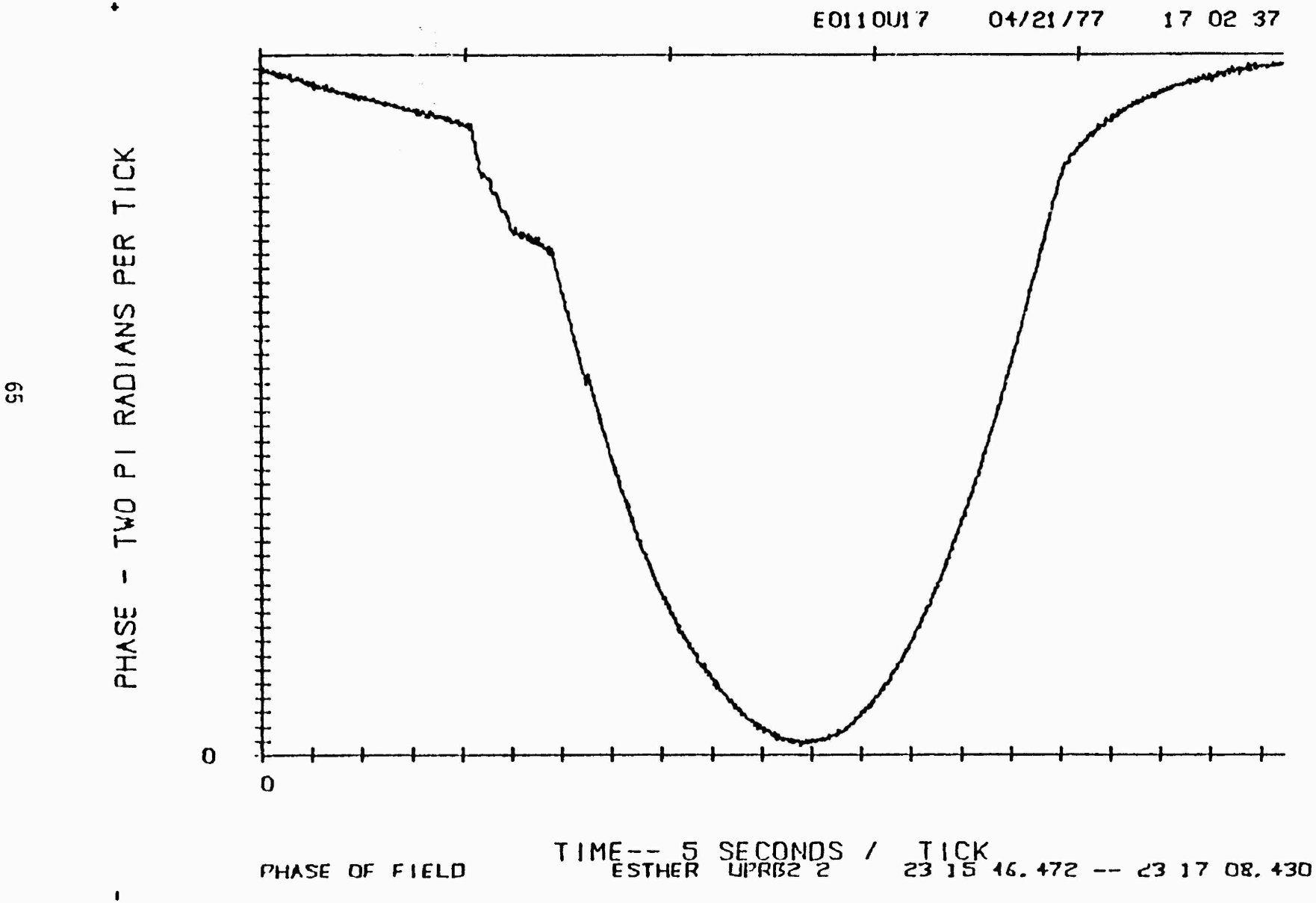

FIGURE 41 Uplink Phase Effects for ESTHER Pass 2

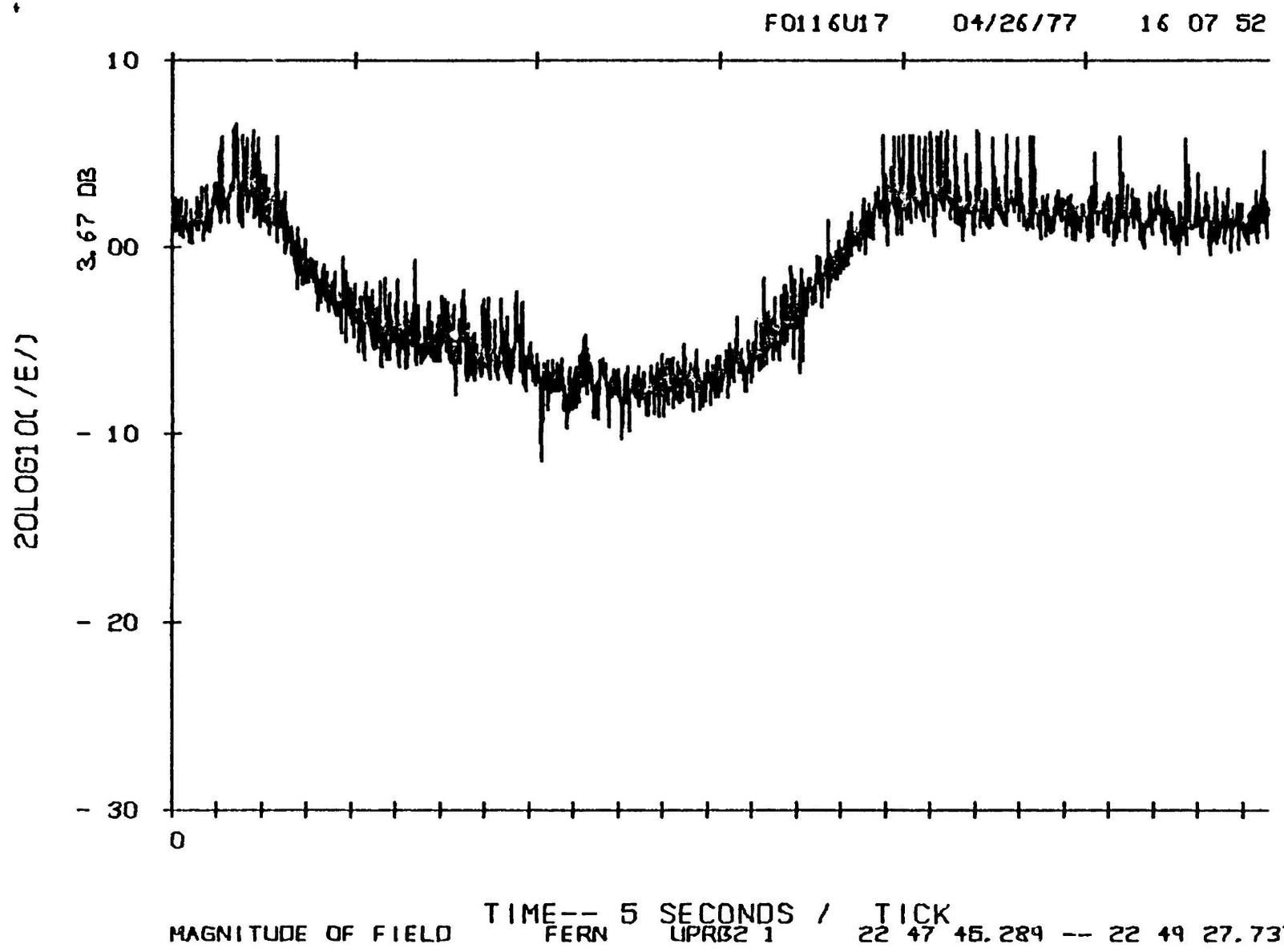

FIGURE 42 Uplink Amplitude Fading for FERN Pass 1

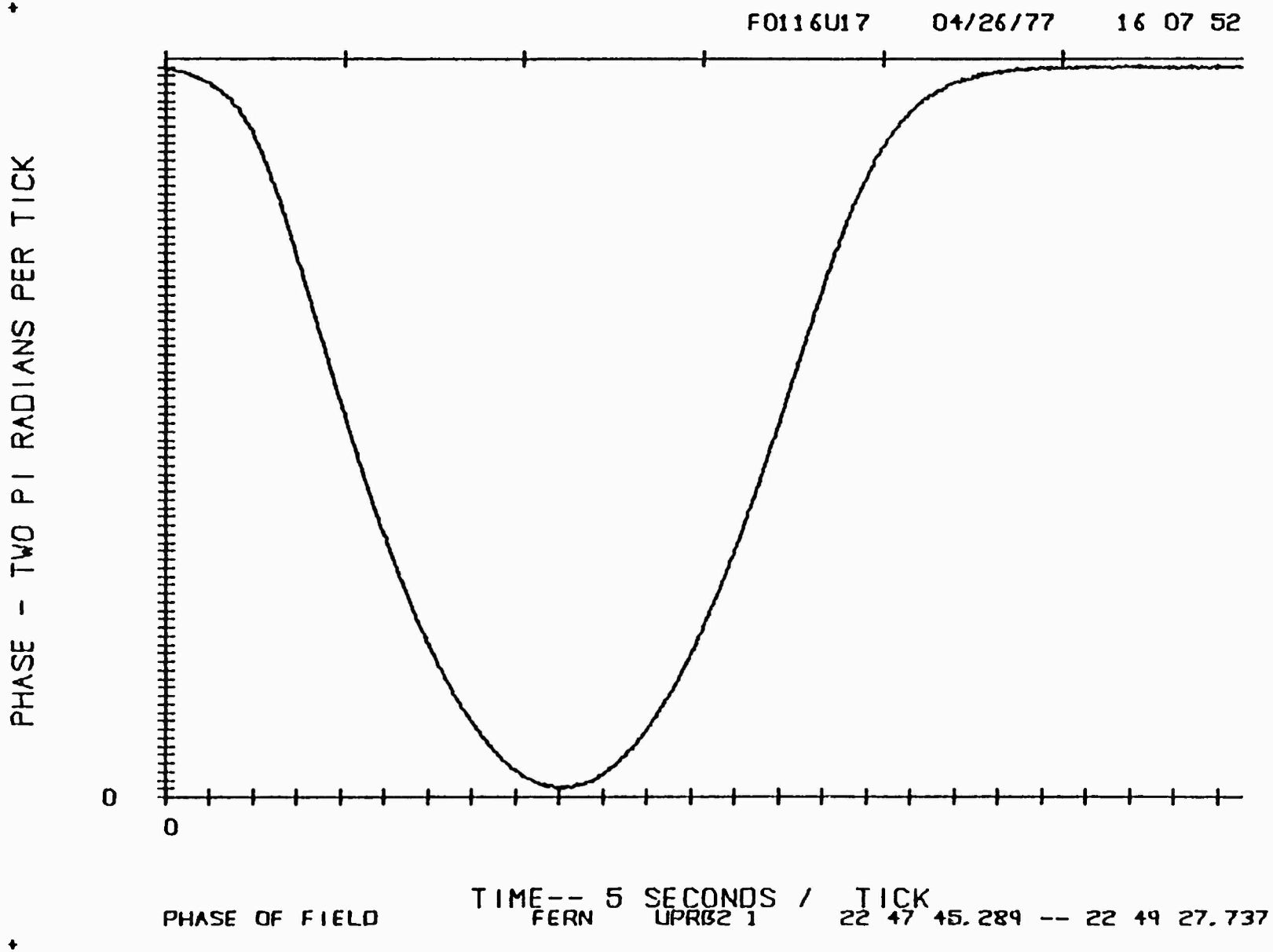

FIGURE 43 Uplink Phase Effects for FERN Pass 1

classical diffraction pattern is unmistakable, however, and easily correlated with the barium induced phase. In the early time runs these phases strongly resembled Gaussian curves (barium phase effects increasing with decreasing values on the plot producing inverted Gaussians) with the phase shifts due to integrated content effects as high as 96 cycles.

Pass 31 of FERN also behaved like an early-time pass which is unusual at this late period in the cloud evolution, Figure 44. Comparison of Pass 31, Figure 44, to the theoretical drawing in Figure 45 shows the theoretical curve to be reproduced very faithfully by the barium cloud structure.

B. Rayleigh-Like Fading: As the cloud developed into a series of individual irregularities, rapid and deep fading was produced often with a ringing type multipath caused by edge diffraction effects at the beginning or end of the pass as seen in FERN, Pass 8, Figure 46. The downlink received signal level during Pass 9 of FERN showed a broad decrease at the initial part of the pass with rapid Rayleigh-like fading toward the end, Figure 47. Figure 48 shows similar results during FERN, Pass 10. Figure 49 shows two additional examples of Rayleigh-like downlink fading lasting a little over 60 seconds each. Excellent examples of Rayleigh-like fading are seen in the uplink ESTHER, Pass 8, data, Figure 50. The diffraction edge in this pass is obvious on the left at the start of the pass. The phase shown in Figure 51 indicates vestiges of the smooth Gaussian early-time behavior. It is, however, corrugated both by changes in path integrated electron content and by diffraction effects which can produced phase jumps associated with deep fades.

C. Parallel Pass Fading: Typically the aircraft flew cross-striation passes, but occasionally a maneuver was flown parallel to the projection of the striations. The fading on these passes differed from that observed

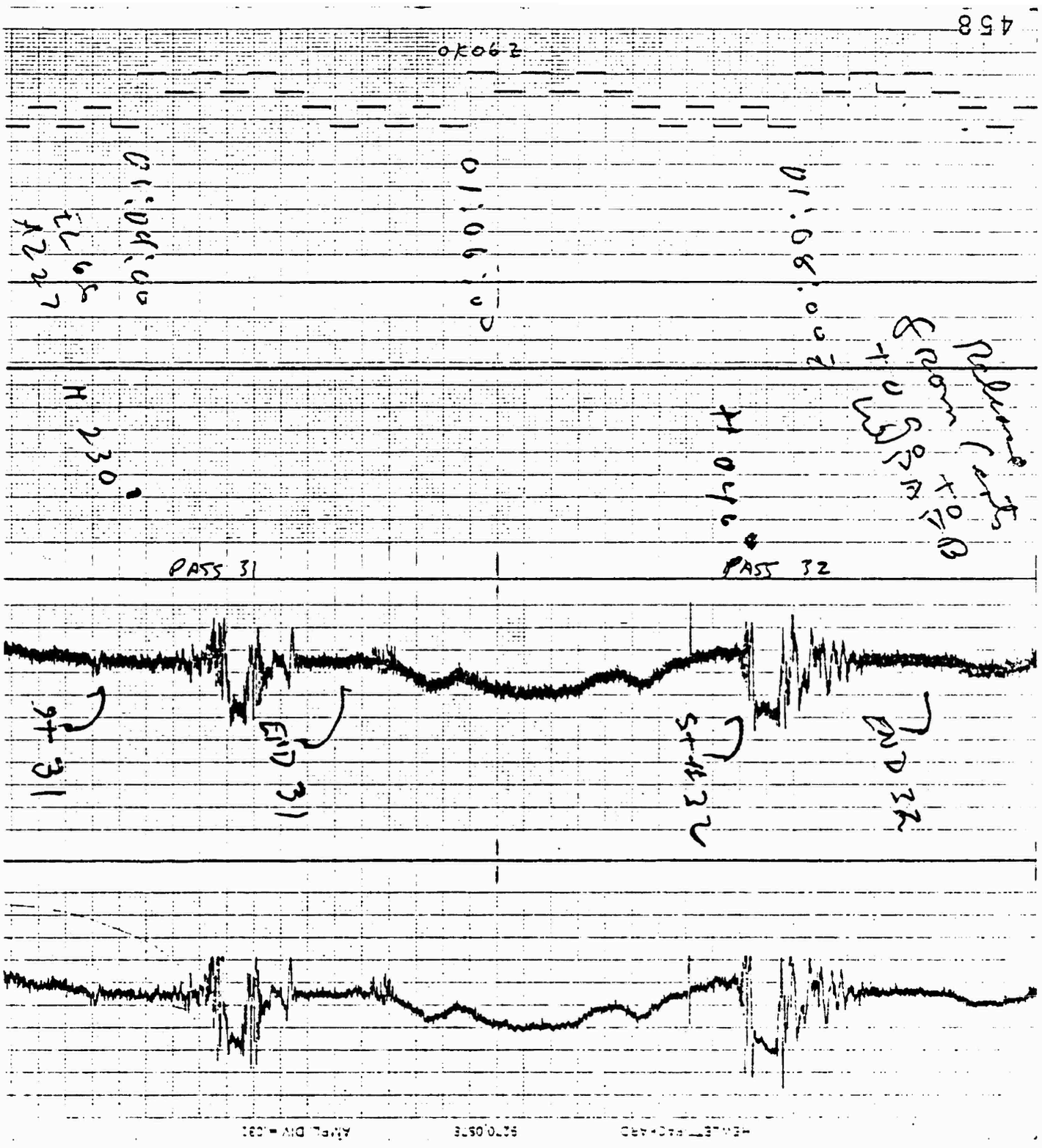

FIGURE 44 Early Time Fading for FERN Pass 31

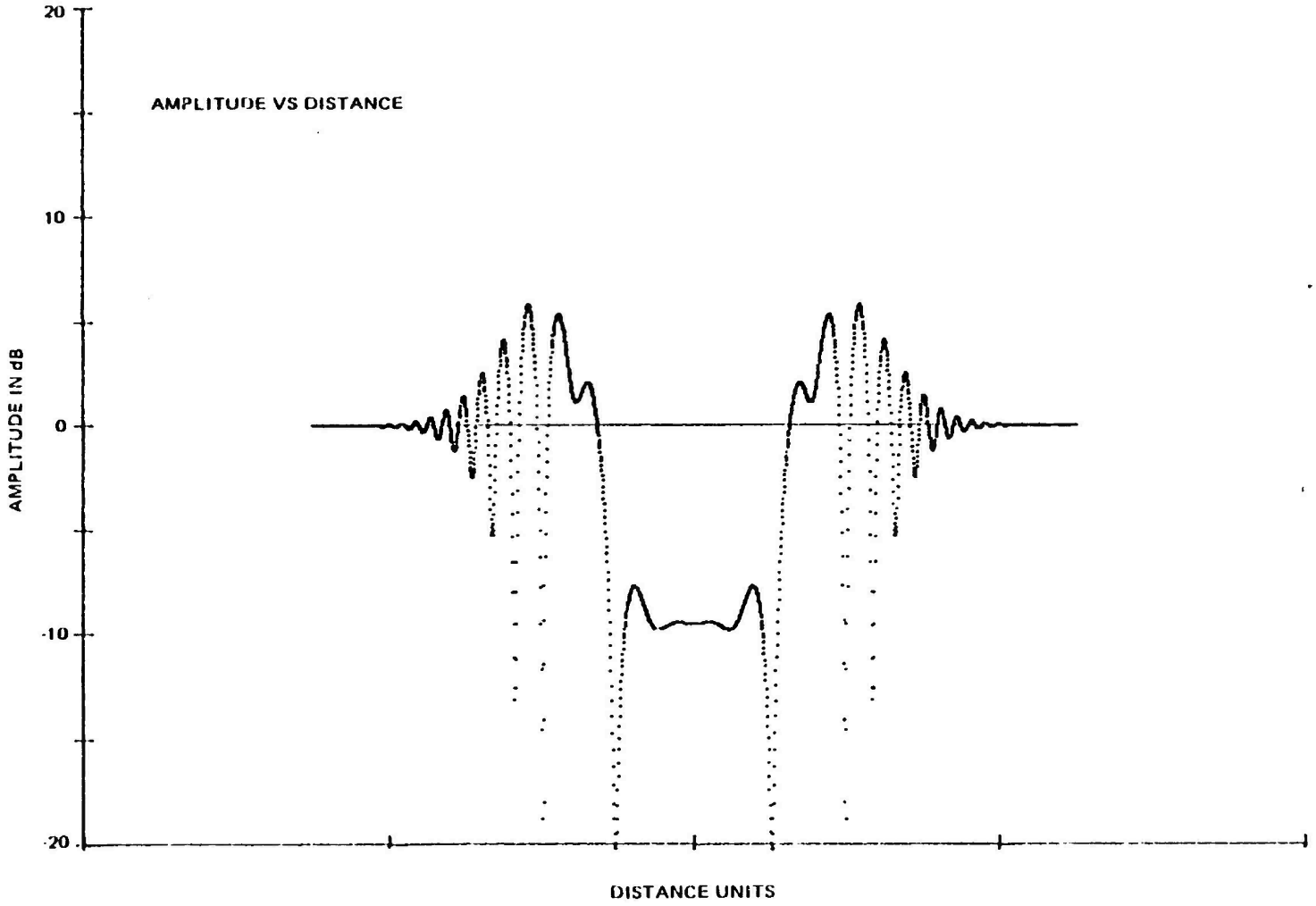

Amplitude in dB Versus Distance (2 km per tic) at the Screen (solid curve) and at the Ground 150 km away (dotted curve) for 300 MHz Propagation Through a 300m Radius Striation with 10^7 Electrons Per cc Peak Density. (U)

FIGURE 45 Theoretical Fading Through Single Striation

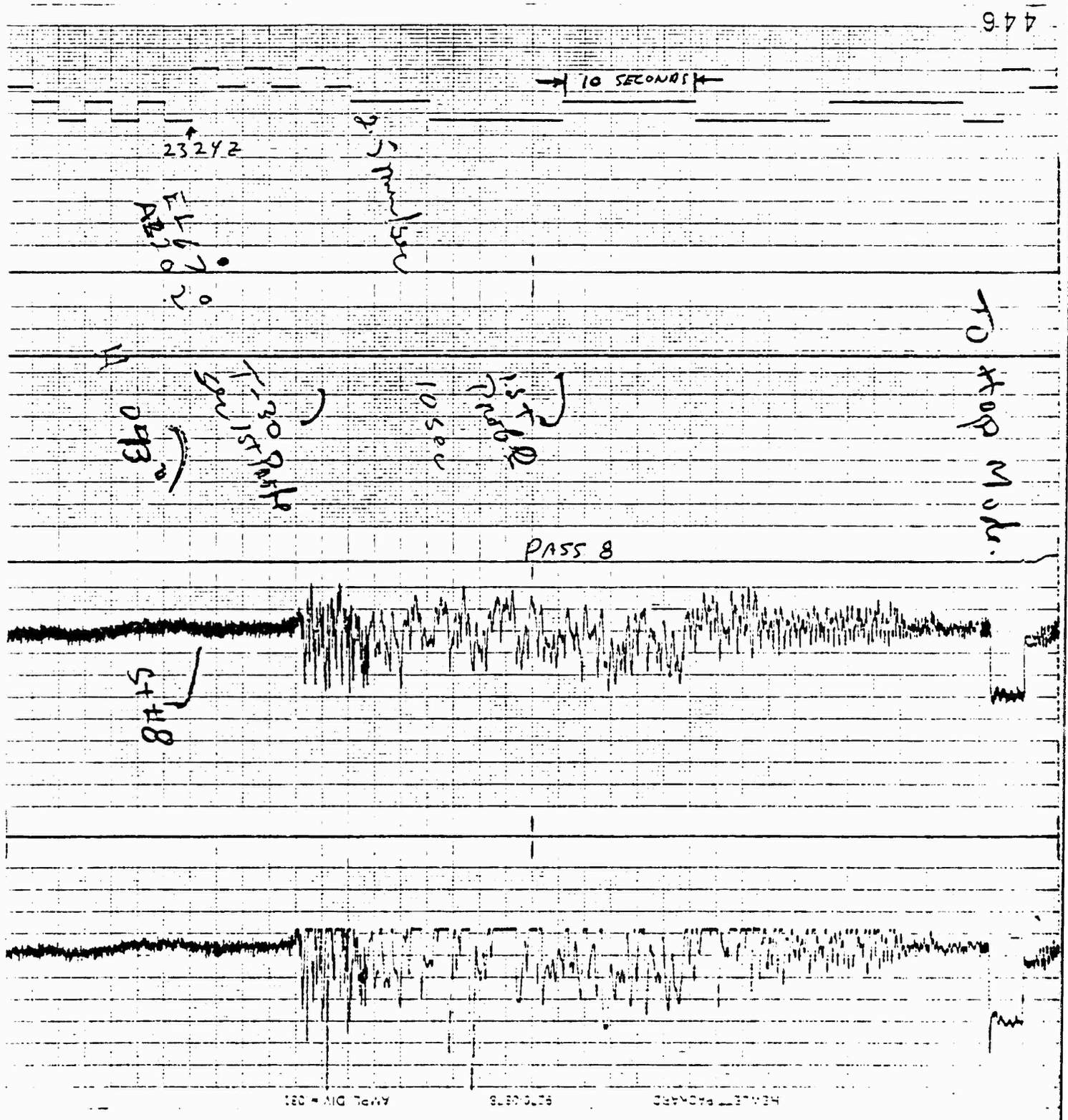

FIGURE 46 Rayleigh Like Downlink Fading on FERN Pass 8

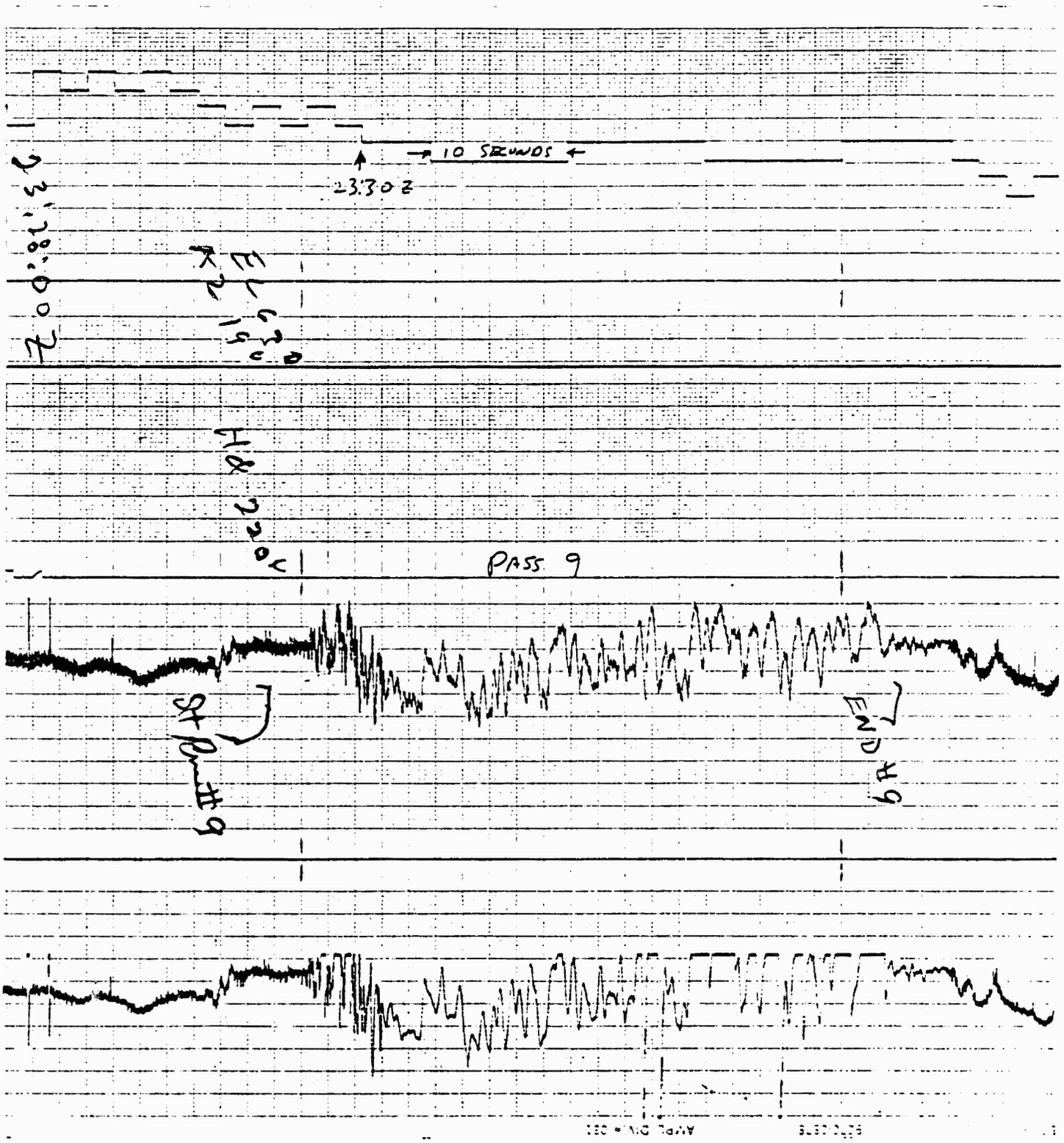

FIGURE 47 Rayleigh Like Downlink Fading on FERN Pass 9

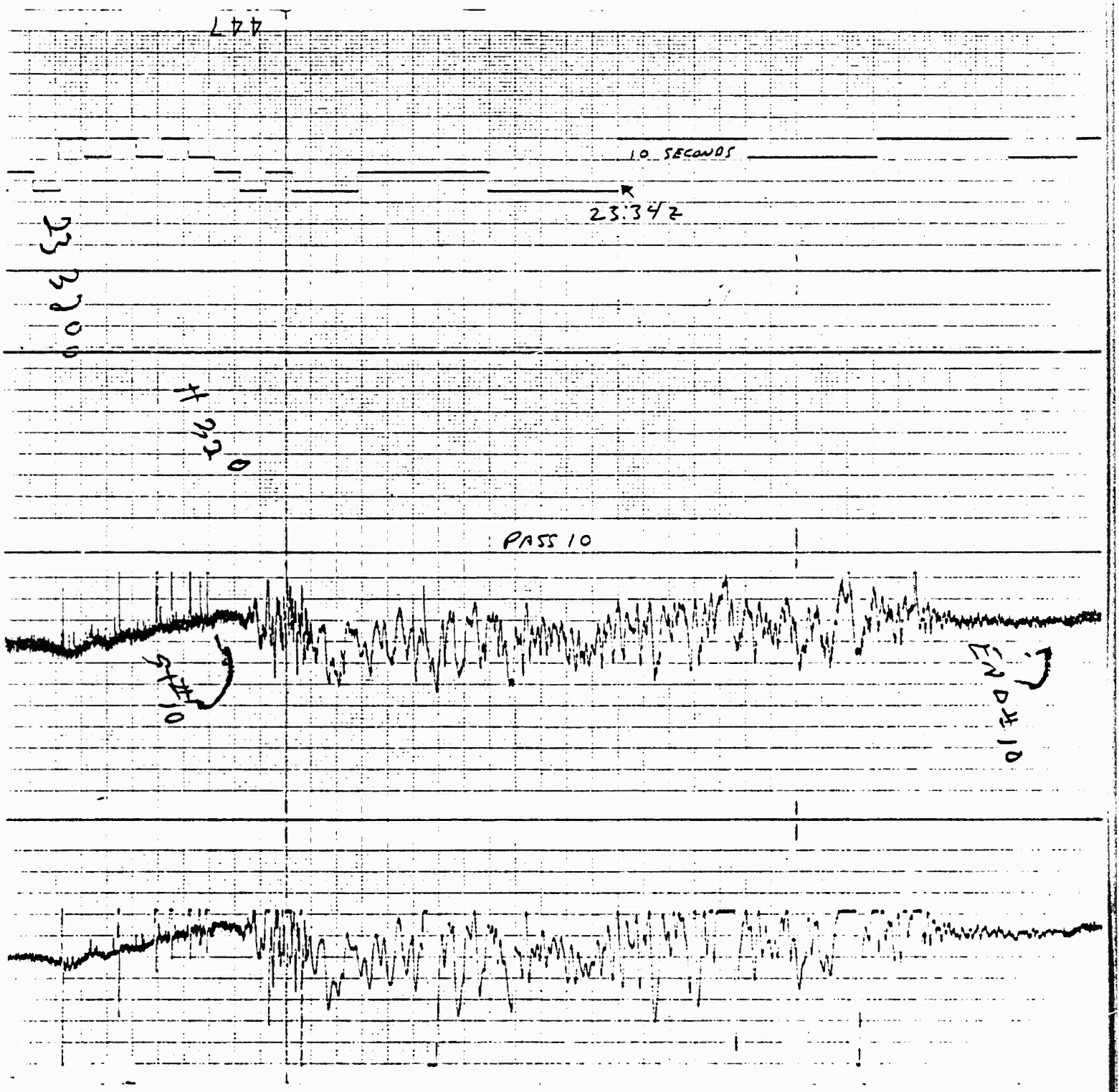

FIGURE 48 Rayleigh Like Downlink Fading on FERN Pass 10

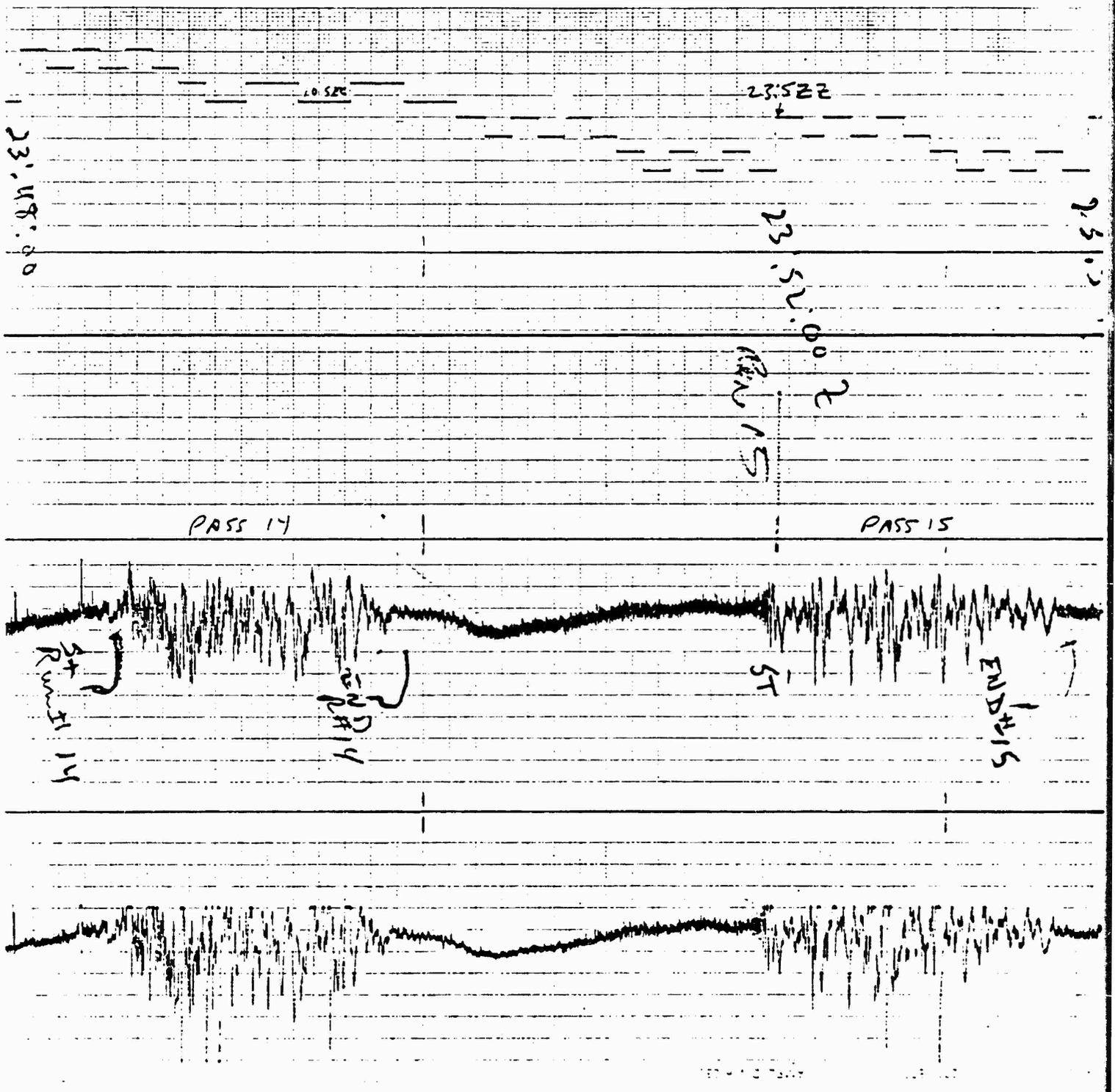

FIGURE 49 Rayleigh Like Downlink Fading on FERN Pass 14

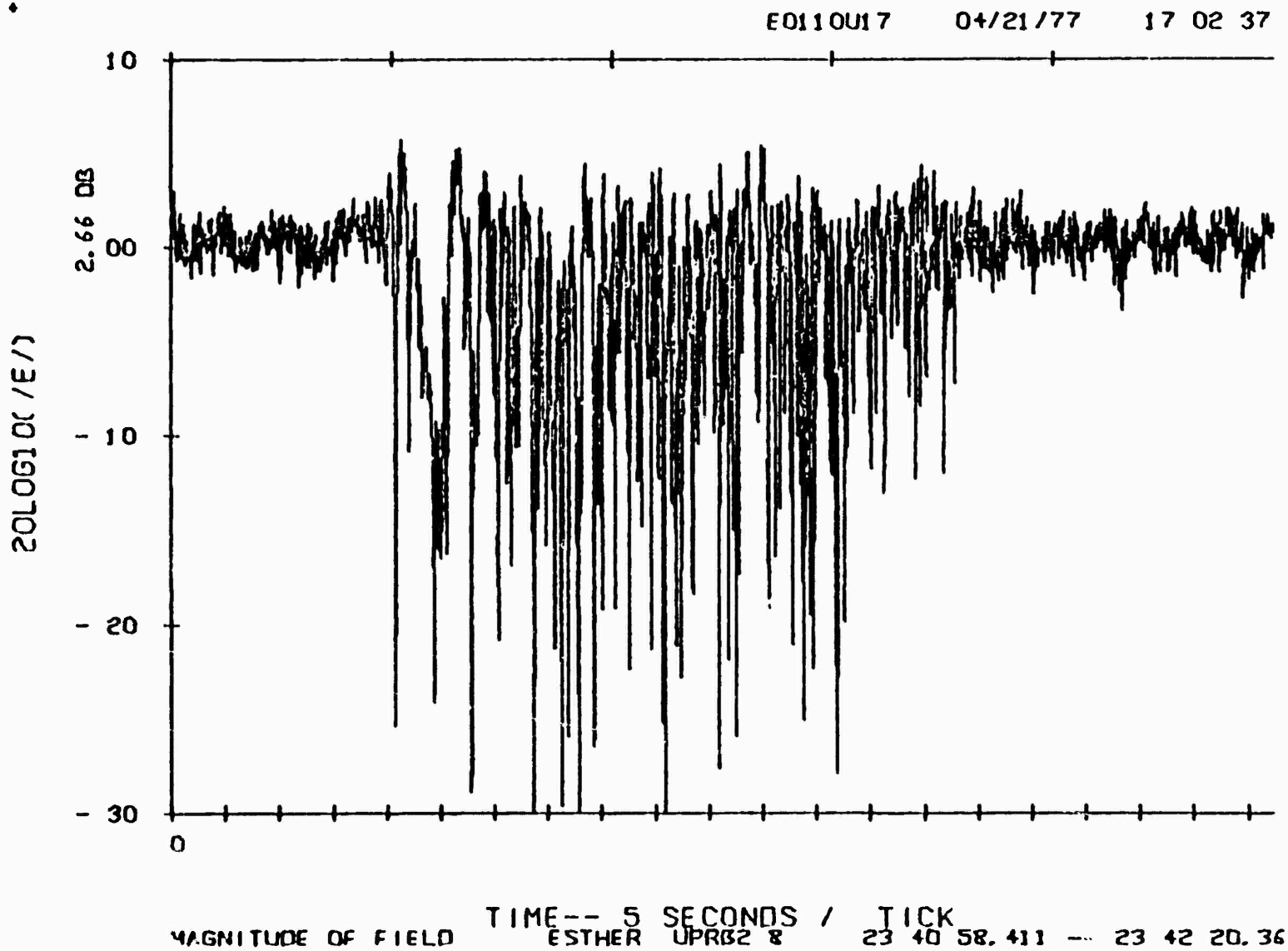

FIGURE 50 Rayleigh Like Uplink Fading on ESTHER Pass 8

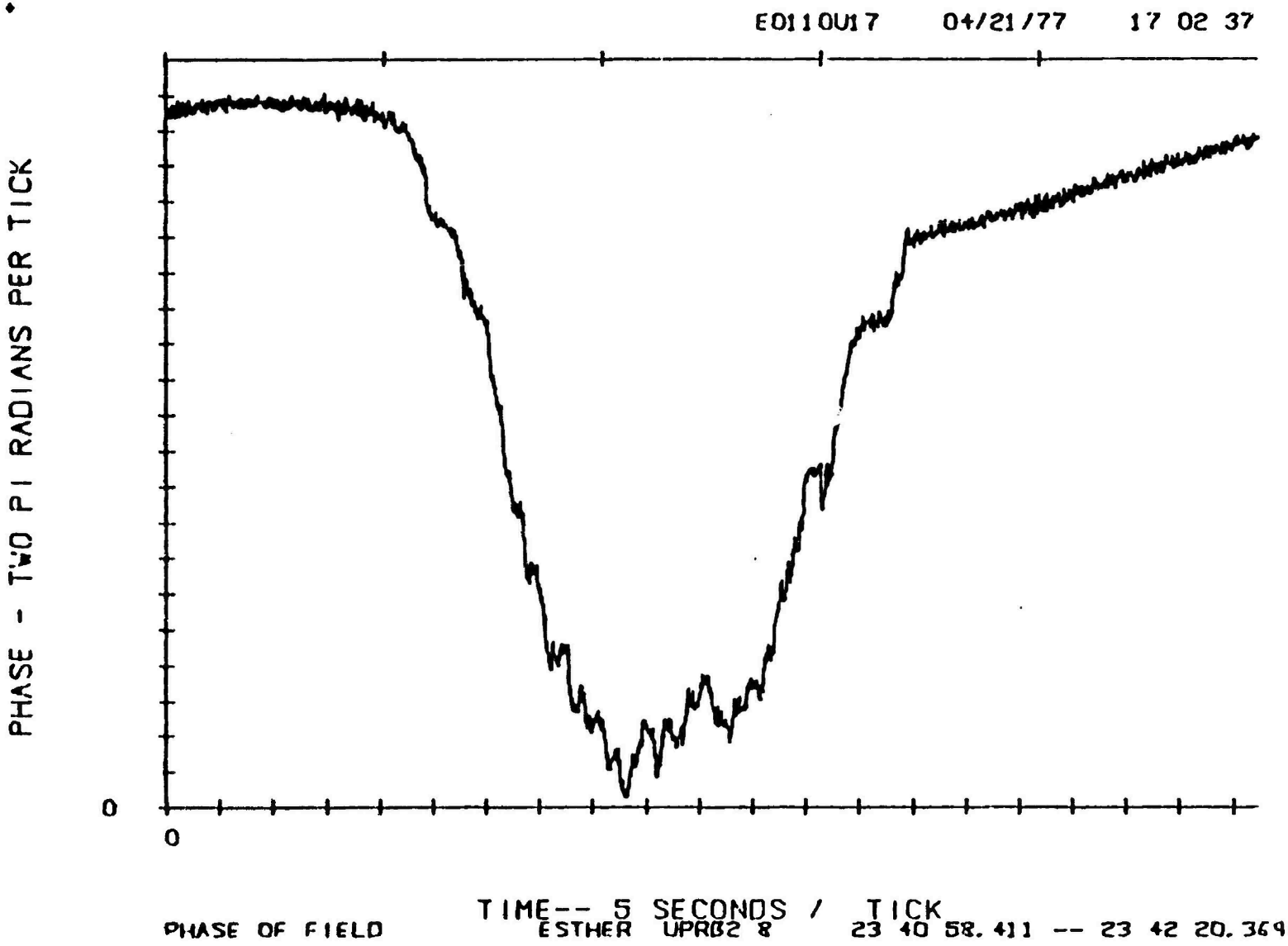

FIGURE 51 Uplink Phase Effects on ESTHER Pass 8

during the cross-striation patterns in that it was much slower. Figures 52 and 53 illustrate the uplink and downlink fading observed respectively during Pass 20 of ESTHER, which was a parallel pass. Figure 54 illustrates the downlink fading observed during a similar pass, Pass 20 of BETTY.

D. Rician-Like Fading: A weaker form of amplitude fading categorized as Rician-like was observed often. Figure 55 shows an example of this type of fading occurring on the uplink during Pass 14 of DIANNE. The fading is noticeably less intense than the Rayleigh fading seen in Figures 46 to 50. Weaker fading such as this is observed more often later in the cloud development and may be attributable to weaker striations and/or poorer cloud tracking. The phase observed on this DIANNE pass, Figure 56, indicates a less intense cloud than seen earlier in the release.

E. Frequency Decorrelation -- Test 3 & Downlink Hop: Comparison of the uplink and downlink tone indicates considerable decorrelation of the fading due to the frequency difference of 90 MHz. Examples of the test configuration #3 uplink and downlink fading for ESTHER, Pass 18, are shown in Figures 57 and 58. Many of the gross features are duplicated in the plots. However, the actual fading generally appears decorrelated. A cross correlation of the received powers on the uplink and downlink produced the plot in Figure 59. A peak of .16 rises significantly out of the noise (with typical peaks of .08) with a relative delay of .9 seconds, versus a completely correlated value of about 1. Degradable by noise on either link, the .16 value reflects considerable but not complete decorrelation.

The downlink UHF hopping signal received on the aircraft was recorded on magnetic tape for further analysis of the spectral decorrelation across the hopping band. By processing the received amplitude with the gross frequency

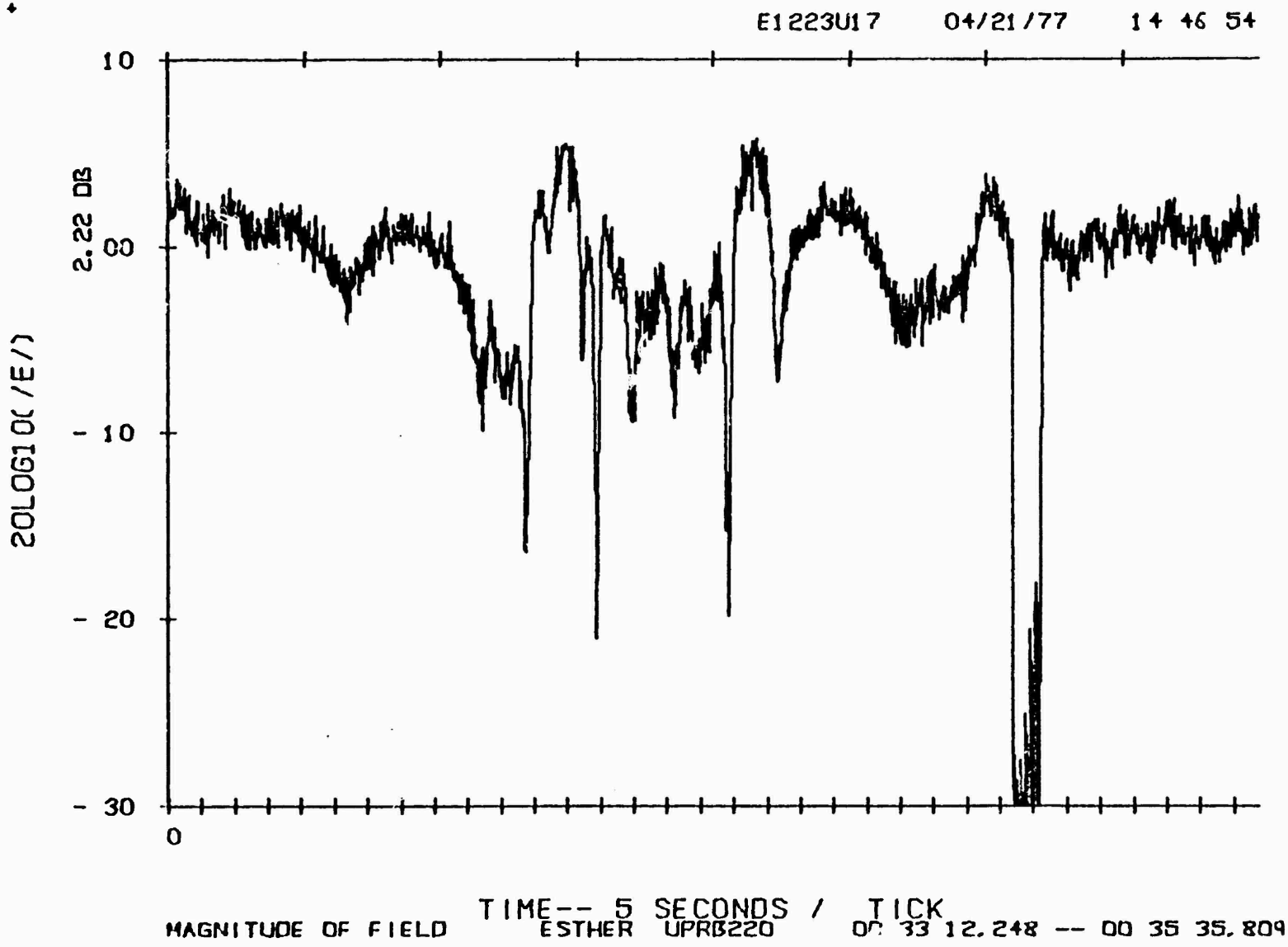

FIGURE 52 Parallel Pass Uplink Fading on ESTHER Pass 20

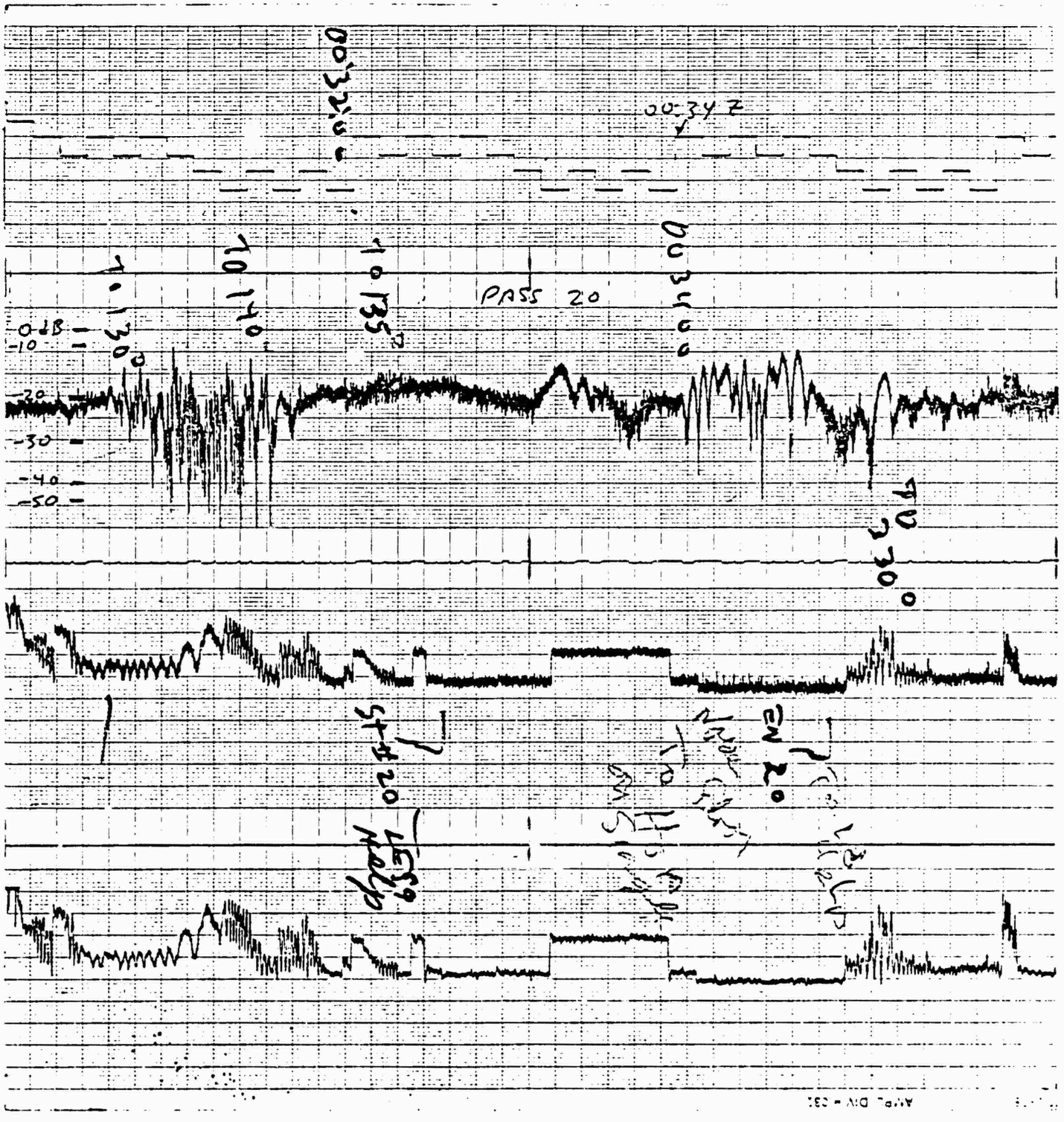

FIGURE 53 Parellel Downlink Fading on ESTHER Pass 20

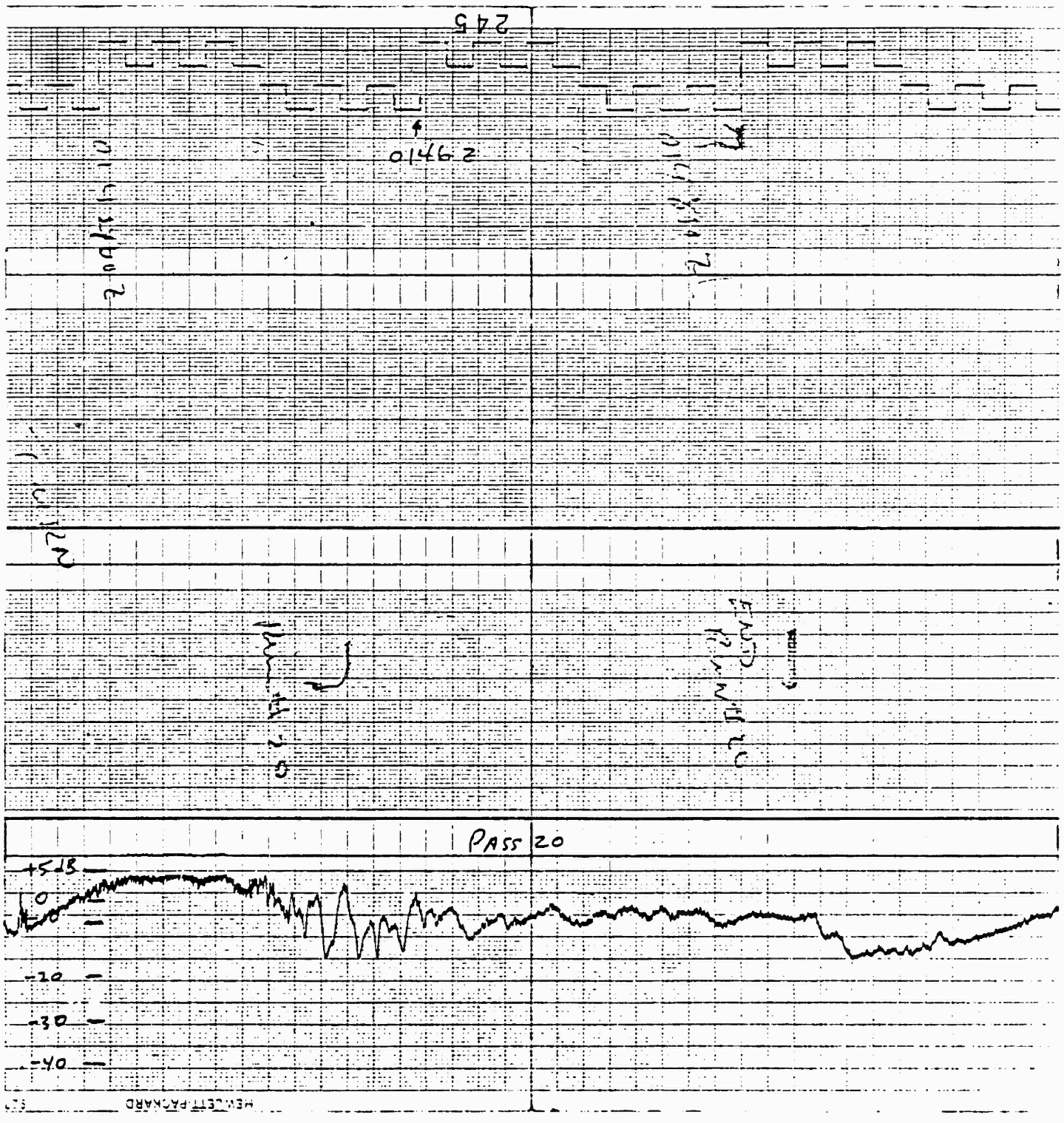

FIGURE 54 Parallel Pass Downlink Fading on BETTY Pass 20

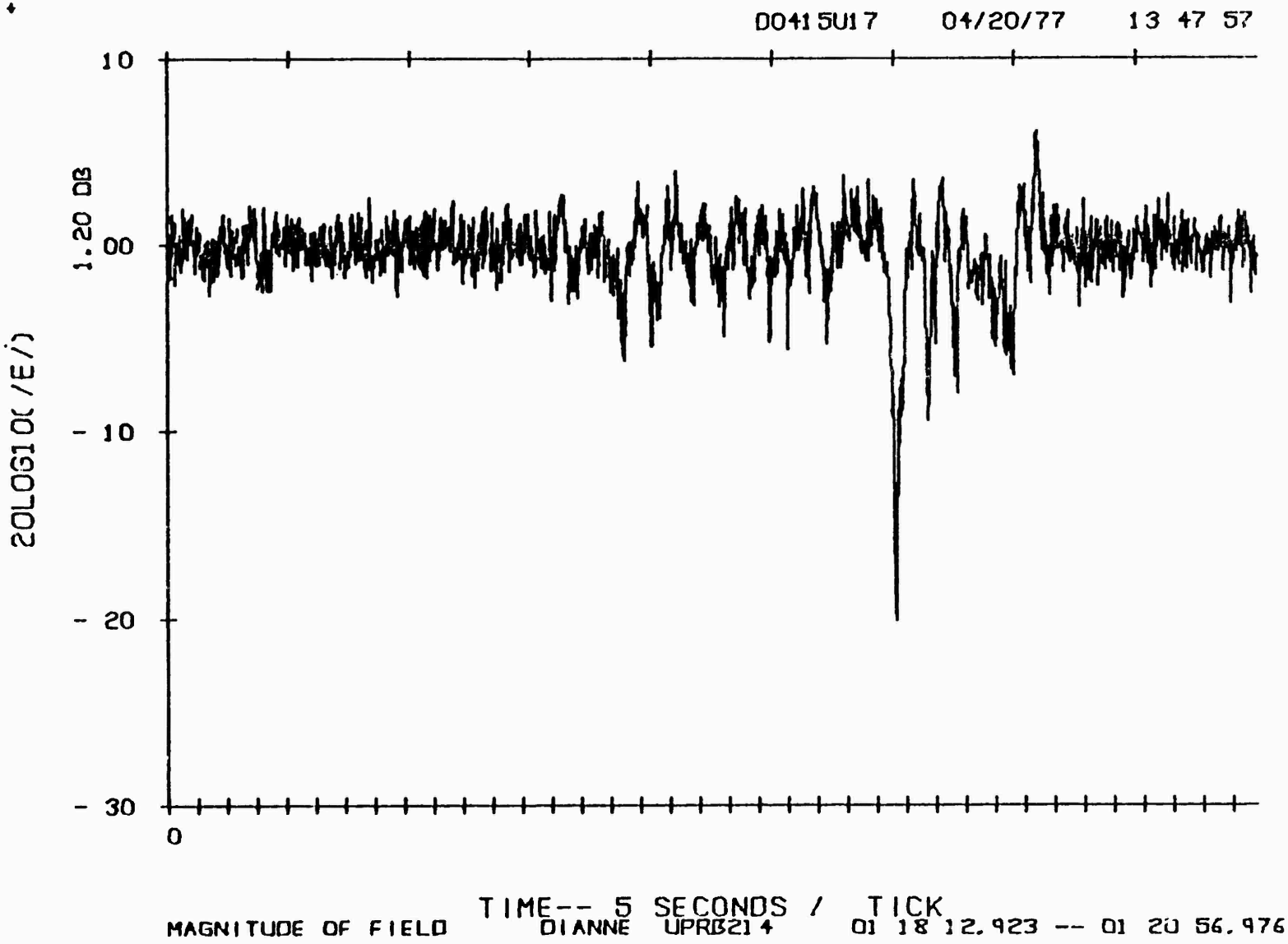

FIGURE 55 Rician Like Uplink Fading on DIANNE Pass 4

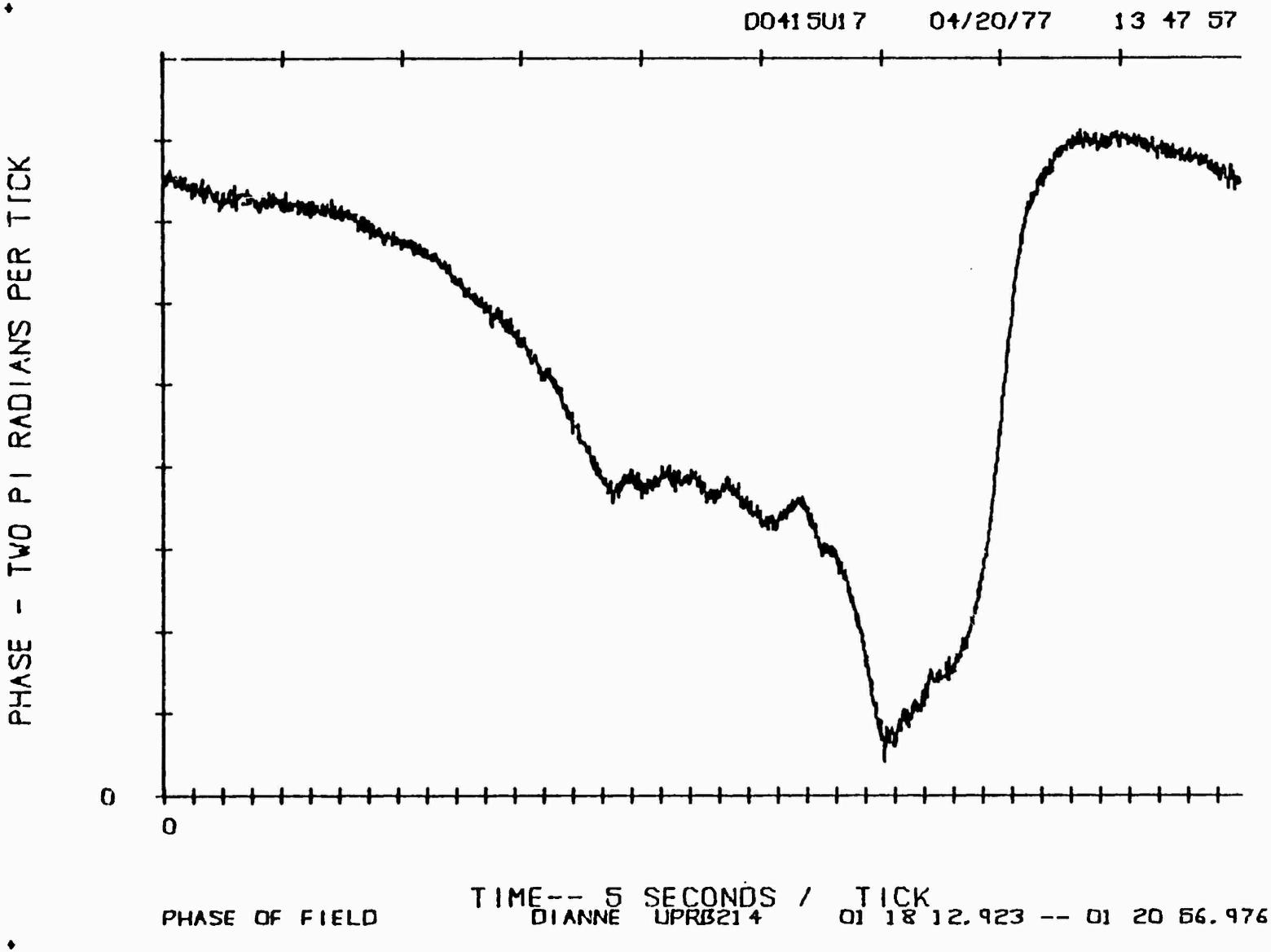

FIGURE 56 Uplink Phase Effects on DIANNE Pass 4

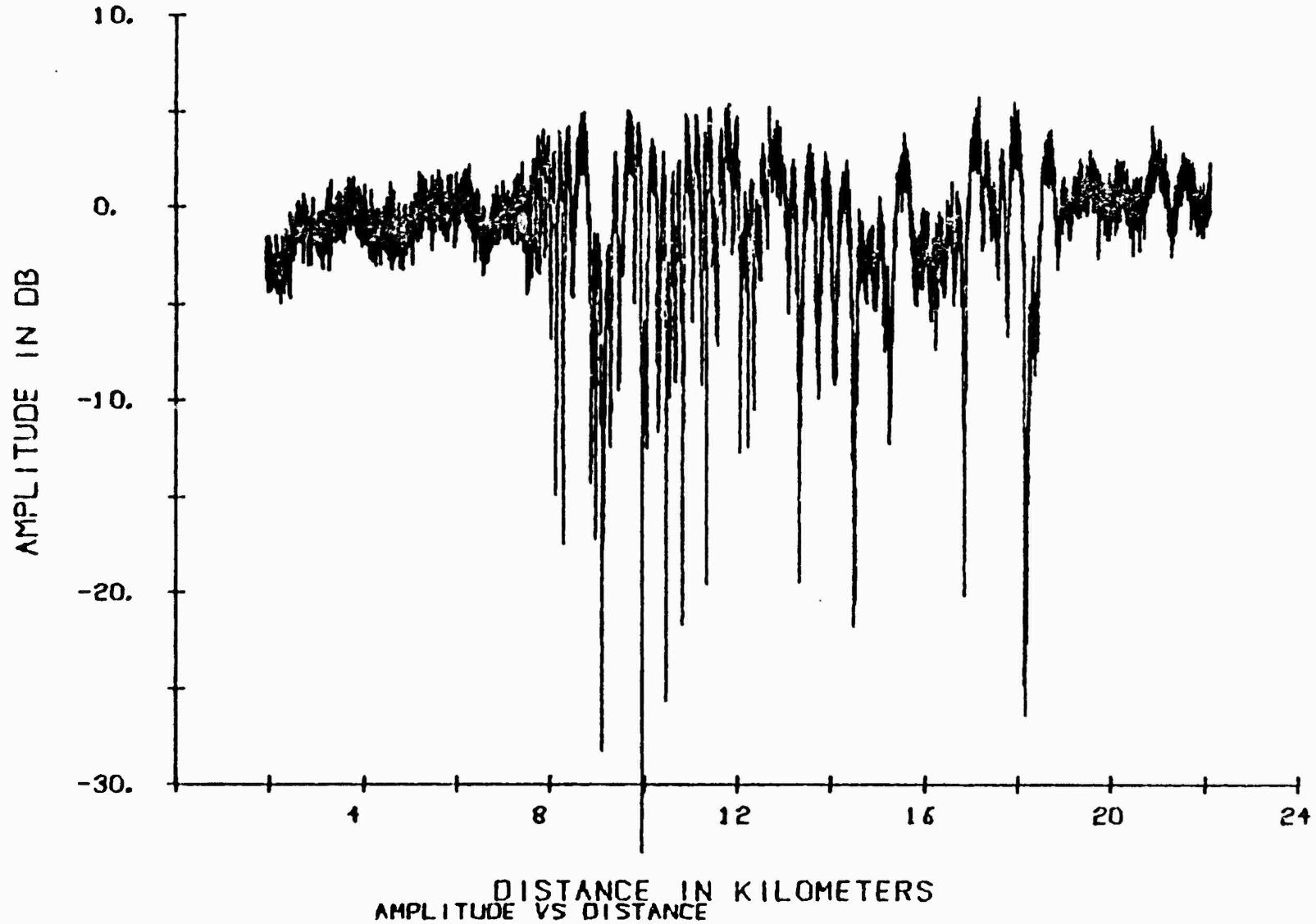

FIGURE 57 Uplink Fading on ESTHER Pass 18

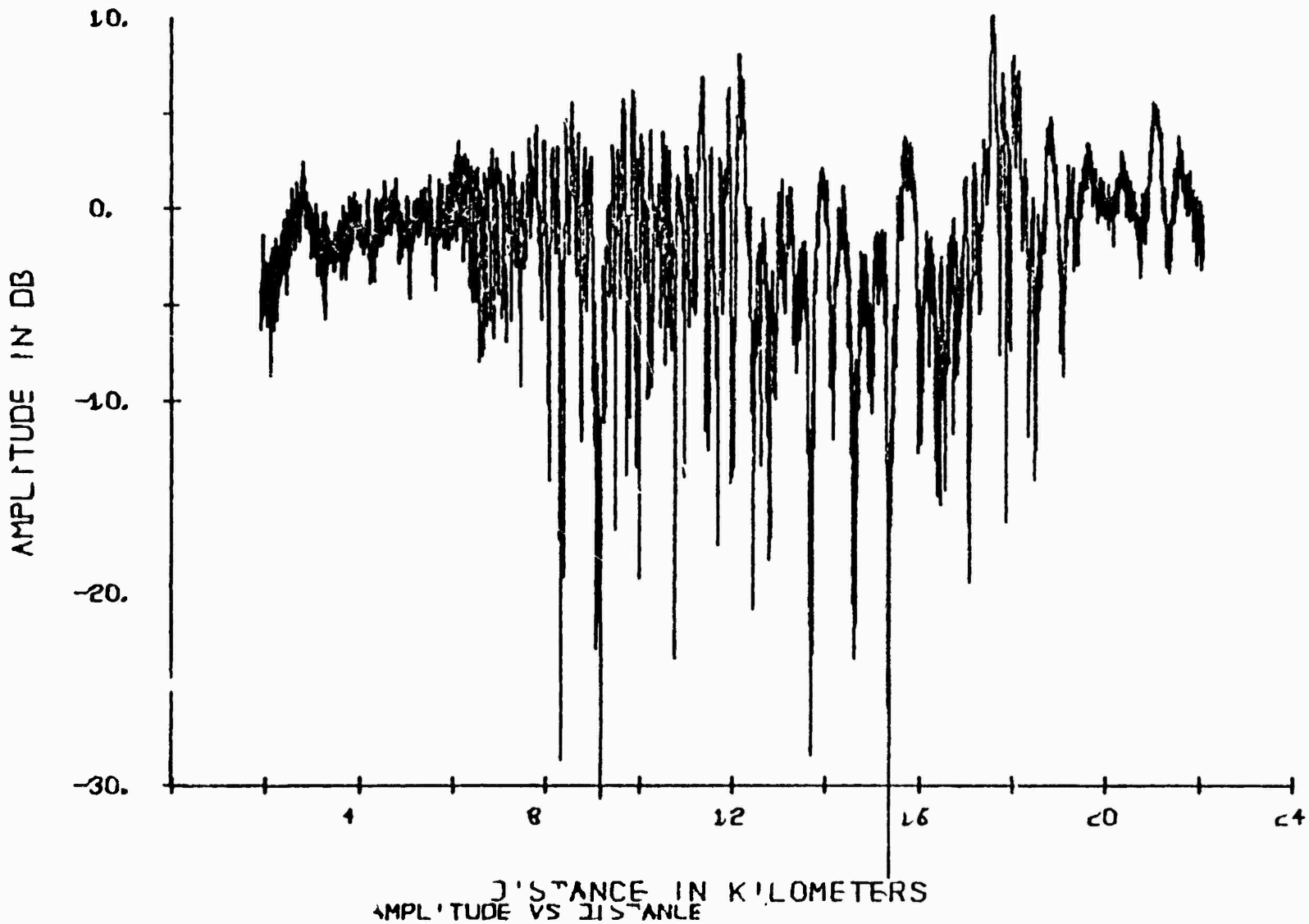

FIGURE 58 Downlink Fading on ESTHER Pass 18

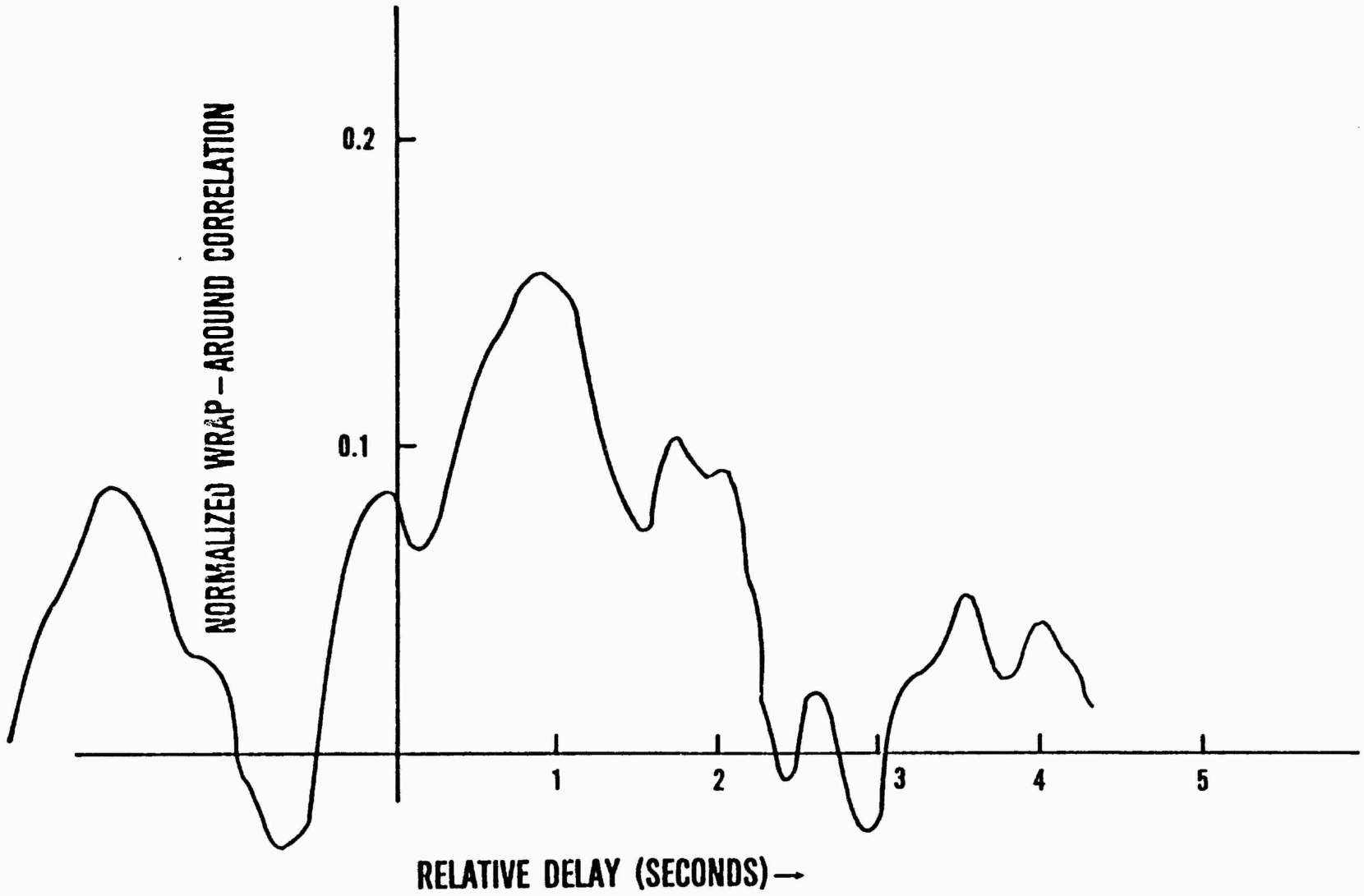

FIGURE 59 Cross Correlation of Uplink and Downlink Fading ESTHER Pass 18

command the decorrelation across the hopping band can be assessed. Visual inspection of this data indicates a potential decorrelation across the band during the early-time passes in ESTHER for fading corresponding to the multipath-like ringing.

F. Systems Effects: The teletype copy received on the UHF down forward link was protected against moderate fading by powerful error-correction coding techniques employing a half-rate code with feedback decoding and full message interleaving. The teletype copy remains basically error free until a channel binary symbol error rate of between 5 and 10 per cent was reached. At that time the teletype copy either exhibited a few errors or did not print due to a print/no-print threshold which excludes all messages exhibiting more than a limited number of errors. The observed range in UHF signal level between the perfect copy and no message copy is rather narrow, on the order of 3 or 4 db for performance in white noise only. Figure 60 is an example of error free copy, while Figure 61 shows a limited number of character errors. Figure 62 shows a larger number of character errors, and Figure 63 is an example of a STRESS pass where most messages were not copied due to the high error rate.

Figure 64 shows a plot of the percentage of messages received correctly versus received signal strength (C)-to-thermal noise power density (N_o) [in inverse Hz] for all passes with significant fading in ESTHER. Also plotted is the system performance without fading that depicts the narrow range between print and no-print. In spite of the full message interleaving (which ideally would average out the received bit energies through fades and focuses) a loss of at least 5 db can be ascribed to the barium induced fading. This loss appears to be dependent upon the nature of the fading, the slower fading characteristic of a late-time barium cloud causing a greater loss.

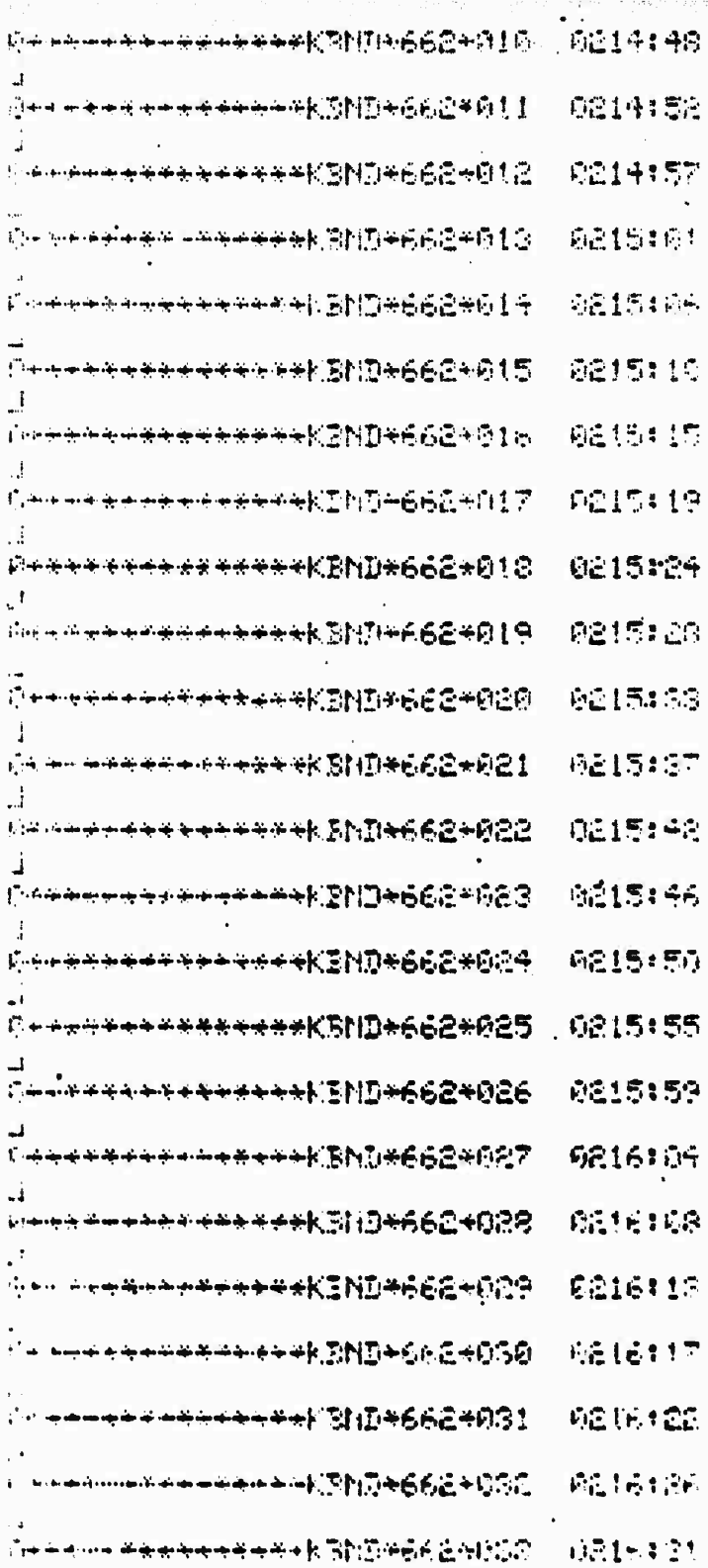

FIGURE 60 Error Free Teletype Copy

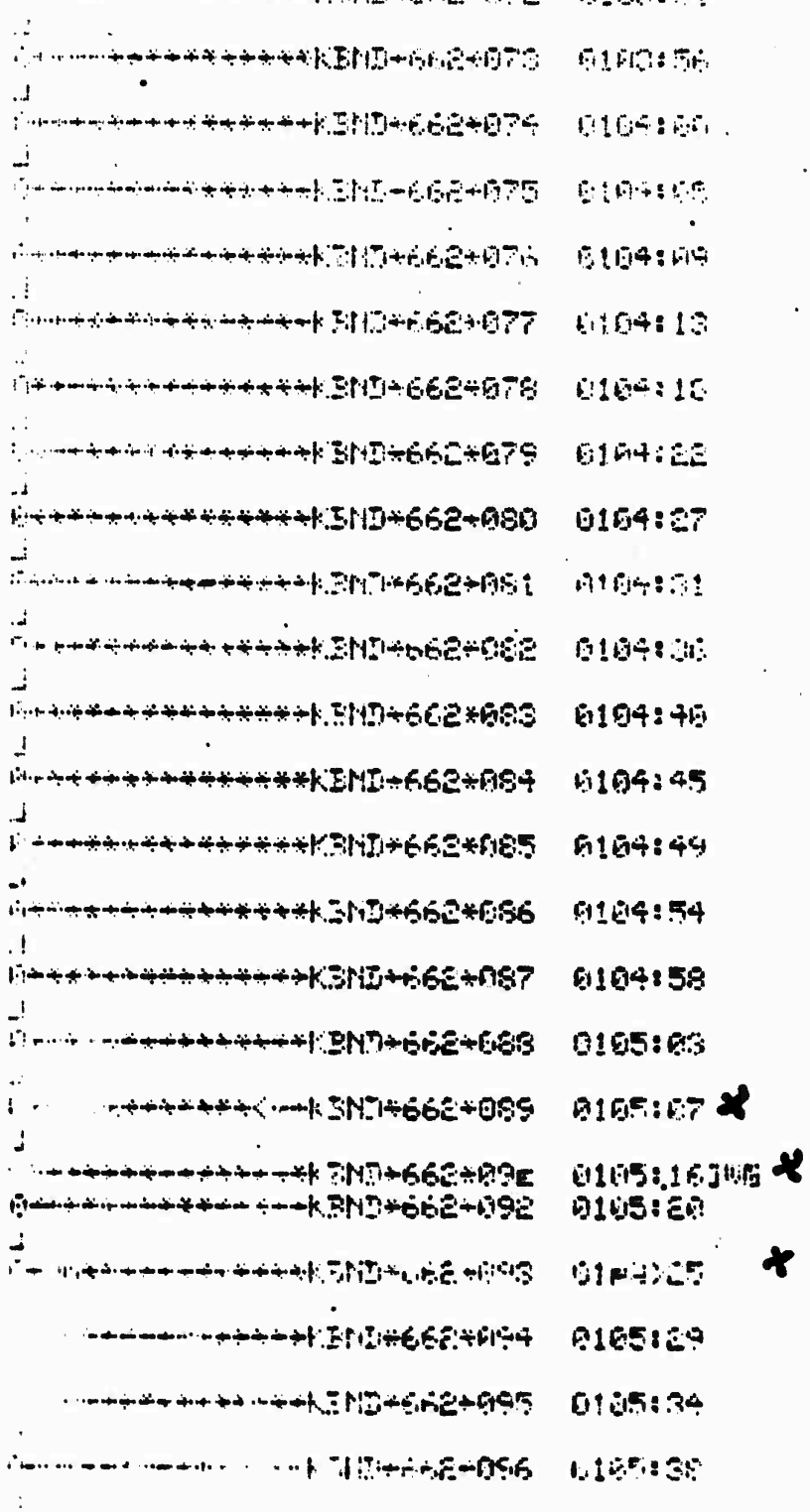

FIGURE 61 Teletype Copy with Limited Errors

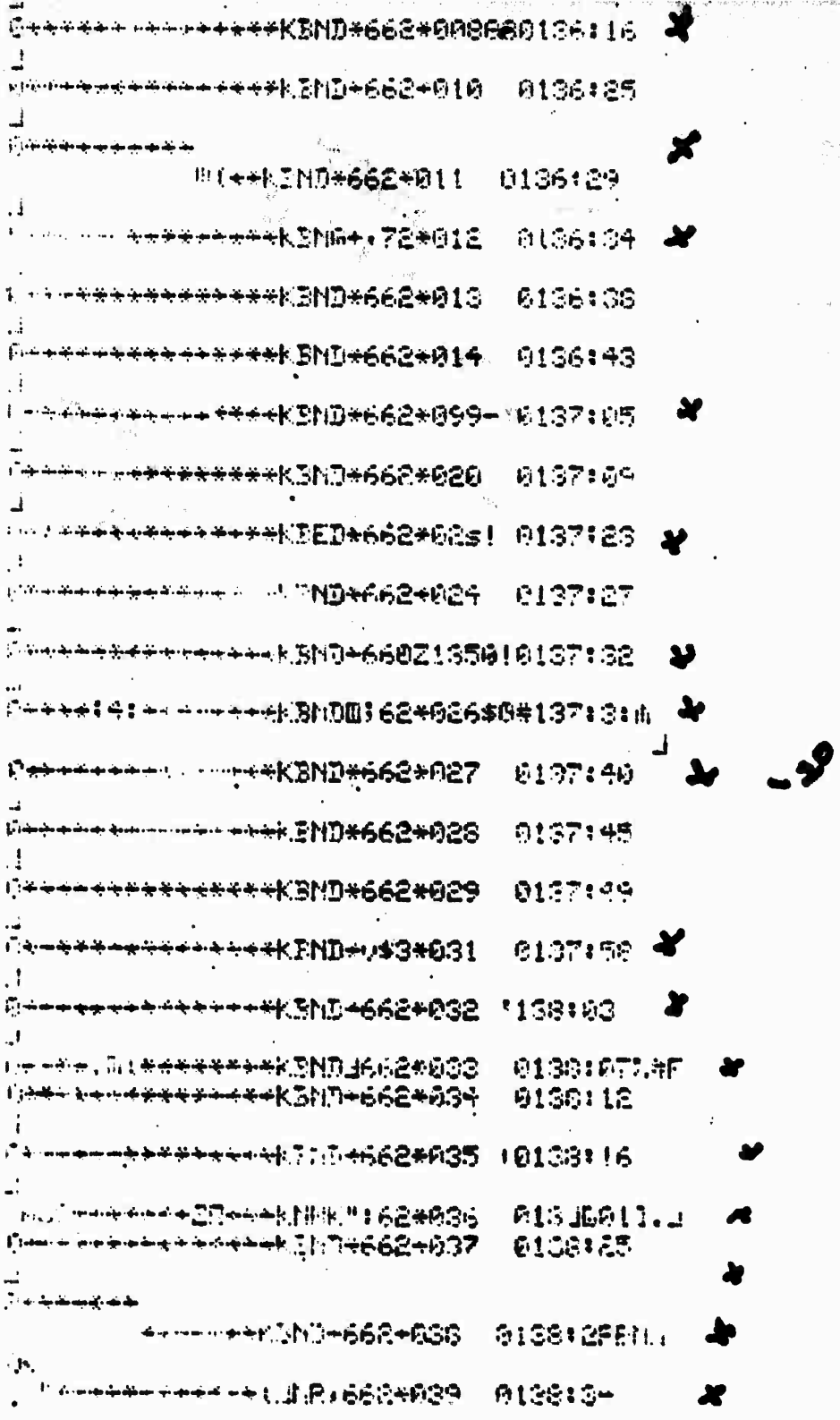

FIGURE 62 Teletype Copy with Moderate Errors

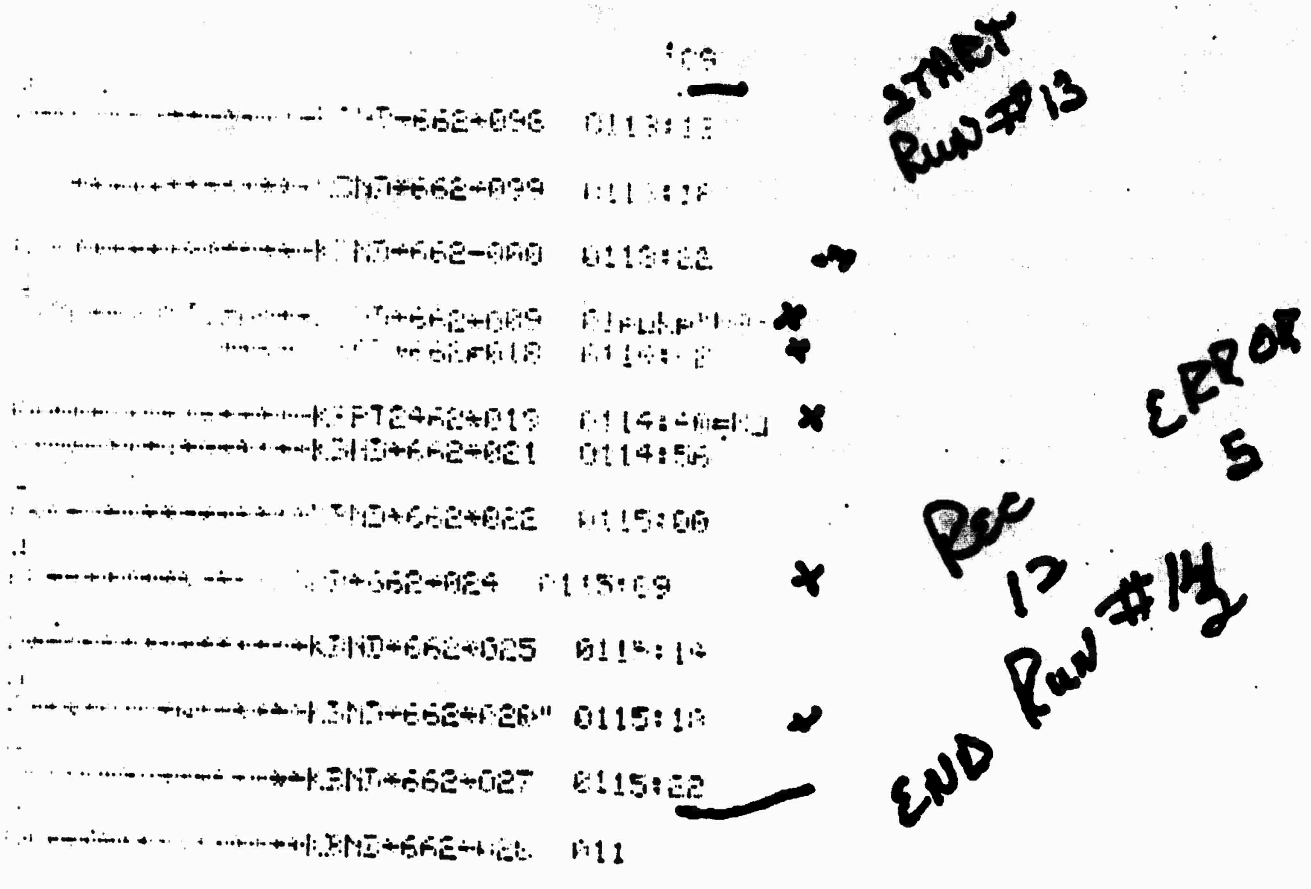

FIGURE 63 Teletype Copy with Many Errors and Deleted Messages

REGULAR MODE ESTHER	PERCENT OF MESSAGES RECEIVED

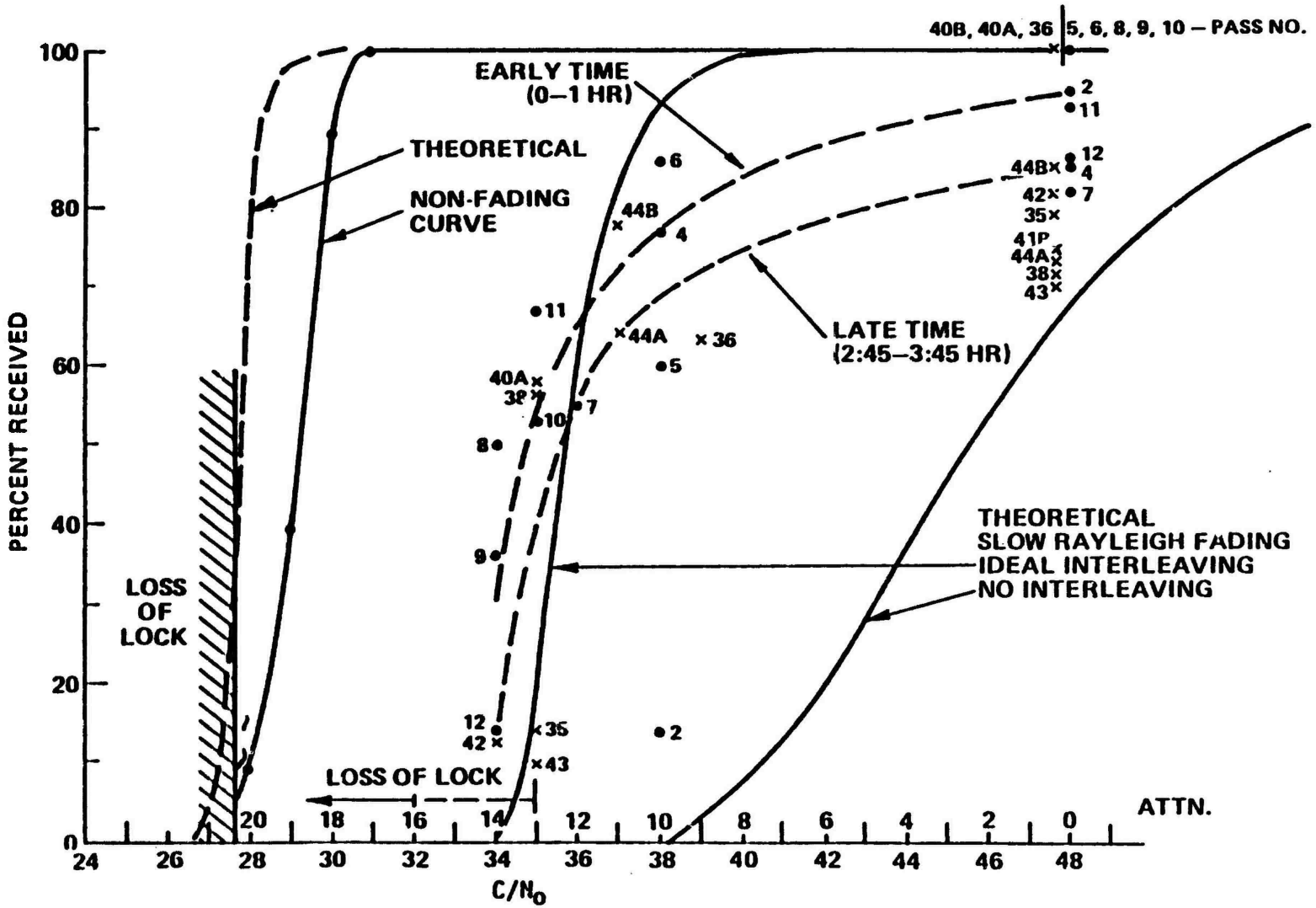

FIGURE 64 Per Cent Messages Received vs. C/No for ESTHER

G. System Effects - Frequency Decorrelation: A comparison was made on the UHF down forward link between a help mode which is a fixed downlink frequency and a hopping mode which hops over a relatively narrow frequency bandwidth. On Pass 8 of the fifth test (FERN) the forward downlink was in the fixed frequency mode (help). Figure 65 shows the received signal level for Pass 8. Also shown on Figure 65 are the UHF link quality for each message and the message character error rate. Approximately 5 minutes after the Pass 8 data the satellite was put in the hopping mode, and data from Passes 9 and 10 can be compared with Pass 8. From Figures 66 and 67 it is obvious that the fading structure remained very similar to that encountered during the fixed frequency Pass 8. The UHF link quality showed no improvement which could be attributed to the frequency diversity of the frequency hopping mode. Likewise, the character error rate per message was no better than that for Pass 8. Table 8 shows a comparison of the average link quality over the 60 seconds of fading for each pass. These results show no improvement for the frequency diversity effect of the frequency hopping on Passes 9 and 10. If the propagation medium exhibited frequency decorrelation, some performance improvement would be expected in the hop mode. Lack of an obvious improvement indicates that the FERN propagation environment traversed was not strong enough to produce significant frequency decorrelation across the downlink hop band.

H. Multipath Test Results: Good quality multipath data was taken during the ESTHER and FERN test flights using LES 9 while the barium fading measurements were being simultaneously performed using LES 8. During ESTHER the aircraft transmitted a PRN sequence from either one of two antennas, the crossed slot and the bottom blade, while during the FERN flight test

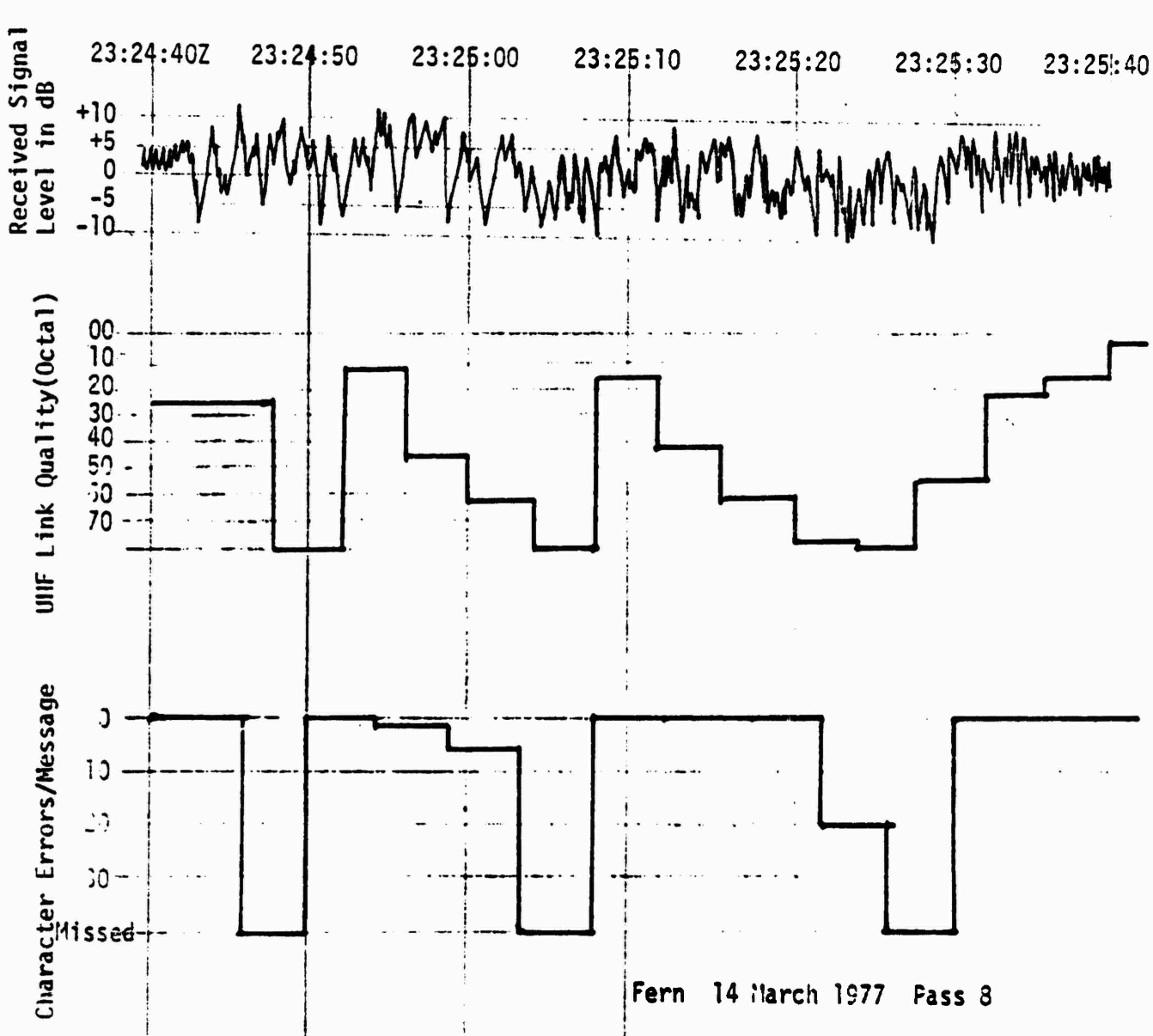

FIGURE 65

Comparison of Signal Level, Link Quality and Character Errors

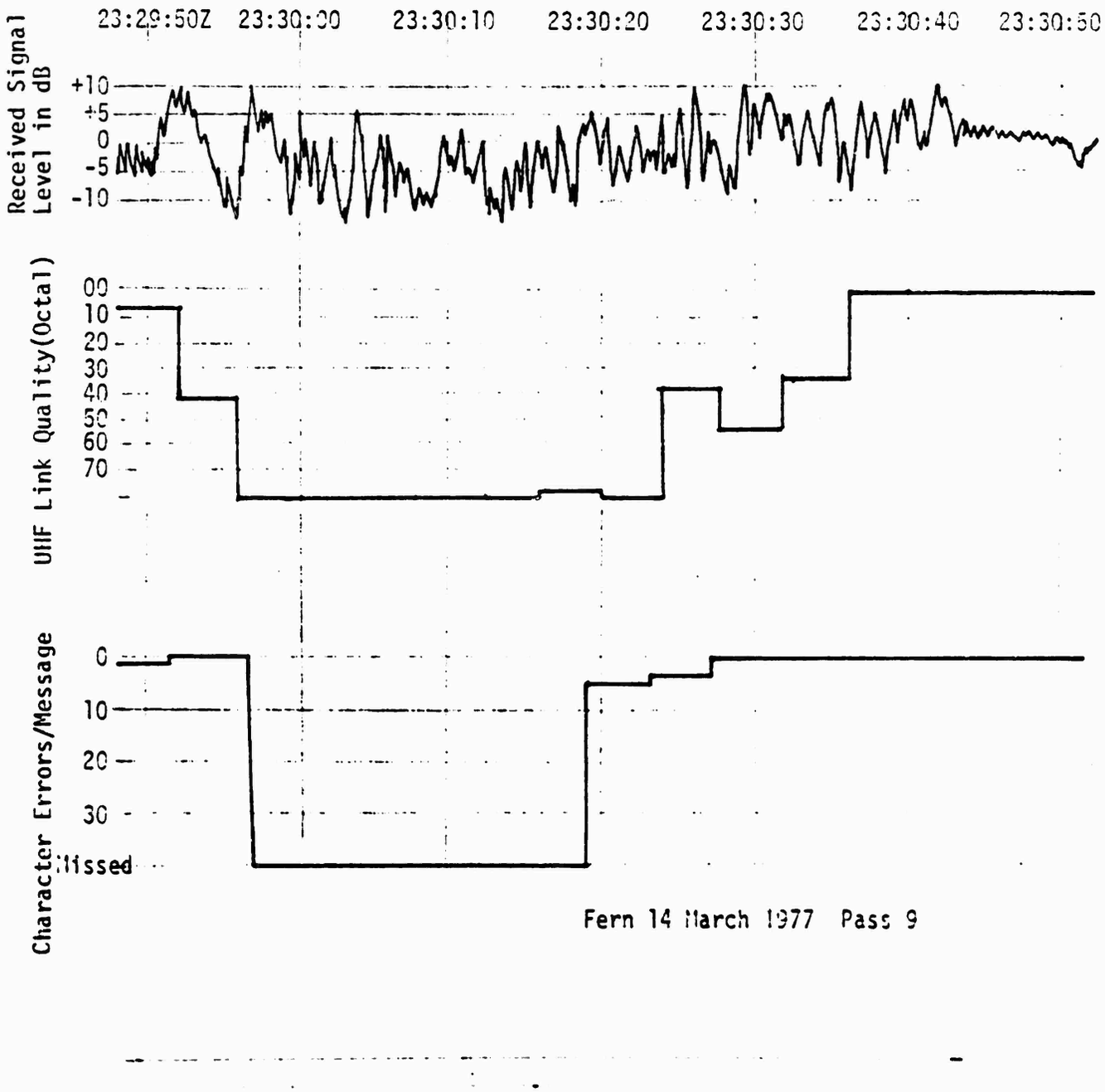

FIGURE 66

Comparison of Signal Level Link Quality and Character Errors

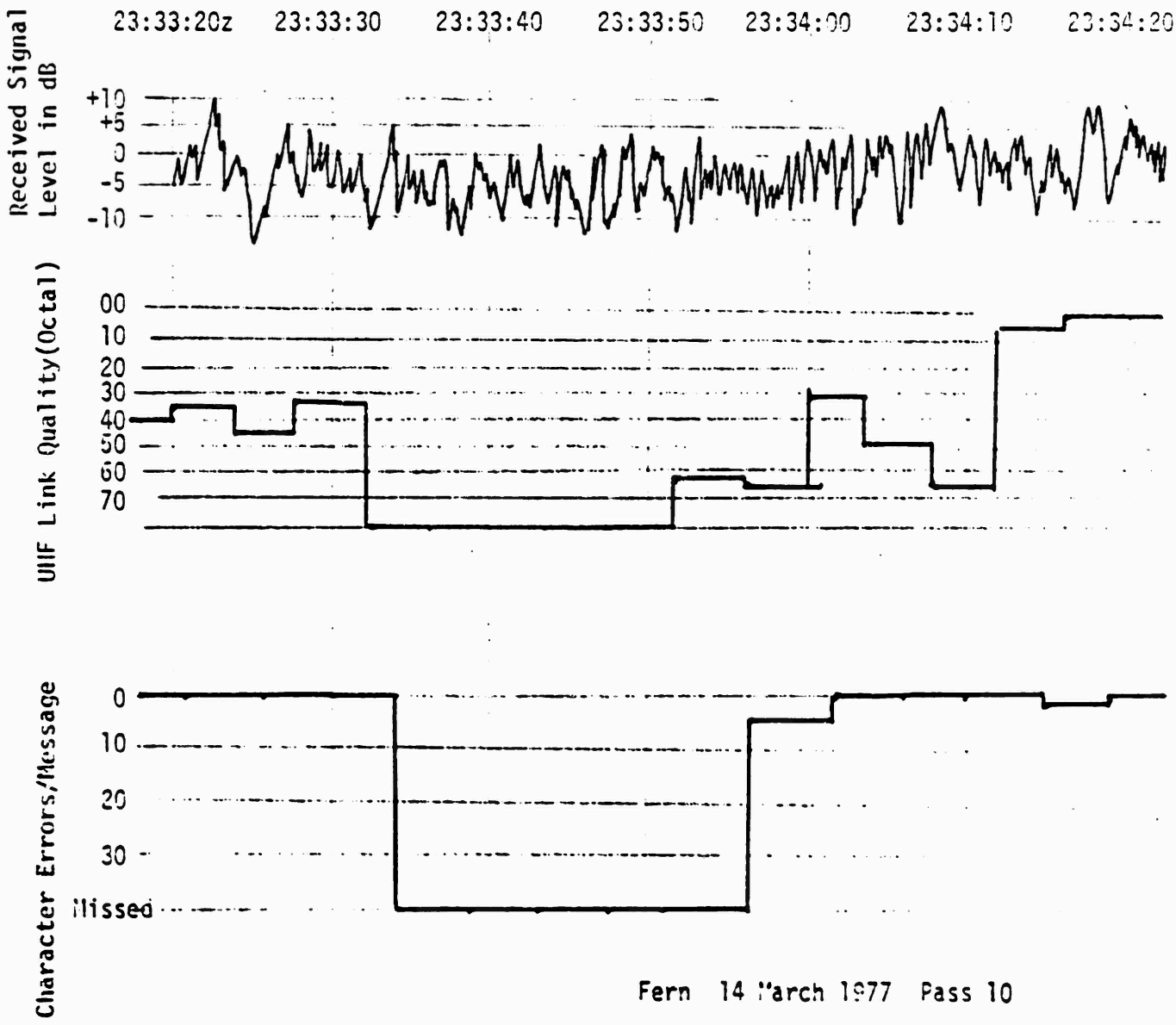

FIGURE 67

Comparison of Signal Level Link Quality and Character Errors

PASS #	MODE	Avg. UHF L.Q.
8	Help	47
9	Hop	54
10	Hop	54

TABLE 8: Comparison of UHF Link Quality For Different Modes

only the bottom blade was used. The PRN correlation receiver at the rooftop facility (RTF) received over 600 returns during the seven-hour ESTHER flight and over 220 returns during the five-hour FERN flight. The nature of the ESTHER returns is summarized in Table 9, which gives the antenna type used and the terrain flown over. Four types of returns were received: crossed slot land returns, crossed slot sea returns, bottom blade land returns, and bottom blade sea returns.

The land returns received during ESTHER from the crossed slot antenna, Figure 68, consisted of one or two peaks rising out of an approximate -146 dbm noise level. The first peak received was the main path signal, typically arriving at the receiver pre-amp with a -115 dbm level. Link calculations of power level received by the RTF helix from the LES 9 low power transmitter give similar numbers indicating that the main path signal-to-noise ratios at the input to the satellite transponder is greater than unity as expected. The main path correlation peak typically had no noise fluctuations greater than the resolution of the strip chart pen. The second peak, when observed, was the land bounce multipath or reflected signal. This signal typically had a -141 dbm received signal level with ±2 db instantaneous fluctuations. The reflected path peak shape was typical of the upper portion of the main path shape indicating an effectively (to the limitation of the noise) specular reflection. Typical delays between the main path and reflected signals were of the order of 12 seconds representing propagation time delays of 40 to 50 microseconds, consistent with aircraft altitude and satellite elevation.

The sea returns received from the crossed slot, Figure 69, were similar to the land returns in nearly all aspects. The prime difference was that the sea multipath returns were received at a level of -133 dbm with ±3 db instantaneous fluctuations in contrast to the -141 dbm land multipath value.

Table 9: ESTHER Multipath Data

	Ant	Return #'s	Approx. Time	Terrain
1	XS	1 - 18	2138 - 2145	Land
		Calibration	2145 - 2200	Land
	BB	19 - 50	2200 - 2230	Land
2	XS	51 - 117	2230 - 2253	Land
		118 - 137	2253 - 2300	Both Land & Sea
	BB	137 - 189	2300 - 2334	Land & Sea
3	XS	190 - 221	2335 - 2354	Land & Sea
		221 - 234	2354 - 0002	Sea
	BB	235 - 388	0002 - 0135	Sea
4	XS	389 - 432	0135 - 0201	Sea
	BB	433 - 475	0211 - 0236	Sea
5	XS	476 - 510	0236 - 0250	Sea
		511 - 523	0250 - 0306	Land
	BB	524 - 555	0306 - 0337	Land
6	XS	556 - 588	0337 - 0405	Land
	BB	589 - 621	0405 - 0436	Land/Landing

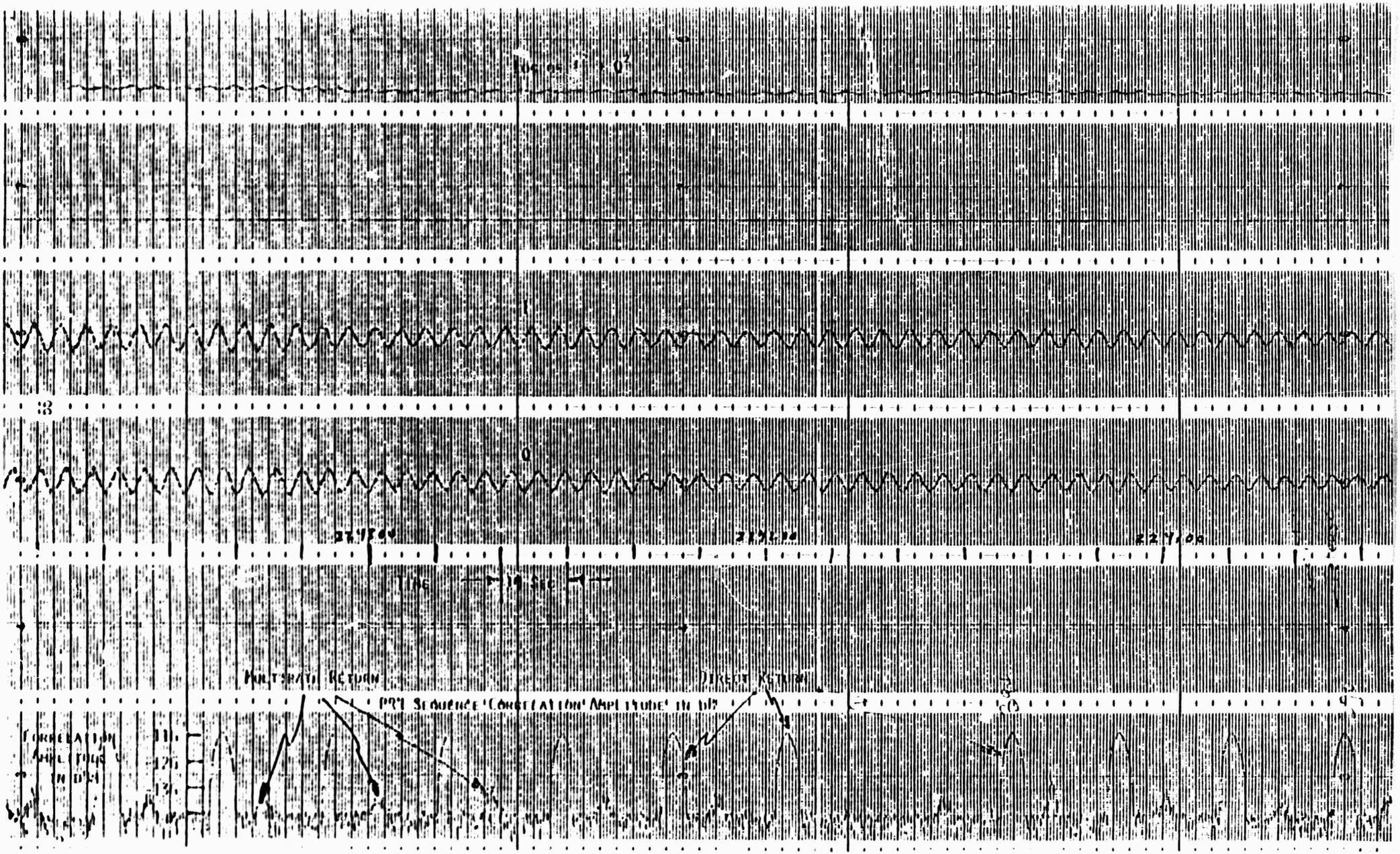

FIGURE 68 Over Land Multipath PRN Correlation Return, Cross Slot Antenna

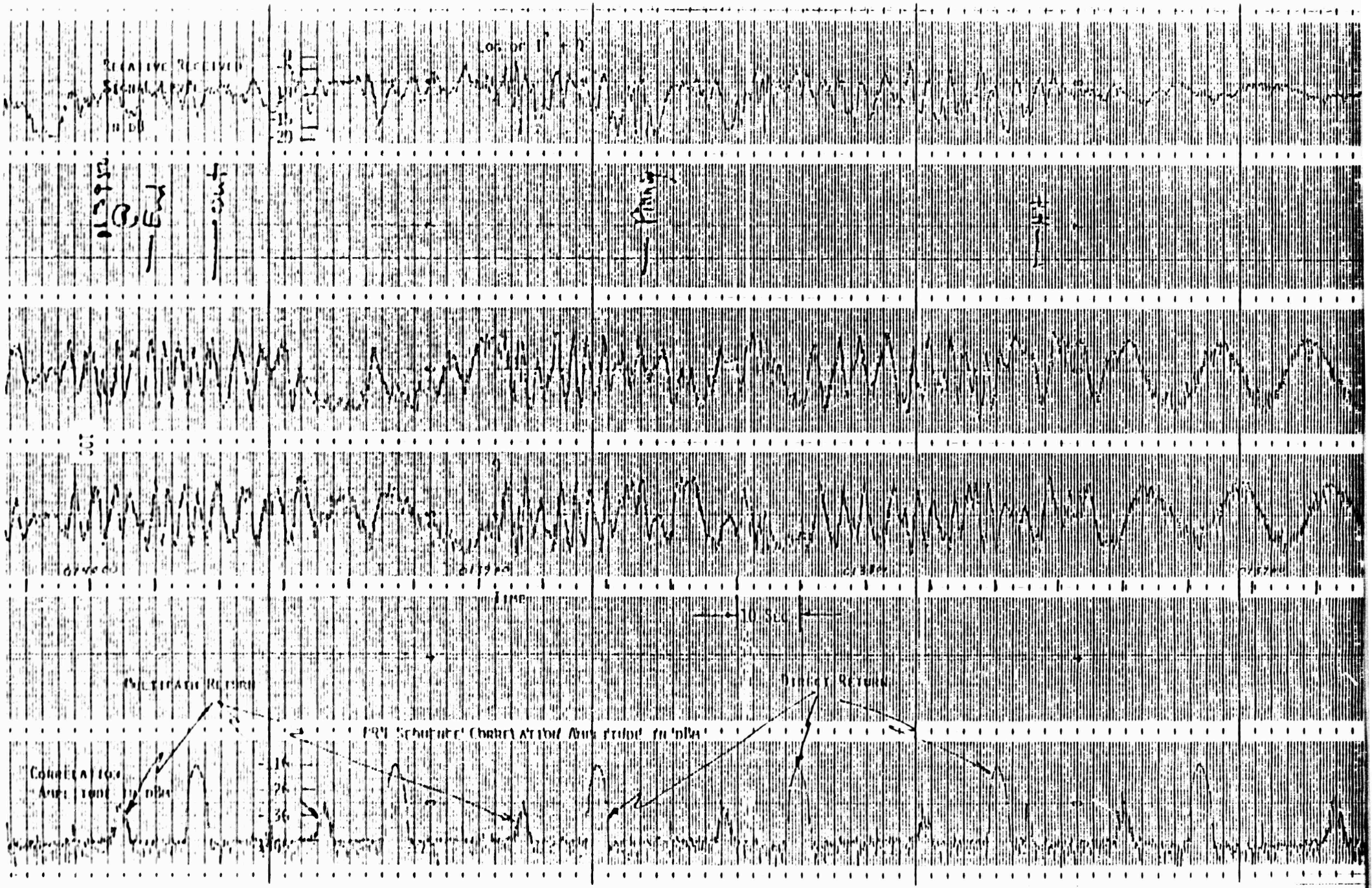

FIGURE 69 Over Water Multipath PRN Correlation Return, Cross Slot Antenna

The land returns received from the bottom blade, Figure 70, were similar to the crossed slot returns in that two similar peaks could be identified. The main path peak represented signal leakage around the aircraft fuselage (with subsequent propagation to the satellite) and its level fluctuated slowly from -118 dbm to -135 dbm on a return-by-return basis. A signal level of -123 dbm represents a nominal return. Typicaliy the main path signal did not fluctuate instantaneously. The multipath peak was typically received with a -128 dbm level with ±3 db instantaneous fluctuations. The onset of this peak corresponded to a 50 microsecond delay from the onset of the main path peak. Nearly 8 microseconds after the onset of the multipath peak a constant signal level 3 db out of the noise was received for more than 100 microseconds.

The sea returns received from the bottom blade, Figure 71, differed from the land returns in a few ways. The main path signal was received with a level that was lower than the land received signal (probably a geometry effect), -132 dbm. It differed from the land main path signals in that ±1 or ±2 dbm instantaneous fluctuations were evident in addition to the expected returns by return fluctuation. The most obvious difference was that the reflected received signal level was a very strong -117 dbm typically with ±2 db fluctuations. Also, the multipath delay profile neither appeared as consistently as in the land return , nor persisted to such long time delays.

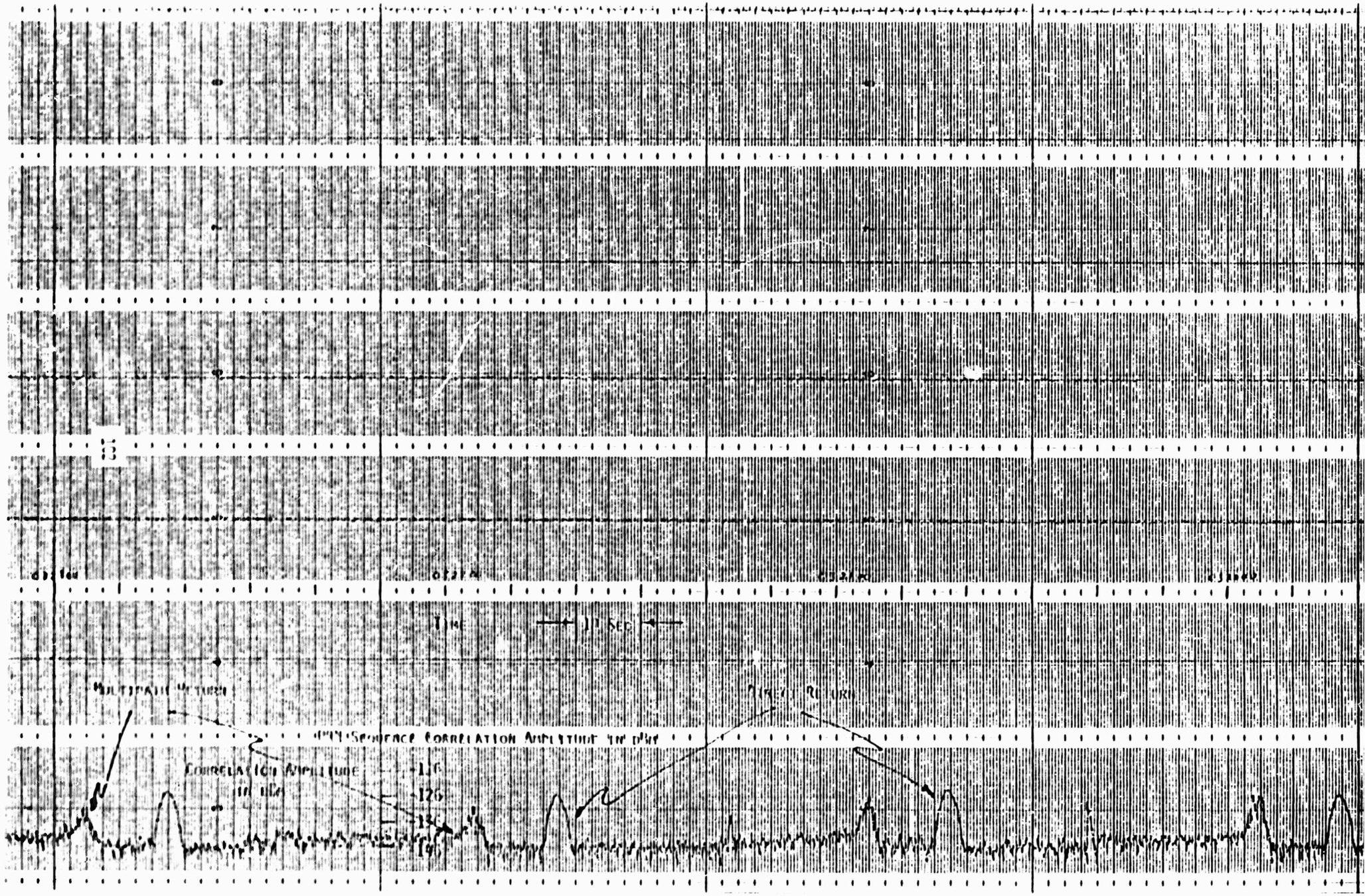

FIGURE 70 Over Land Multipath Correlation Return, Bottom Blade Antenna

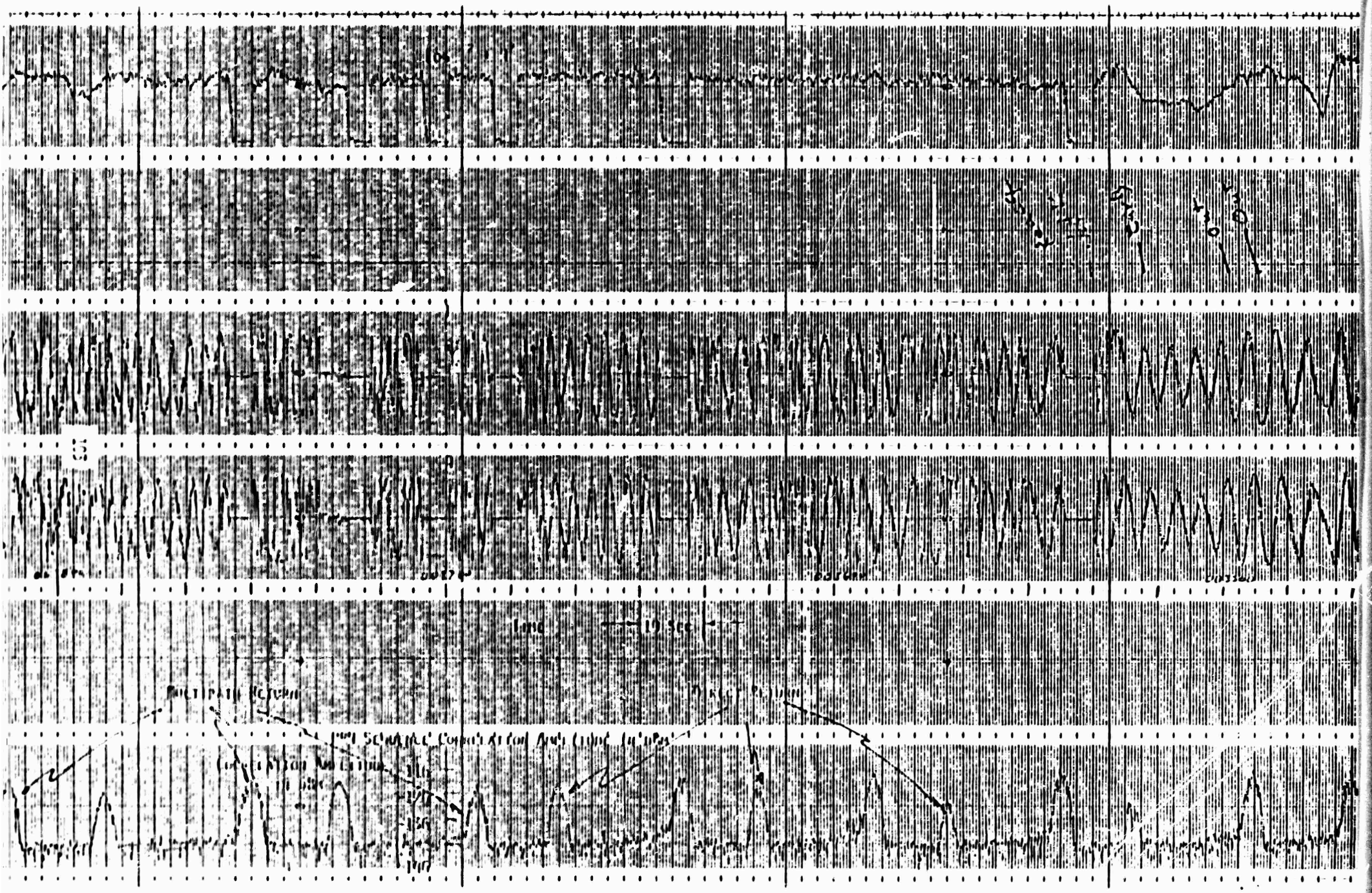

FIGURE 71 Over Water Multipath PRN Correlation Return , Bottom Blade Antenna

VII. CONCLUSIONS

During the five STRESS tests a wide variety of ionospheric scintillation fading was encountered. Fades during the early development of the cloud usually consisted of a single, long defocus, roughly 10 db deep with a single enhancement (focus) prior to and following the defocus. The mid-time fading was Rayleigh-like, usually with rapid fades from 15 to 30 db deep with enhancements of 5 to 10 db. During the late-time the fading was often patchy and Rician-like with slower fading.

The effect of the fading on the teletype character error rate has been estimated for various fading models. Figure 72 shows a series of curves depicting the expected symbol error rate into the decoder for the cases of no fading, flat Rayleigh fading, and selective Rayleigh fading. The difference in symbol energy required to achieve a 5×10^{-2} symbol error rate both in no fading and in flat fading is a representative figure of the expected system performance loss in the barium environment. At the 5×10^{-2} symbol error rate into the decoder the message error rate is expected to be approximately one-half. This loss can be seen to be about 8 db in Figure 72 which is close to the performance loss of 6 db actually observed in the data reduced to date (ESTHER). Sources of error in this comparison are: 1) the assumption of Rayleigh fading, the barium fading used to determine the 6 db loss figure may have been less intense than Rayleigh; 2) the assumption of 5×10^{-2} symbol error representing a message error rate of one-half; and 3) the assumption that the fading was flat, some frequency selectivity could be mitigating the fading. Further investigation should be fruitful in this area.

Regarding Assumption 3), the assumption of flat fading, there is some quick-look evidence that the barium induced fading during FERN is indeed non-selective. The effect of frequency decorrelation on the forward UHF downlink

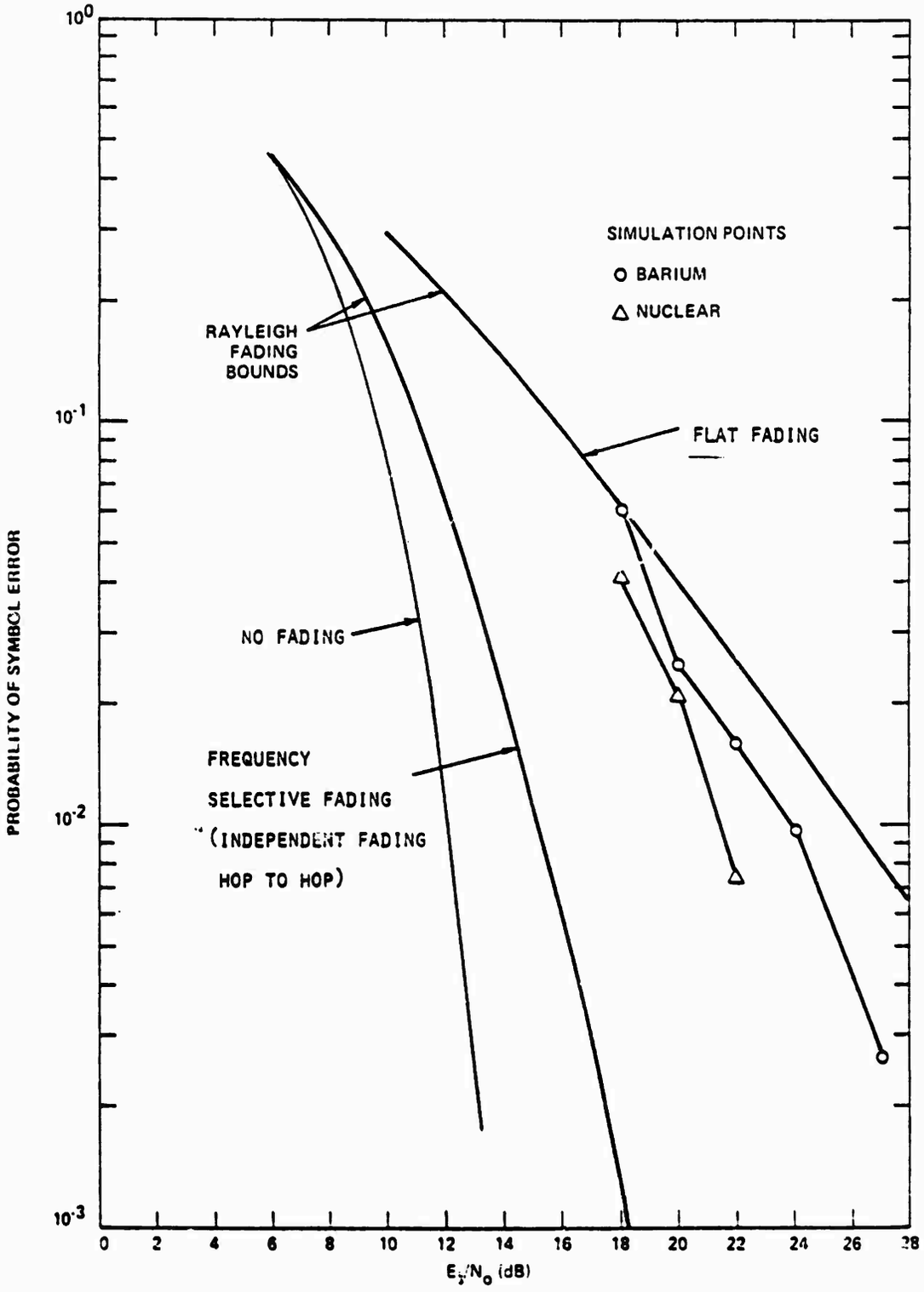

FIGURE 72 Average Character Error Rate Probability, Slow Fading

appeared to be insufficent to change the fading performance during FERN. The error rate in the hopped, or frequency diversity mode, appeared to be almost identical in the fixed frequency "HELP" mode. Note, however, that decorrelation of the uplink and downlink tone, which are separated by 90 MHz, was evident. Frequency diversity of the order observed over the 90 MHz could be used to improve system performance if used in conjunction with an error correction coding system similar to that employed in the LES 8/9 system.

The ionospheric irregularities produced during the STRESS test by the barium cloud produced fading quite similar to that encountered in the equatorial ionosphere. Figures 73 through 77 show examples of fading encountered during an AFAL ionospheric scintillation test in the area of Lima, Peru during March 1977. The rate of fading and depth of fading appeared quite comparable. The physical extent of the fading was naturally much smaller for the STRESS test. In the equatorial region scintillation is often encountered for periods of hours. The barium cloud scintillation also appeared to have a more regular repetitive structure than that encountered in the natural equatorial scintillation situation.

One of the main objectives of the STRESS test was to obtain fading information or to characterize the fading situation of a disturbed ionosphere for extrapolation to a nuclear environment. For this reason it is appropriate to make a comparison between the barium and the expected nuclear environments with considerations to the validity of a systems test, as is summarized in Table 10. The barium induced propagation disturbance was observed to cause UHF Rayleigh fading. This aspect of barium induced fading is a key point of commonality since the signal fading expected to result from nuclear detonation induced ionospheric irregularities also has a Rayleigh amplitude distribution. Apart from this important aspect, the fading from barium will differ from those

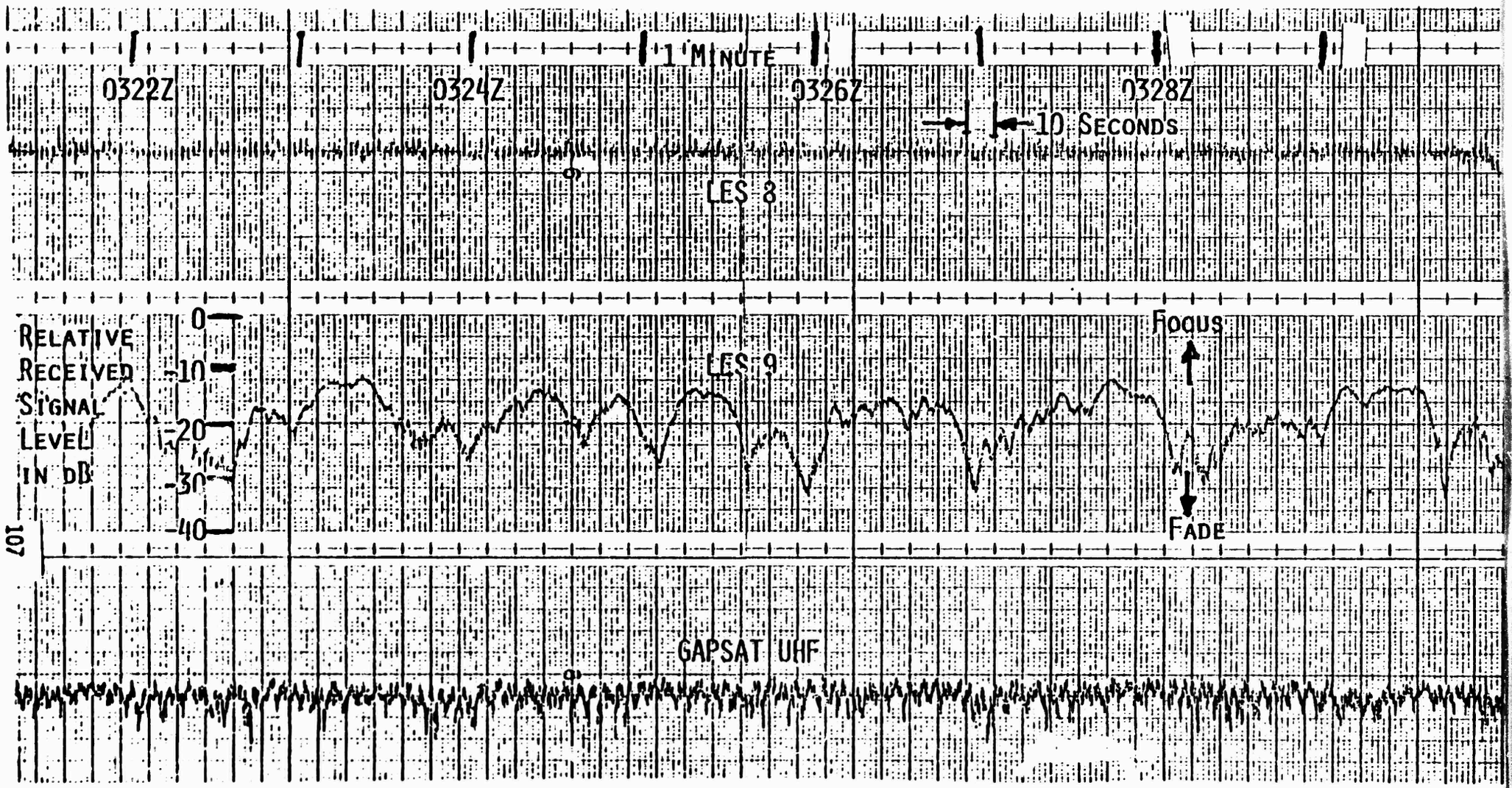

FIGURE 73 Natural Scintillation Peru 27 March 77

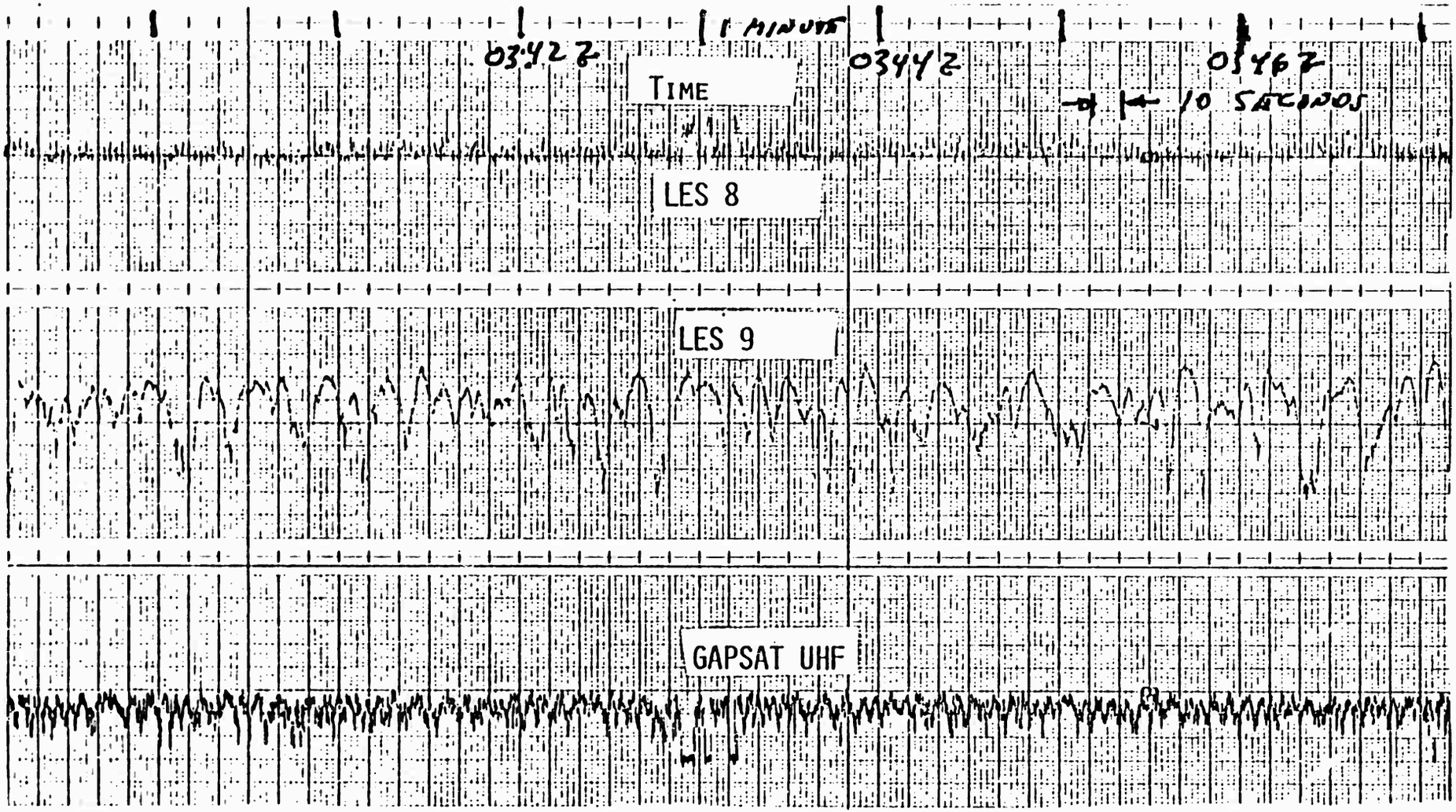

FIGURE 74 Natural Scintillati Peru 27 March 77

FIGURE 75 Natural Scintillation Peru 27 March 77

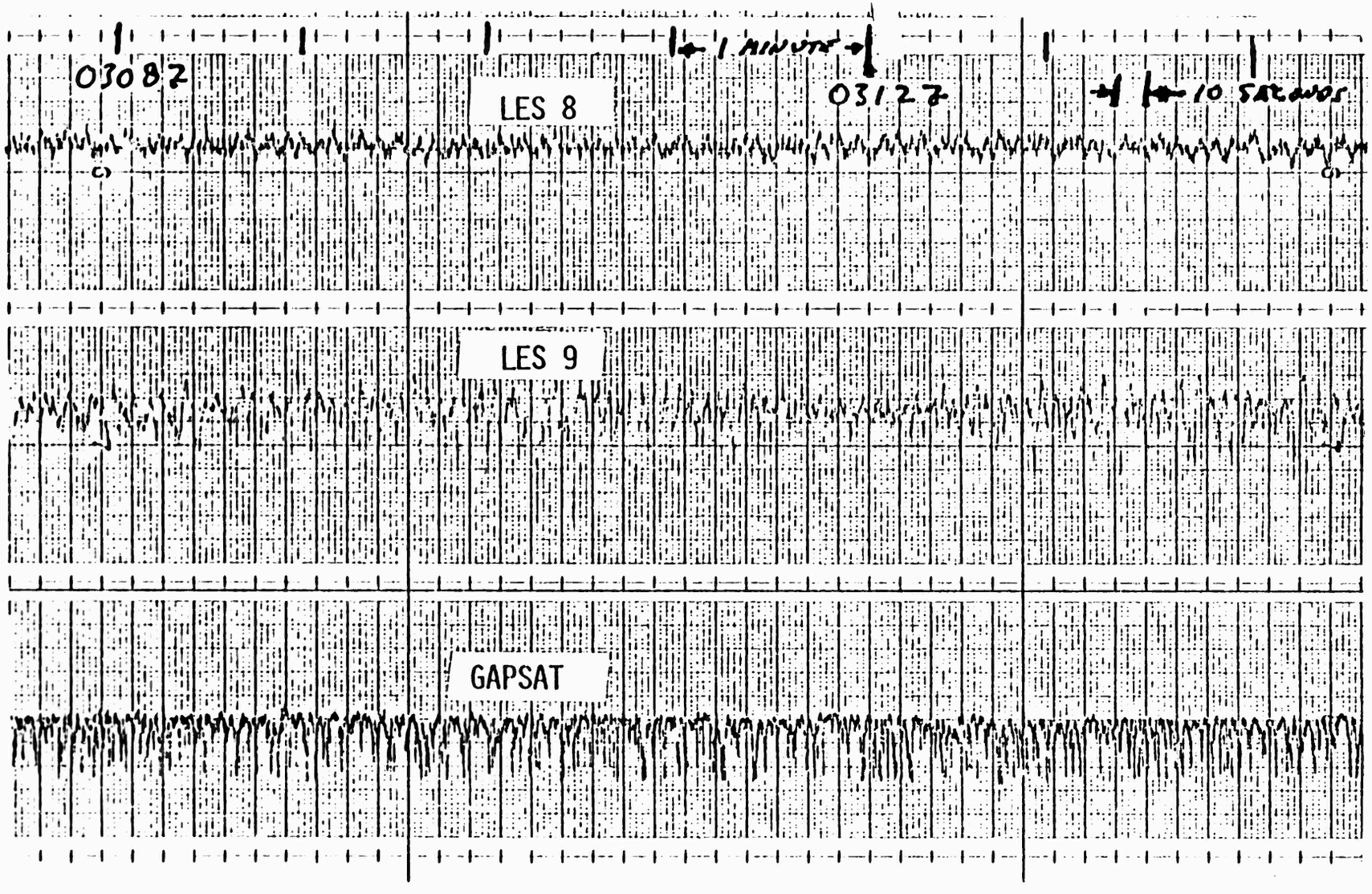

FIGURE 76 Natural Scintillation Peru 27 March 77

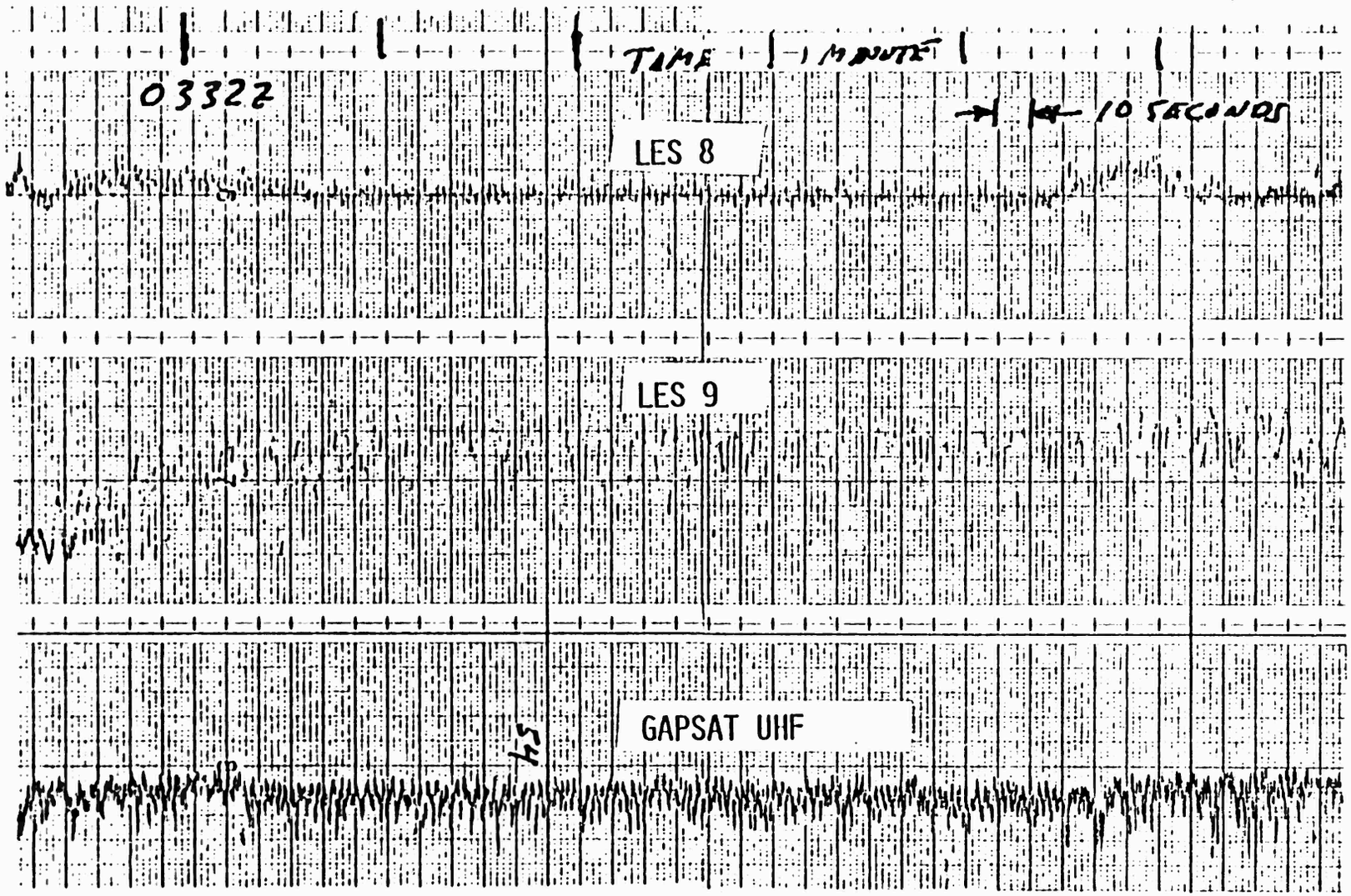

FIGURE 77 Natural Scintillation Peru 27 March 77

* Barium Environment causes Rayleigh Fading at UHF

* Nuclear Environment causes Rayleigh Fading at UHF
  - But Faster Fading
  - Smaller Correlation Bandwidth

* Coded System will operate better in faster fading

* Coded frequency-hopped system will operate better if correlation bandwidth is smaller than hopping bandwidth (but larger than signal spectrum)

Table 10: Barium/Nuclear Similarities For System Testing

predicted for a nuclear environment in one major and two minor areas. The major difference is that the nuclear environment is expected to cause long-lived signal absorption. Barium clouds produce no absorption of significance, and thus, they cannot be straightforwardly used to simulate nuclear induced system effects. However, it is believed that a meaningful test can be conducted if the predicted values of nuclear induced signal absorption are artificially injected into the system channel. Signal attenuation of the UHF system signals received by the subject modem was used in the STRESS experiment for this purpose. The two minor differences between the barium fading and nuclear environments are that generally the barium fading is expected to be slower than the nuclear fading and that the barium fading is expected to be less frequency selective. Although these differences will exist for most nuclear geometries, it should be noted that geometries through the nuclear environment with weaker or less extensive irregularities that have fading rates and frequency selectivities similar to barium are not ruled out. It should also be noted that for the range of fading rates and fading correlation bandwidths involved in most nuclear modelling, those presented by the barium environment are worst case conditions for error correction coded frequency hopping systems (LES 8/9 forward and report-back in particular). Decoders and hard decision demodulators in such systems generally perform better for a given average channel symbol error rate as the channel fading they must correct for causes a more random channel symbol error pattern. A slow fade rate causes an undesirable organization of channel symbol error patterns in time as does a large fading correlation bandwidth, which to a wideband hopped signal presents the same fading from hop to hop. If the system's effects were less severe when produced by slower fading or large fading correlation bandwidths, then some doubts might prevail with regard to the ability to use

barium in a systems test. However, because of the worst case conditions of these differences, it is felt that systems tests with barium are meaningful in the assessment of nuclear detonation induced systems effects, given that the attenuation has been set according to the expected absorption.

The PRN multipath testing brought forth several conclusions. Multipath returns obtained while using the crossed-slot antenna indicated that the isolation of the direct from the reflected propagation path was of the order of 17 db ±3 db over sea and 30 db ±5 db over land for 30° to 40° satellite elevation angles. The sea isolation value is in good agreement with data taken from the crossed-slot antenna on the 16 January 1977 test flight. The values of multipath isolation set confidence limits on the determination of the depth of barium induced fading from crossed-slot antenna data. Although fades deeper than the isolation may be observed, it is not possible to attribute them solely to barium cloud effects. (Thermal noise sets similar confidence limits on fading data.) The sea multipath isolation of any antenna is dependent upon three parameters: the direct path antenna gain, the sea state reflection coefficient, and the antenna gain (due to leakage around the aircraft fuselage) in the direction of the received multipath. The first two parameters are relatively uniform over the set of upward looking topside UHF antennas on the aircraft C135/662. The last parameter may change moderately and, as a result, the multipath isolation of the topside upward looking antennas may vary by 5 or 10 db from antenna to antenna. The best sea multipath isolation available is 25 to 30 db from Dorne-Margolin hybrid antenna based on the results of pre-STRESS, STRESS, and the 16 January 1977 test flight. This antenna was used in STRESS for transmission of the uplink probe.

Returns obtained while using the bottom blade indicated that sea specular reflections cause a loss of only a few (more than 1 less than 10) db of signal strength. In contrast land reflections cause a greater (more than 10 db but less than 20 db) loss. The strong sea multipath returns point to the possibility of the use of the sea bounce path as a spatial diversity path through ionospheric fading. Conventional spatial diversity techniques are not implemented in airborne receiver platforms to mitigate ionospheric fading because of the large antenna separations typically required. Use of the multipath bounce channel would overcome the separation problem with the sacrifice of some signal level.

In the bottom blade results a clearer picture of the multipath delay profile is available than previously available in the topside antenna results of pre-STRESS. This picture indicates a multipath profile that is predominantly specular to the 8 microsecond resolution of the PRN measurement. Some diffuse energy arrived after this specular return in both sea and land results. However, it was observed more consistently in the land results. In the land results diffuse energy arrived at the satellite as late as 100 microseconds after the start of the main path reflection in many returns. This delay corresponds to energy arriving with a 30 kilometer longer path length over and above the extra 15 kilometer specular multipath length.

VIII. RECOMMENDATIONS FOR FUTURE EFFORTS

Additional reduction and analysis of the STRESS data is planned. As discussed previously, the downlink hop data can be reduced along with coarse frequency command recordings to give information on the frequency decorrelation of the downlink hop propagation medium. It is also possible to back-propagate the recorded propagation probe data to determine the true integrated electron content of the barium cloud for phenomenological purposes. Such a technique has been used with downlink data from Pass 18, ESTHER, the amplitude fading of which is shown in Figure 58. Figure 78 shows the scintillation index (S_4) of the data versus back propagation distance. The minimum of about 165 kilometers indicates that most of the fading effects seen at the ground were due to barium structure at this altitude. The dotted curve in Figure 79 is the phase of the field at this altitude (contrast the phase at the ground in the solid curve) which is a very good indicator of the actual integrated electron content. Back propagation analyses such as these are planned to assist phenomenological interpretation of ion cloud behavior and to check propagation prediction techniques. A thorough data reduction effort is planned to extend through June 1978.

Further ionospheric testing is planned in the future. STRESS multipath measurements indicate that signals reflected off the ocean provide a signal path through the ionosphere both spatially distinct from main path signals and strong enough to establish a spatial diversity gain through ionospheric fading. The 600 meter spatial correlation lengths of ionospheric fading prevent the use of conventional spatial diversity techniques on airborne force elements. Plans exist for future testing of the sea multipath

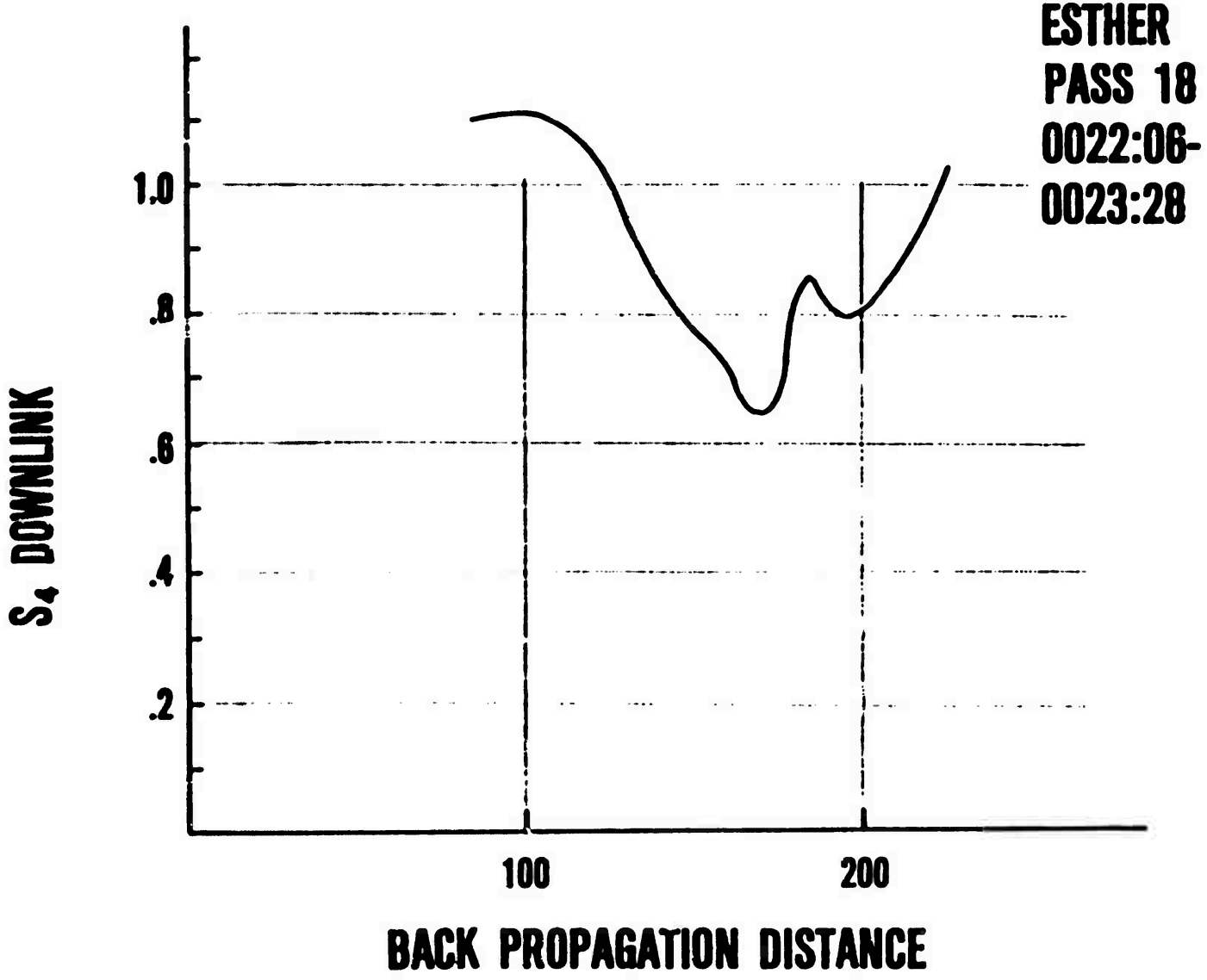

FIGURE 78 Back Propagation of ESTHER PASS 18 Downlink Data

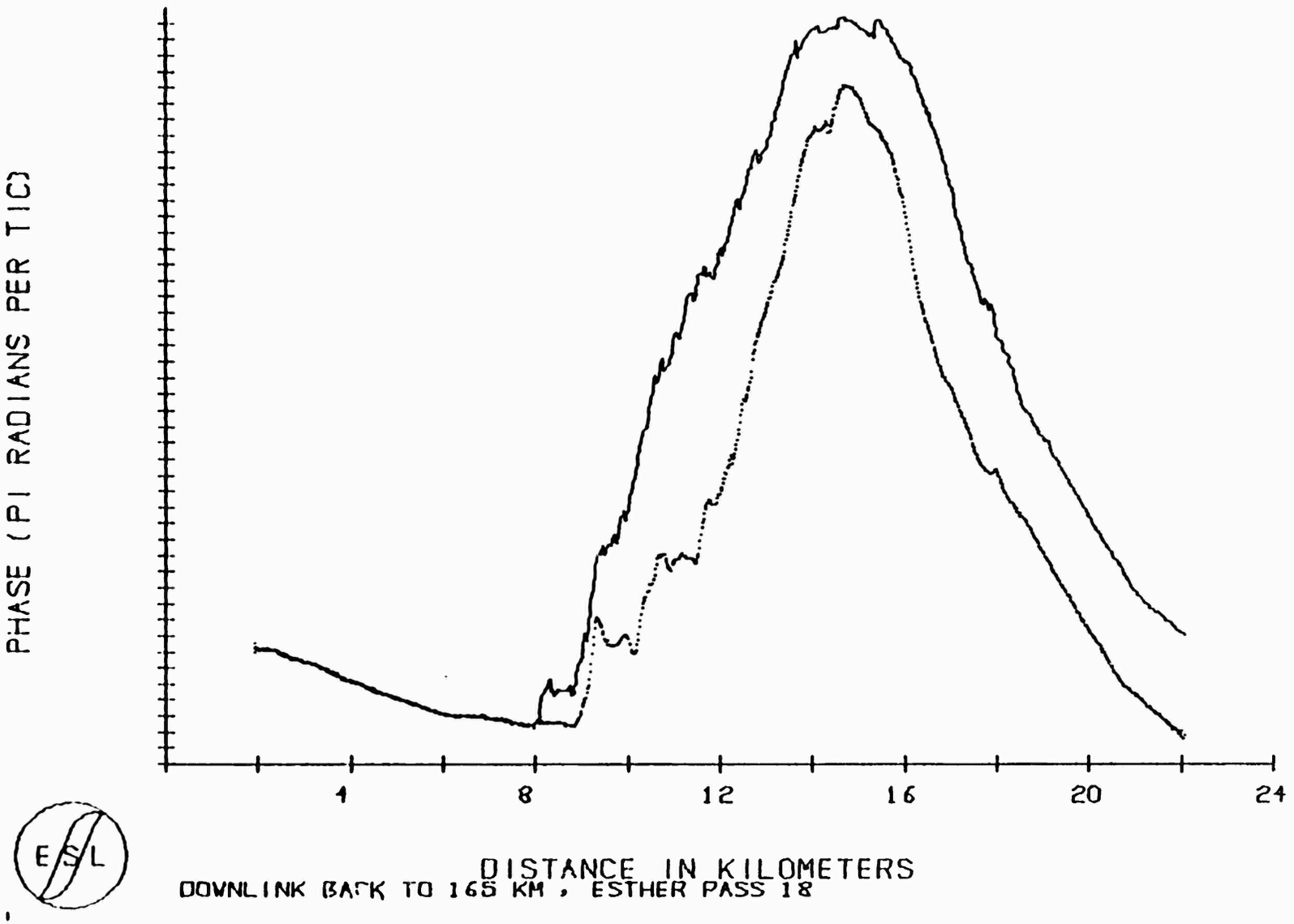

FIGURE 79 Back Propagation Distance for ESTHER Pass 18 Downlink Data

spatial diversity path against equatorial fading using LES 8 or LES 9 to evaluate the usefulness of the concept. Such a test could occur in the Fall of 1977.

Additional testing/simulation is planned to further evaluate the relationship between fading level, acquisition time, and bit-error rate. Magnetic tape recordings have been made of the UHF signal levels received during the STRESS test and during natural, equatorial ionospheric scintillation fading tests. These tape recordings will be used to generate a fading signal for the additional evaluation. AFAL's Communication System Evaluation Laboratory is equipped with a LES 8/9 satellite simulator. This satellite simulator can produced a UHF forward downlink signal which will be modified by the signal level traces recorded during the STRESS and equatorial scintillation tests. The UHF satellite receiving system utilizing the single UHF modem or the dual UHF modem can be subjected to repeated tests using a selected fading pattern and varying the median signal level. This technique will allow meaningful evaluations of acquisition times during various fading structures with various signal level margins. These tests are planned for Fall 1977.

REFERENCES

1. D. R. McDaniel, editor. Project SECEDE Final Program Review, Vol. II, SRI 2-5462, October 1972, p. 19.

2. L. M. Linson. Private Communication, February 1977.

3. C. Prettie, et. al. Final Report of the Feasibility Study for the STRESS Experiment, DNA Report by ESL; Sunnyvale, California, 20 August 1976.

4. J. Marshall. Preliminary Quick-Look Data Summary Communication/Propagation Test Data For Project STRESS; ESL, Sunnyvale, California, 15 March 1977.

5. D. R. McDaniel. STRESS Field Operations Plan; SRI Report for DNA; SRI, Menlo Park, California, February 1977.

6. Joint Report On Peru Scintillation Tests; AFAL/AFGL Report, AFAL: Wright Patterson AFB, Ohio; 28 February 1977.

7. Dr. C. Prettie. Project STRESS Barium Release Experiment; ESL SR-226; ESL; Sunnyvale, California, 29 April 1976.